

©[2016]

Irene M. Wohlman

ALL RIGHTS RESERVED

CHEMICAL-INDUCED ALTERATIONS IN THE ENDOCANNABINOID SYSTEM
IN MOUSE SKIN

By

Irene M. Wohlman

A Dissertation submitted to the
Graduate School-New Brunswick
Rutgers, The State University of New Jersey
and

The Graduate School of Biomedical Sciences

In partial fulfillment of the requirements

For the degree of

Doctor of Philosophy

Graduate Program in Toxicology

written under the direction of

Jeffrey D. Laskin

and approved by

New Brunswick, New Jersey

May, 2016

ABSTRACT OF THE DISSERTATION

Chemical-Induced Alterations in the Endocannabinoid System in Mouse Skin

By IRENE M. WOHLMAN

Dissertation Director:

Jeffrey D. Laskin, PhD.

Vesicants including sulfur mustard (SM) and nitrogen mustard (NM) are bifunctional alkylating agents that cause skin inflammation, edema and blistering. This is associated with alterations in keratinocyte growth and differentiation. Endogenous cannabinoids, including N-arachidonylethanolamine (anandamide) and 2-arachidonoyl glycerol, are important in regulating inflammation, keratinocyte proliferation and wound healing. Their activity is mediated by binding to classical cannabinoid receptors, CB1 and CB2, as well as peroxisome proliferator-activated receptor alpha (PPAR α). Levels of endocannabinoids are regulated by fatty acid amide hydrolase (FAAH); inhibitors of this enzyme are known to suppress inflammation. Each of the endocannabinoid proteins was found to be expressed in epidermis and epidermal appendages in mouse skin. Treatment of the skin with SM or NM, at concentrations that induce tissue injury, was found to markedly upregulate FAAH, CB1, CB2 and PPAR α ; increased expression of these proteins persisted in the tissue during the wound healing process. To determine if the endocannabinoid system regulated the action of vesicants, mouse skin was treated with a novel class of vanilloid carbamates that are potent inhibitors of FAAH. These compounds were found to be highly effective in suppressing vesicant-induced inflammation in mouse skin. These data demonstrate that markers of the

endocannabinoid system are expressed in mouse skin. Our findings that NM and SM cause changes in the endocannabinoid system and that FAAH inhibitors have the capacity to reduce skin injury support the idea the endocannabinoids contribute to the pathogenic responses to vesicants.

DEDICATION

I would like to thank my family members and friends who supported me throughout my studies, and especially to my partner John Sassone for his patience and sense of humor, who kept me smiling through it all.

A special dedication is given to my father, who supported my decision to return to school for a Ph.D. late in life.

ACKNOWLEDGEMENTS

I would like to thank my advisor, Dr. Jeffrey Laskin, for all his patience, guidance and encouragement throughout the course of my research. I also wish to thank Dr. Laurie Joseph for her invaluable assistance and advice in the lab and in organizing this project. I would also like to acknowledge the contributions of my other thesis committee members, Dr. Ned Heindel, whose knowledge and suggestions helped me with the chemistry aspects of my research and Dr. Michael Gallo, who was always there to support and guide me and the other RATS throughout our graduate studies. Also a special thanks to all the JPGT faculty, especially Drs. Kenneth Reuhl, Jason Richardson and Marion Gordon for putting me on the spot and asking questions that guided me and helped me put my data in better perspective.

Special thanks to Gabriella Composto for all her assistance and advice on the immunohistochemistry and mouse treatment techniques I acquired in the Joseph lab, which directly contributed to me finishing this project. Special thanks also to Dr. Yi-Hua Jan and Dr. Vladimir Mishin for providing mentorship and encouragement in all things thioredoxin and FAAH. Thank you to the other EOHSI Laskin lab members: Dr. Ruijin Zheng, Dr. Shaojin Yang, and Dr. Yun Wen for their advice and help with experiments; to members of the EMSOP Laskin lab: Dr. Debbie Laskin, Dr. Carol Gardner, Mary Francis, Kinal; and Jessica Cervelli for all her help with the VS scope; and Dr. Chris Gibson and other members of Dr. Aleksunes' lab for help with my microglia project; and assistance from Rita Hahn and Adele Miller from Dr. Gordon's lab with the cryostat and reviewing of seminar presentations.

I would also like to thank everyone in Dr. Heindel's group at Lehigh, Dr. C. Jeff Lacy, Dr. Christophe Guillon and Jaya Saxena for all their assistance with the chemistry aspects of this project. I'd also like to thank the other members of the CounterACT group for their contributions to our work at Rutgers and my thesis project: Dr. Diane

Heck, Dr. Robert Casillas, Dr. Claire Croutch, Dr. Michael Shakarjian, Dr. Hong Duck Kim, and to Dr. MT-Huang and for his work with the MEVM and use of his laboratory for cell culture.

I would also like to acknowledge the members of the administrative staff past and present: Bernadine Chmielowicz, Liz Rossi, Eva Link, Sandi Selby, Toni Meyers and Kristin Borbely for their guidance and support in navigating through the Rutgers system.

TABLE OF CONTENTS

ABSTRACT.....	ii
ACKNOWLEDGEMENTS.....	v
DEDICATION.....	vii
TABLE OF CONTENTS.....	viii
LIST OF TABLES.....	xiii
LIST OF FIGURES.....	xviii
ABBREVIATIONS.....	xv
<u>INTRODUCTION</u>	1
1.0 Skin and Dermal Appendages	
1.1 Skin.....	1
1.2 Epidermis.....	1
1.3 Dermis & Hypodermis.....	3
1.4 Hair Follicles.....	4
1.5 Sebaceous Glands.....	5
1.6 Mouse vs. Human Skin.....	6
1.7 Keratinocyte Migration & Proliferation in Wounding.....	7
2.0 Sulfur & Nitrogen Mustards	
2.1 History & Background.....	9
2.2 Mechanism of Mustard Activation.....	11
2.3 Vesicant-Induced Skin Injury.....	12
2.4 Histopathological Effects.....	15
3.0 Mechanisms of Vesicant Toxicity in Skin	
3.1 Oxidative Stress.....	16
3.2 Proinflammatory Cytokines.....	17
3.3 Inflammatory Mediators.....	18

3.4 Apoptosis & Terminal Differentiation.....	19
4.0 Endocannabinoid System	
4.1 Endocannabinoids.....	21
4.2 Biosynthesis, Transport & Metabolism of Anandamide.....	22
4.3 Palmitoylethanolamine.....	25
4.4 Endocannabinoid receptors.....	26
4.5 Involvement or interaction of other receptors with the ECS.....	28
a. Peroxisome proliferator-activated receptor (PPAR α).....	28
b. Transient receptor potential vanilloid receptor-1 (TRPV-1).....	29
c. GPR55.....	29
4.6 Fatty Acid Amide Hydrolase (FAAH).....	30
4.7 FAAH Inhibition.....	31
4.8 Endocannabinoid System Role in Skin and Skin Inflammation	
a. FAAH.....	33
b. CB1 receptor.....	34
c. CB2 receptor.....	36
d. PPAR α	37
4.9 Endocannabinoid System in Wound Healing.....	37
<u>SUMMARY AND RATIONALE</u>	39
<u>PART 1: SPECIFIC AIMS 1 AND 2</u>	
1. Experiments.....	43
a. Animals	44
i. Mouse strains	
b. Chemical Treatments	
i. Nitrogen Mustard application to mouse dorsal skin.....	45
ii. Sulfur Mustard application to mouse dorsal skin.....	46

iii. MEVM.....	47
c. Immunohistochemistry.....	48
2. Results.....	49
3. Discussion.....	54
<u>PART 2: SPECIFIC AIM 3</u>	82
1. Experiments	
a. FAAH inhibitors and enzyme inhibition assays.....	83
b. COX-1 and COX-2 inhibition assays.....	83
c. Acetylcholinesterase inhibition assays.....	84
2. Results.....	85
3. Discussion.....	93
<u>CONCLUDING REMARKS</u>	160
<u>REFERENCES</u>	163

LIST OF FIGURES

1. Structures of NM, SM and CEES	11
2. Vesicant mechanism of action (NM).....	12
3. Structural changes in mouse skin following NM exposure.....	60
4. Effects of NM on CB1 receptor expression.....	62
5. Effects of NM on CB2 receptor expression.....	64
6. Blocking peptides inhibit binding of antibodies specific for FAAH, CB1, CB2 and PPAR α to NM treated mouse skin.....	66
7. Effects of NM on PPAR α nuclear receptor expression.....	68
8. Effects of NM on FAAH expression.....	70
9. Structural changes in mouse skin following SM exposure.....	72
10. Effects of SM on CB1 receptor expression.....	74
11. Effects of SM on CB2 receptor expression.....	76
12. Effects of SM on PPAR α nuclear receptor	78
13. Effects of SM on FAAH expression.....	80
14. General structures of FAAH inhibitors.....	104
15. Chemical components of vanillyl alcohol carbamates.....	106
16. Activity of vanillyl alcohol carbamates with N-conjugated ring R-groups as inhibitors of FAAH enzyme activity.....	110
17. Ability of vanillyl alcohol carbamates with N-conjugated alkane R-groups to inhibit FAAH.....	114
18. Chemical components of Class II hydroxamate compounds.....	116
19. Activity of the hydroxamate class of compounds as inhibitors of FAAH enzyme activity.....	120
20. Chemical components of Class III compounds.....	122
21. Structures of conjugate NSAID substituents.....	128

22. General structure of Olvanil-NSAIDs.....	130
23. Comparison of Olvanil-NSAID and URB597 structures.....	132
24. Activities of the Olvanil-NSAID compounds and URB597 as inhibitors of FAAH enzyme activity.....	136
25. Activities of the NSAIDs ibuprofen and indomethacin as inhibitors of FAAH enzyme activity.....	140
26. Comparison of NDH Compound Structures with and without O-phenoxy group.....	142
27. Comparison of NDH Compound Structures with and without additional amide group.....	146
28. General structure of Ester-Carbonate and Ester series NSAIDs.....	148
29. General structure of Class V(a) Ester-Carbonate NSAID (4338).....	150
30. General structure of Class V(b) Galantamine-NSAID.....	152
31. Activity of the Ester-carbonate 4338 as an inhibitor of FAAH.....	156
32. Activities of the Galantamine-NSAID compounds as inhibitors of FAAH enzyme activity.....	158

LIST OF TABLES

1. Ability of vanillyl alcohol carbamates with N-conjugated ring R-groups to inhibit FAAH enzyme activity and suppress inflammation in the mouse ear vesicant model (MEVM).	108
2. Ability of vanillyl alcohol carbamates with C ₄ -C ₁₂ alkane R-groups to inhibit FAAH enzyme and suppress inflammation in the mouse ear vesicant model (MEVM).....	112
3. Ability of hydroxamates to inhibit FAAH and suppress inflammation in the mouse ear vesicant model (MEVM).....	118
4. Activity of vanillyl amides and vanillyl amide carbamates as FAAH enzyme inhibitors and suppressors of inflammation in the mouse ear vesicant model (MEVM).....	124
5. Comparison of the activity of phenyl- and phenyl hydroxyl carbamates (hydroxamates) as inhibitors of inflammation in the mouse ear vesicant model.....	126
6. Activities of 4369, olvanil-NSAIDs and URB597 as FAAH, COX-1, COX-2 and AChE enzyme inhibitors and suppressors of inflammation in the mouse ear vesicant model (MEVM).....	134
7. Activities of indomethacin and ibuprofen as FAAH, COX-1, COX-2 enzyme inhibitors, and suppressors of inflammation in the mouse ear vesicant model (MEVM).....	138
8. Activities of the vanillyl amide compounds as FAAH enzyme inhibitors and suppressors of inflammation in the mouse ear vesicant model (MEVM)	142
9. Activities of the Class V compounds as FAAH, COX-1, COX-2 and AChE inhibitors, and suppressors of inflammation in the mouse ear vesicant model (MEVM).....	152

ABBREVIATIONS

2-AG	2-arachidonoyl glycerol
AA	arachidonic acid
ACEA	<i>N</i> -(2-Chloroethyl)-5Z,8Z,11Z,14Z-eicosatetraenamide
AChE	acetylcholinesterase
AChEI	acetylcholinesterase inhibitor
ACPA	arachidonylcyclopropylamide
AD	atopic dermatitis
AEA	anandamide
AG	2-arachidonoyl glycerol
AMT	anandamide membrane transporter
AP-1	activator protein 1
Asp	aspartic acid
ATP	adenosine triphosphate
cAMP	cyclic AMP
CB	cannabinoid
CB1	cannabinoid receptor 1
CB2	cannabinoid receptor 2
CD-1	general purpose, white Swiss mouse strain
CEES	2-chloroethyl ethyl sulfide
CNS	central nervous system
COX-2	cyclooxygenase 2
CP	cytosolic port
CYP450	cytochrome P450
DLD1	Dukes' type C, colorectal adenocarcinoma cell line
DNA	deoxyribonucleic acid

DNFB	dinitrofluorobenzene
DNMT	DNA methyltransferase
EA	ethanolamide
EC	endocannabinoid
EC ₅₀	half-maximal effective concentration
ECM	extracellular matrix
ECS	endocannabinoid system
EDTA	ethylenediaminetetraacetic acid
EET	epoxyeicosatrienoic acid
EET-EA	epoxyeicosatrienoic acid ethanolamide
EGF	epidermal growth factor
EPO	eosinophil peroxidase
ERK	extracellular-signal-regulated kinases
FAAH	fatty acid amide hydrolase
FADD	Fas-associated protein with death domain
FITC	fluorescein isothiocyanate
GPR55	G-protein receptor 55
GSH	glutathione
4-HNE	4-hydroxynonenal
H&E	hematoxylin and eosin stain
HB-EGF	heparin-binding EGF-like growth factor
HCL	hydrochloric acid
HETE	hydroxyeicosatetraenoic acid
HETE-EA	hydroxyeicosatetraenoic acid ethanolamide
HF	hair follicle
HFG	human gingival fibroblasts

His	histidine
HpETE	hydroperoxyeicosatetraenyl
HpETE-EA	hydroperoxyeicosatetraenyl-EA
HT29	human adenocarcinoma cell line
IBD	inflammatory bowel disease
IC ₅₀	half-maximal inhibitory concentration
IHC	immunohistochemistry
IL-1	interleukin 1
IL-1 β	interleukin 1 beta
I κ B α	nuclear factor of kappa light polypeptide gene enhancer in B-cells inhibitor, alpha
iNOS	inducible nitric oxide synthase
JNK	c-Jun N-terminal kinase
K1	keratin 1
K4	keratin 4
K5	keratin 5
K6	keratin 6
K10	keratin 10
KC	keratinocyte
LOX	lipxygenase
LPA	lysophosphatidic acid
LPI	lysophosphatidylinositol
LTB ₄	leukotriene B ₄
LTC ₄	leukotriene C ₄
Lys	lysine
MAC	membrane access channel

MAGL	monoacylglycerol lipase
MAPK	mitogen-activated protein kinase
MEVM	mouse ear vesicant model
MMP-2	matrix metalloproteinase 2
MOMP	mitochondrial membrane permeability
NAAA	<i>N</i> -acylethanolamine-hydrolyzing acid amidase
NAD ⁺	nicotinamide adenine dinucleotide
NAE	<i>N</i> -acylethanolamine
NAT	<i>N</i> -acyltransferase
NAPE	<i>N</i> -acylphosphatidylethanolamine
NAPE-PLD	<i>N</i> -acylphosphatidylethanolamine-phospholipase D
NFκB	nuclear factor kappa-light-chain-enhancer of activated B cells
NHEK	normal human epidermal keratinocytes
NK	natural killer cells
NM	nitrogen mustard
NSAID	non-steroidal anti-inflammatory
OAE	oleylethanolamide
OP	organophosphate
PARP	poly (ADP-ribose) polymerase
PBS	phosphate buffered saline
PE	phosphatidylethanolamine
PEA	palmitoylethanolamide
PGD ₂ -EA	prostaglandin D ₂ (ethanolamide)
PGDS	prostaglandin-D synthase
PGE ₂ -EA	prostaglandin E ₂ (ethanolamide)
PGES	prostaglandin-E synthase

PGF ₂ -EA	prostaglandin F ₂ (ethanolamide)
PGF _{2α} -EA	prostaglandin F ₂ alpha (ethanolamide)
PGG ₂ -EA	prostaglandin G ₂ (ethanolamide)
PGI ₂	prostaglandin I ₂
PI3-K	phosphoinositol 3-kinase
PKC	protein kinase C
PPARα	peroxisome proliferator activated receptor alpha
PUFA	polyunsaturated fatty acid
QSAR	quantitative structure-activity relationship
RE	response elements
RNA	ribonucleic acid
ROS	reactive oxygen species
RXR	retinoid X receptor
SAR	structure-activity relationship
Ser	serine
SG	sebaceous gland
SKH1-Hr	hairless mouse strain
SM	sulfur mustard
TGF-α	transforming growth factor alpha
THC	tetrahydrocannabinol
TNFα	tumor necrosis factor alpha
TPA	12-O-tetradecanoylphorbol-13-acetate
TRPV-1	transient receptor potential vanilloid-1
UVA	ultraviolet A

INTRODUCTION

1.1 Skin

The skin is the largest organ in the body (Wickett R.R., 2006). It protects the organism from the environment (i.e. microbes, heat, cold), assists in temperature regulation and sensations of touch, heat and cold (Wickett R.R., 2006; Darlenski, 2011).

Mammalian skin consists of three major layers:

1. The outermost layer, the epidermis, which provides a waterproof barrier.
2. The dermis, which lies deep to the epidermis and contains tough connective tissue, and dermal appendages including hair follicles, sebaceous glands, sweat glands.
3. The bottommost layer, the hypodermis or subcutaneous layer, consists of adipose and connective tissue (Wickett R.R., 2006).

1.2 Epidermis

The epidermis comprises four main layers, the stratum basale, the stratum spinosum, stratum granulosum and stratum corneum (Wikramanayake *et al.*, 2014; Matsui and Amagai, 2015). Epidermal boundary homeostasis is maintained by keratinocytes which undergo terminal differentiation, a process involving a switch from a proliferative state to a differentiated state as they ascend from the basal layer toward the skin surface (Blanpain and Fuchs, 2009; Bikle *et al.*, 2012). In each layer, different sets of keratin intermediate filaments are expressed by keratinocytes (Wikramanayake *et al.*, 2014; Matsui and Amagai, 2015). Keratins are elastic, fibrous proteins which form heterodimers between acidic (type I) and basic (type II) proteins. The heterodimers form a three-dimensional cytoskeleton within the cytoplasm and surrounding the nucleus (Wikramanayake *et al.*, 2014; Matsui and Amagai, 2015). Basal keratinocytes express the intermediate filament proteins keratin 4, 5 and 15 and are attached to the basement

membrane by hemidesmosomes and focal adhesions (Blanpain and Fuchs, 2009; Pastar *et al.*, 2014).

Keratinocyte stem cells are located in the basal layer and in the hair follicle bulge region (Blanpain and Fuchs, 2009). In adult skin, proliferating stem cells asymmetrically divide to produce two daughter cells: one which remains a stem cell and the other which commits to a program of terminal differentiation (Blanpain and Fuchs, 2009; Sotiropoulou and Blanpain, 2012). The differentiating basal keratinocytes withdraw from the cell cycle, lose their ability to adhere to the basement membrane and move upward through the epidermal layer, changing their morphology and composition as they ascend (Wikramanayake *et al.*, 2014). Apical to the basal layer is the spinous layer, consisting of larger, polyhedral, flattened keratinocytes (Wikramanayake *et al.*, 2014). As keratinocytes differentiate, they switch from synthesis of K4, K5 and K15 to that of K1, K10 and caspase-14, forming a sturdy, spinous network of desmosomes resistant to mechanical stress (Pastar *et al.*, 2014; Wikramanayake *et al.*, 2014).

As the cells continue ascending, basophilic keratohyalin granules appear in the cytoplasm; these cells comprise the epidermal granular layer (Wikramanayake *et al.*, 2014). Granules contain keratin filaments and the keratin-binding proteins profilaggrin and loricrin (Pastar *et al.*, 2014). At the uppermost layer, keratinocytes undergo apoptosis and begin formation of the stratum corneum (Matsui and Amagai, 2015). Keratin filaments form disulfide bonds with mature filaggrin and assemble a cornified cell envelope directly beneath the plasma membrane, which disintegrates along with the cellular organelles and nucleus (Matsui and Amagai, 2015). Corneocytes, the cells comprising the stratum corneum, form when the resulting calcium influx activates transglutaminase to catalyze crosslinking of involucrin and loricrin proteins, forming a tough, insoluble cell envelope around the keratin filaments (Pastar *et al.*, 2014; Matsui and Amagai, 2015). Lipids extruded into the extracellular space form a continuous lipid

matrix, filling the space between corneocytes and sealing them together (Wikramanayake *et al.*, 2014). Finally, through the process of desquamation, apical corneocytes dissociate and slough off into the environment (Wikramanayake *et al.*, 2014).

Biochemical changes that occur during terminal differentiation are regulated in part by a steep calcium (Ca^{2+}) gradient present in the epidermis (Menon *et al.*, 1992; Elias and Feingold, 2001). The lowest levels of Ca^{2+} are found in the basal layer, increasing upward to the granular layer (Arabzadeh *et al.*, 2009; Bikle *et al.*, 2012). Increased extracellular calcium [Ca^{2+}_o] triggers a release of intracellular free calcium [Ca^{2+}_i] promoting keratinocyte differentiation (Bikle *et al.*, 1996; Tu *et al.*, 2012). Disruption of the epidermal barrier can alter the Ca^{2+} gradient, resulting in increased proliferation and disorganized epidermal layers (Tu *et al.*, 2012).

1.3 Dermis & Hypodermis

The dermis is subdivided into two main layers, the papillary and the reticular (Smith *et al.*, 1982). The superior papillary layer contains a thin arrangement of collagen fibers, while the inferior reticular layer is thicker, and comprised of dense collagen fibers arranged parallel to the skin surface (Smith *et al.*, 1982). Structures within the dermis include fibroblasts, eccrine and apocrine sweat glands, and the pilosebaceous units, comprised of a hair follicle, hair shaft, erector pili muscle, and sebaceous glands (Smith *et al.*, 1982). It also contains a network of blood vessels to supply nutrients, remove wastes, regulate temperature and allow entry of immune cells (Smith and Holbrook, 1982; Schmid and Harris, 2014). Finally, between the skin and underlying deep fascia lies the hypodermis, a fatty layer of adipose tissue which stores large quantities of lipids and acts as a cushion (Wosicka and Cal, 2010).

1.4 Hair Follicles (HF)

The HF functions as a mini-organ, and is formed through interaction between the neuro- and mesoectoderm (Rishikaysh *et al.*, 2014). The follicle is divided into a lower segment or bulb/suprabulbar region; a middle segment or isthmus located between the opening of the sebaceous gland duct and the bulge region; and an upper segment or infundibulum, the region between the point where the sebaceous gland duct opens into the hair canal and the skin surface (Wosicka and Cal, 2010; Rishikaysh *et al.*, 2014). The bulb surrounds the dermal papilla, which is responsible for stimulating hair growth, and the hair matrix, which is the actively growing portion of the follicle (Wosicka and Cal, 2010). Surrounding the hair follicle is the outer root sheath, a stratified epithelium continuous with the epidermis (Wosicka and Cal, 2010).

HFs undergo cyclic phases known as the hair cycle (Alonso and Fuchs, 2006; Rishikaysh *et al.*, 2014). Phases of the cycle include anagen (growth), catagen (regression) and telogen (resting) (Alonso and Fuchs, 2006; Rishikaysh *et al.*, 2014). Exogen, where the telogen club is released (hair shedding) does not occur at every cycle (Alonso and Fuchs, 2006; Rishikaysh *et al.*, 2014). Duration of anagen depends upon continued proliferation and differentiation of follicle-base matrix cells and determines the length of the hair shaft (Alonso and Fuchs, 2006; Rishikaysh *et al.*, 2014). Daughter cells move upwards from the follicle base to form layers of the inner root sheath and hair shaft (Alonso and Fuchs, 2006; Rishikaysh *et al.*, 2014). The inner root sheath keratinizes to form a structural support, then its dead cells degenerate as they reach the upper follicle and release the hair shaft to extend through the skin (Alonso and Fuchs, 2006; Rishikaysh *et al.*, 2014). During catagen cell-cycling decreases, while increased apoptosis occurs in the epithelial cells of the bulb, outer root sheath and outermost epithelial layer. Hair shaft differentiation ends, and the bottom of the hair shaft forms a club-shaped bulb (Alonso and Fuchs, 2006; Rishikaysh *et al.*, 2014).

Catagen is followed by telogen, a resting phase (Alonso and Fuchs, 2006; Rishikaysh *et al.*, 2014).

Hair follicle stem cells play a role in epidermal reepithelialization after wounding (Ito *et al.*, 2005; Ansell *et al.*, 2011). Epidermal wound repair involves activation, then migration and proliferation of keratinocytes from the wound edge and from the adnexal structures, such as hair follicles and sweat glands (Ito *et al.*, 2005; Ansell *et al.*, 2011). Cells from the HF infundibulum migrate into the epidermis, while bulge cells migrate to the infundibulum, then to the epidermis to cover the wound bed (Ito *et al.*, 2005). However, during normal conditions, bulge cells do not migrate to the epidermis therefore do not contribute to homeostasis (Ito *et al.*, 2005).

1.5 Sebaceous glands (SG)

Except for the palms of the hands and soles of the feet, most regions of the body contain sebaceous glands (Zouboulis *et al.*, 2008; Schneider and Paus, 2010). They are part of the pilosebaceous unit, associated with the upper portion of the hair follicle and connected to the skin surface via the sebaceous duct (Zouboulis *et al.*, 2008). Their main function is to produce and release an oily, waxy substance called sebum through holocrine secretion, a process of terminal differentiation and degeneration of mature sebocytes (Schneider and Paus, 2010).

Sebocytes are cells of the sebaceous gland whose biological activity is regulated by steroid hormone receptors, peroxisome proliferator-activated receptors and liver X receptor (Zouboulis *et al.*, 2008). The basal layer of the gland contains small, mitotically active cells which undergo terminal differentiation (Schneider and Paus, 2010). As the cells are displaced toward the center of the gland, they leave the cell cycle, accumulate lipid and lose subcellular structures (Schneider and Paus, 2010). Once they reach the sebaceous duct, they disintegrate and release their contents (Schneider and Paus, 2010).

Human and mouse sebum differ in composition. Human sebum consists primarily of triglycerides, diglycerides and free fatty acids (57%), wax esters (26%), squalene (12%), and cholesterol (2%) (Ottaviani *et al.*, 2010; Schneider and Paus, 2010). In humans, accumulation of squalene, an intermediate in cholesterol synthesis, is significantly higher in human sebocytes than in other body organs (Smith and Thiboutot, 2008; Zouboulis *et al.*, 2008). Squalene in other organs is converted to lanosterol and finally to cholesterol; the reason for its accumulation in human sebum is presently unknown (Smith and Thiboutot, 2008). Mouse sebum contains fewer triglycerides, diglycerides and free fatty acids (9%) and wax esters (5%), but more cholesterol (13%) (Smith and Thiboutot, 2008). The differences in composition may be due to the specific needs of the animal relating to the environment, *i.e.* waterproofing, temperature, skin exposure to bacteria or UV light (Smith and Thiboutot, 2008).

Free fatty acids in sebum are known to participate in the inflammatory process of acne (Ottaviani *et al.*, 2010; Zouboulis *et al.*, 2014). Sebum linoleic and arachidonic acids can be oxygenated to proinflammatory products by COX-2 (Zouboulis *et al.*, 2014). Arachidonic acid upregulates the proinflammatory cytokines IL-6 and IL-8 in sebocytes, and activates PPARs which regulate lipogenesis (Zouboulis *et al.*, 2014). In HaCaT keratinocytes, lipoxygenase activation by squalene peroxides induce an inflammatory response, increase in IL-6 production and stimulate their proliferation (Ottaviani *et al.*, 2006; Zouboulis *et al.*, 2014).

1.6 Mouse vs. Human Skin

Mouse models are used extensively in toxicology studies. Mice are easy to handle and inexpensive to maintain. Transgenic models of many human diseases exist and provide valuable pathology data. However, some differences between mouse and human skin should be noted.

Human skin is less compliant than thinner mouse skin, an important

consideration in mechanical aspects of wound healing (Garcia *et al.*, 2010; Avci *et al.*, 2013). Mouse skin is covered with thick hair which cycles similarly to humans (anagen, catagen, telogen), however, the mouse hair cycle only lasts approximately 3 weeks, while in humans the cycle in scalp can last several years (Wong *et al.*, 2011; Avci *et al.*, 2013). Epidermal turnover time in the mouse takes approximately 8 – 10 days versus 40-56 days in humans (Potten *et al.*, 1987; Koster, 2009). Rete ridges and dermal papillae found in human skin are absent in mouse skin except during wound healing. Mice also lack apocrine sweat glands. Mouse skin has a panniculus carnosus, a layer of thin muscle which produces rapid wound contraction after injury. After the wound contracts, it is filled by granulation tissue (Greenhalgh, 2005; Avci *et al.*, 2013). In contrast, human skin heals first by re-epithelialization, followed by formation of granulation tissue (Greenhalgh, 2005; Avci *et al.*, 2013). There are also gender differences to consider; the dermis is thicker in males, while the epidermis and hypodermis are thicker in females. Despite these and other differences, mouse models remain an important tool for studying the effects of toxicants on the skin (Wong *et al.*, 2011).

1.7 Keratinocyte Migration & Proliferation in Wounding

Keratinocytes play a major role in the restoration of the epidermal boundary following injury. Re-epithelialization is important in both boundary maintenance and restoration. If the epithelium is inadequately restored, there is risk of infection and wound reoccurrence (Pastar *et al.*, 2014). When the epidermis is breached through wounding, monocytes, neutrophils and macrophages are the first responders, while keratinocytes become activated through expression of growth factors and cytokines (Pastar *et al.*, 2014). The activated phenotype is characterized by expression of K6 and K16, which allows the keratinocytes to migrate and fill in the wound bed (Paladini *et al.*, 1996; Ramot *et al.*, 2013; Pastar *et al.*, 2014).

In order to migrate to the wound site, the KCs must first break their cell-to-cell desmosomal and cell-to-matrix hemidesmosomal contacts (Pastar *et al.*, 2014).

Through activation of protein kinase C α , desmosomes switch from calcium-independent to calcium-dependent, which decreases their adhesive properties (Pastar *et al.*, 2014).

Migrating keratinocytes move in a sheet or tongue; as the sheet moves, the KCs behind the migrating edge begin to proliferate. Growth factors, integrins, keratins, matrix metalloproteinases (MMPs), cytokines and chemokines, and extracellular macromolecules are involved in the proliferation process (Pastar *et al.*, 2014). EGFR, a growth factor, is transactivated by HB-EGF, EGF, and TGF- α which directly stimulate both keratinocyte migration and proliferation, and induce expression of K6 and K16 (Lee *et al.*, 2005; Pastar *et al.*, 2014). MMPs release growth factors from the wound matrix, and can activate growth factors such as IGF-1 (Pastar *et al.*, 2014).

Fibroblast growth factors stimulate epithelialization through paracrine signaling (Pastar *et al.*, 2014). FGF2 (KGF) increases KC proliferation and migration during wound healing by signaling through a KGFR2IIIb receptor exclusive to keratinocytes (Werner *et al.*, 1994; Pastar *et al.*, 2014). TGF β 1 stimulates MMPs, which facilitate KC detachment from the basal lamina and movement through the fibrin and extracellular matrix forming in the wound (Krampert *et al.*, 2004; Pastar *et al.*, 2014). A2 β 1 integrin sustains KC migration on type 1 collagen through MMP-1, which is abundant in wound edges (Pilcher *et al.*, 1999; Pastar *et al.*, 2014). The ratio between MMPs and TIMPs (tissue inhibitors of metalloproteinases) is also important; MMP/TIMP ratio is affected in chronic wounds (Pastar *et al.*, 2014).

Working together, MMPs, the ECM and integrins play an integral role in the proliferation and migration of keratinocytes in acute wounds. Once the wound is fully covered with a layer of keratinocytes and with no drainage, it is considered healed. The

proliferation stage ends and the stratification (differentiation) stage begins (Pastar *et al.*, 2014).

In intact epidermis and acute wounds, mitotically active keratinocytes are only present in the basal layer (Pastar *et al.*, 2014). However, in chronic wounds, mitotically active keratinocytes divide throughout the suprabasal layers (Pastar *et al.*, 2014). Hyperproliferation occurs, marked by the activation and overexpression of c-myc, a nuclear protein involved in cell cycle progression, apoptosis and cellular transformation (McMahon *et al.*, 2000; Pastar *et al.*, 2014). Differentiation and activation pathways are dysregulated resulting in suppression of K1, K10 and filaggrin, and activation of involucrin and transglutaminase 1 (Stojadinovic *et al.*, 2008; Pastar *et al.*, 2014). Hyperkeratosis, a thickening of the cornified layer, and parakeratosis, nuclei present in the stratum corneum, are characteristic of chronic wounds (Stojadinovic *et al.*, 2008; Pastar *et al.*, 2014).

2.0 Sulfur & Nitrogen Mustards

2.1 History & Background

Sulfur mustard (SM), also known as mustard gas (Figure 1), was first synthesized in 1822 by the Belgian, Cesar Mansuete Despretz (Mansour Razavi *et al.*, 2012). Albert Guthrie first characterized its vesicant properties after being exposed while repeating Despretz's experiments in 1860 (Pita and Vidal-Asensi, 2010). In 1886 the German chemist Viktor Meyer synthesized a purer, more toxic form of mustard by reacting thiodiglycol and chlorine (Balali-Mood and Hefazi, 2005; Pita and Vidal-Asensi, 2010). In 1916, German scientists Wilhelm Lommel and Wilhelm Steinkopf developed a process for large-scale production of Meyer's mustard for the German Imperial Army, and the compound was named "LOST", an acronym combining the first two letters of their last names (Pita and Vidal-Asensi, 2010; Mansour Razavi *et al.*, 2012).

Sulfur mustard was first used as a chemical warfare agent in Ypres, Belgium in 1917 (Mansour Razavi *et al.*, 2012). Although subsequently banned by the Geneva Protocol in 1928, the manufacture, stockpiling and deployment of SM continued throughout the 20th century, and was used by Iraq's Saddam Hussein in the Iran-Iraq war (1983-1988) (Mansour Razavi *et al.*, 2012). The terror group ISIS captured the Muthanna State Establishment, the center of Iraqi chemical agent production, where according to a letter to the UN from the Iraqi government, 2,500 chemical rockets remained in the facility and officials witnessed intruders looting equipment before surveillance cameras were shut down (Chivers, 2014). ISIS militants reportedly used sulfur mustard in attacks against Kurdish forces as recently as last August (Starr *et al.*, 2015). In addition, soldiers and civilians alike run the risk of exposure from repurposed weapons used in attacks and abandoned, corroding weapons releasing their contents into the environment (Chivers, 2014).

Nitrogen mustard, a sulfur mustard analog (Figure 1), was originally developed as a chemical warfare agent, however it was unsuitable for battle and never used in war (Korkmaz *et al.*, 2008; Shakarjian *et al.*, 2010). In 1942, Alfred Gilman and Louis Goodman at Yale School of Medicine were studying the effects of mustard exposure (DeVita and Chu, 2008). Medical records of soldiers exposed to SM during WWI indicated they had reduced levels of lymphocytes, leading Goodman and Gilman to hypothesize that mustards could be used to treat lymphoma. After success in a mouse model, they convinced their colleague Gustaf Lindskog to administer their "synthetic lymphocidal chemical", or mustine, to a patient with advanced non-Hodgkins lymphoma (DeVita and Chu, 2008). The treatment reduced the patient's tumor mass and added months to his life. This breakthrough marked the beginning of chemotherapy, and the use of nitrogen mustard (Mechlorethamine, mustine, Mustargen®) as a

chemotherapeutic agent (DeVita and Chu, 2008). Today it is used as a topical treatment for mycosis fungoides, a form of T-cell lymphoma (Lindahl *et al.*, 2013).

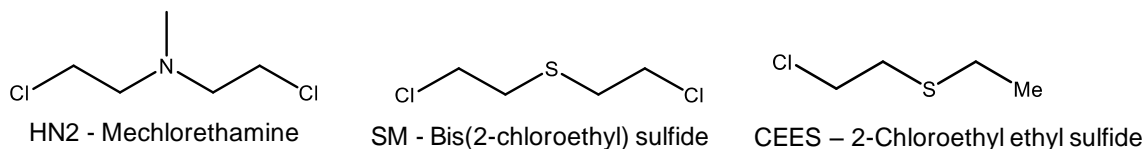


Fig. 1 Structures of NM, SM and CEES

2.2 Mechanism of Mustard Activation

Sulfur mustard is a bifunctional alkylating agent (Shakarjian *et al.*, 2010; Kumar *et al.*, 2015). The first step (in aqueous solution) one of the chloroethyl side chains undergoes a nucleophilic substitution via S_N1 reaction. Chloride is then released and a positively charged ethylsulfonium ring is formed (Figure 2) (Shakarjian *et al.*, 2010). This highly electrophilic intermediate reacts with nucleophilic sites on most cellular macromolecules, including DNA, RNA and proteins (Papirmeister *et al.*, 1985; Kehe *et al.*, 2009a). The remaining chloroethyl side chain cyclizes and can react with another nucleophile, or with water (Shakarjian *et al.*, 2010). In each reaction, one mole of H^+ and Cl^- are released (Shakarjian *et al.*, 2010). SM readily forms adducts with the N7 position of 2-deoxyguanosine residues on DNA, forming inter- and intrastrand crosslinks (Kehe *et al.*, 2009a). It also reacts with carbohydrates, lipids, and amino acid residues in proteins (cysteine, histidine, glutamic and aspartic acids - i.e. sulfhydryl groups, phosphates, ring nitrogens and carboxyl groups) (Laskin *et al.*, 2010; Shakarjian *et al.*, 2010).

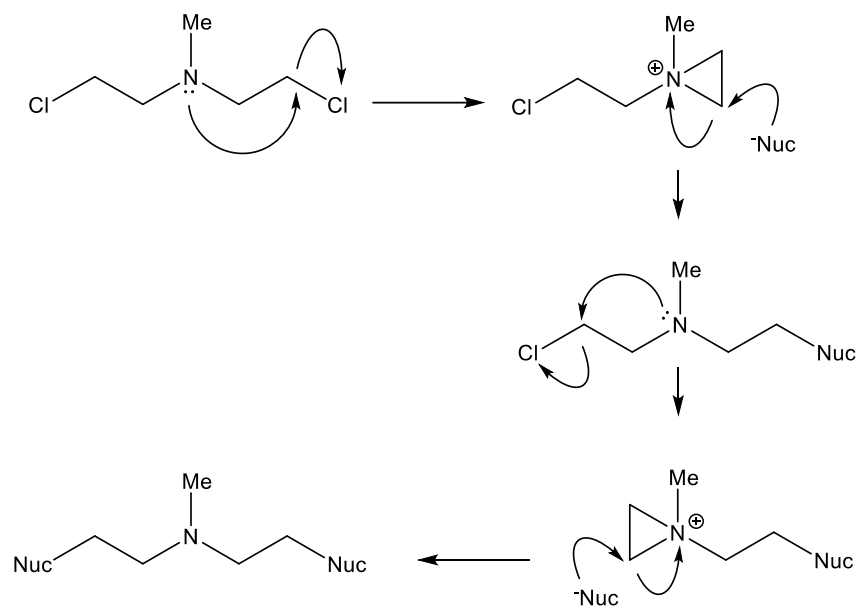


Fig. 2 Mustard Mechanism of Action (NM)

2.3 Vesicant-Induced Skin Injury

Sulfur mustard is an oily liquid soluble in water at a level of only 0.07% at 10°C, but is highly soluble in organic solvents (Balali-Mood and Hefazi, 2005). Because of its low solubility in aqueous media it persists in the environment; most surfaces and objects exposed are contaminated for an extended time. SM is light yellow to dark brown in color, and has a characteristic odor of garlic, onion or mustard (Balali-Mood and Hefazi, 2005).

Exposure to SM can occur through inhalation, absorption through the skin or surface of the eye, or through the gastrointestinal tract after consumption of tainted food (Balali-Mood and Hefazi, 2005). As a liquid or vapor, SM has been reported to penetrate human skin at 1 – 4 mg.cm²/min at 21°C, with greater absorption at increased ambient temperatures (Balali-Mood and Hefazi, 2005). Approximately 80% of liquid SM evaporates; of the 20% absorbed, 12% remains in the skin and 8% enters the circulation (Balali-Mood and Hefazi, 2005). Unhydrolyzed mustard may remain in the stratum

corneum and upper epidermis, which could explain occurrence of secondary blisters as long as 30 days post SM exposure (Kehe *et al.*, 2009a). High doses of SM vapor (1000-10,000 mg. min/m³) or liquid (40-100 mg/cm²) over a long exposure period can cause significant toxicity, however there have been few reports of lethality (Balali-Mood and Hefazi, 2005). The estimated LD₅₀ for humans exposed to liquid SM through the skin is 100 mg/kg (7g/70 kg person) (Poursaleh *et al.*, 2012). A dose of 20 µg/cm² liquid or 4 µg/cm² vapor can produce blisters (Poursaleh *et al.*, 2012). Factors contributing to increased SM toxicity include profuse sweating, greasy skin, and high ambient temperature (Ghabili *et al.*, 2010; Shakarjian *et al.*, 2010). Warm, moist areas covered with thin skin, including the axilla, genitalia and groin are more susceptible to SM-induced injury (Hefazi *et al.*, 2006; Ghabili *et al.*, 2010). In addition to being covered with moisture, these areas tend to contain more hair follicles, leading to better SM penetration (Hefazi *et al.*, 2006; Ghabili *et al.*, 2010).

Skin exposure is usually followed by a dose-dependent latency period (Wattana and Bey, 2009; Ghabili *et al.*, 2010). Two to twenty-four hours post exposure, erythema and itching occur at a threshold dose of 100-300 mg.min/m³ (Kehe *et al.*, 2009j; Ghabili *et al.*, 2010). The appearance of small epidermal vesicles (blisters) within the area of erythema is evident after 4-18 hours (Ghabili *et al.*, 2010; Shakarjian *et al.*, 2010). Rubbing the area can induce more blistering, indicating damage to the basal membrane (Kehe *et al.*, 2009j; Ghabili *et al.*, 2010). The blisters increase in size and number, then coalesce to form pendulous bullae filled with a clear, yellow fluid (Balali-Mood and Hefazi, 2005; Kehe *et al.*, 2009j). Approximately 48 hours post-exposure, larger blisters rupture leading to full-thickness skin loss, erosions, and ulceration (Balali-Mood and Hefazi, 2005; Ghabili *et al.*, 2010). A necrotic layer or eschar forms at 72 hours which sloughs by 4 – 6 days, succeeded by a pigmented scar after 3 weeks (Balali-Mood and Hefazi, 2005; Ghabili *et al.*, 2010). In a low-dose exposure, the erythematous skin

region becomes hyperpigmented within 2 weeks then desquamates with no other effect (Graham *et al.*, 2005; Ghabili *et al.*, 2010). However, high-dose exposures can be very painful and full-thickness regions of skin can be lost (Ghabili *et al.*, 2010). In cases of severe injury, the blisters heal in 2 – 3 weeks, full-thickness erosions after 6 – 12 weeks (Balali-Mood *et al.*, 2005; Ghabili *et al.*, 2010). Hypopigmentation is often visible in the healed area, while hyperpigmentation can be observed within the region of damaged cells surrounding the original wound (Balali-Mood and Hefazi, 2005; Ghabili *et al.*, 2010). Hyper- and hypo-pigmentation can persist for months or years, along with scarring (Ghabili *et al.*, 2010; Poursaleh *et al.*, 2012). Vesicant-induced burn injuries generally heal slower than thermal burns (Balali-Mood and Hefazi, 2005), and in large wounds this delay can be much longer than for a thermal burn of equivalent area (Rice, 2003; Balali-Mood and Hefazi, 2005).

Chronic effects of vesicant-induced injury can persist years after the first exposure (Balali-Mood *et al.*, 2005; Graham *et al.*, 2005; Dachir *et al.*, 2012). In a study on 34,000 Iranians 13 – 20 years post-SM exposure, 24.5% of the complications were found on skin (Khateri *et al.*, 2003). In another study by Balali-Mood *et al.*, 2005, toxic effects of SM poisoning were reported in a group of 40 Iraqi veterans 16 – 20 years post exposure, in which 75% had persistent effects in skin (Balali-Mood *et al.*, 2005). Hyperpigmentation and xerosis were the two most common findings (Balali-Mood *et al.*, 2005). In cases of xerosis, the individuals complained of itching, a burning sensation, and scaly skin (Khateri *et al.*, 2003; Hefazi *et al.*, 2006; Ghabili *et al.*, 2010). Other complications included seborrheic dermatitis, psoriasis, discoid lupus erythematosus, eczema, and keratosis pilaris (Khateri *et al.*, 2003; Hefazi *et al.*, 2006; Ghabili *et al.*, 2010).

2.4 Histopathological effects

During the erythematous phase of injury, nuclear swelling, chromatin dispersion, and cytoplasmic vacuole formation are observed in a few scattered basal keratinocytes in the epidermis (Kehe *et al.*, 2009a). Over time, increased numbers of basal keratinocytes are affected; pyknotic nuclei are observed followed by fragmentation of the cytoplasmic membrane. Regions of necrotic cells appear at the epidermal-dermal junction, which coalesce to form microblisters and eventually bullae (Kehe *et al.*, 2009a). Cases have been reported where bullae did not form and necrosis involved the full-thickness of the epidermis (Shakarjian *et al.*, 2010). Hyperemia can occur during the erythematous phase at low doses, but at higher doses, more damage to capillaries is noted. Inflammatory cells are also present in cases of SM-induced injury, mononuclear cells appearing first followed by neutrophils before vesication occurs (Shakarjian *et al.*, 2010).

Previous studies have shown that the dermal appendages, including pilosebaceous units, are targets for NM and SM-induced injury (Haslam *et al.*, 2013; Joseph *et al.*, 2014). In 14-day time course experiments where mice were exposed to SM using a vapor cup model, loss of outer root sheath cells from the infundibulum to the root bulb were observed along with morphological changes as early as one-day post exposure (Joseph *et al.*, 2014). Karyolysis occurred in cells of the outer root sheath and interfollicular epidermis (Joseph *et al.*, 2014). Over time, the hair follicles degraded and by 14 days, only follicular cysts remained in the wound region (Joseph *et al.*, 2014). In sebaceous glands, degenerative changes in sebocytes were found from days 3-7. The number of intact sebocytes decreased over the time course; by day 14 none were observed in the wound area (Joseph *et al.*, 2014). Xerotic, flaky skin was apparent in the wound, consistent with earlier studies in guinea pigs and previous observations in human skin (Benson *et al.*, 2011; Firooz *et al.*, 2011; Tewari-Singh *et al.*, 2013).

3.0 Mechanisms of Vesicant Toxicity in Skin

3.1 Oxidative Stress

SM has been reported to produce oxidative and electrophilic stress in skin (Shakarjian *et al.*, 2010). Under normal conditions, glutathione (GSH), a nucleophilic antioxidant, protects against the effects of reactive oxygen species (ROS) and electrophiles by maintaining a net reducing environment in the cell (Laskin *et al.*, 2010; Shakarjian *et al.*, 2010). Oxidative stress occurs after injury when an imbalance occurs between the generation of ROS and their detoxification (Khansari *et al.*, 2009; Laskin *et al.*, 2010). Markedly reduced GSH levels are observed in cells treated with SM and related vesicants, leading to increases in intracellular ROS and formation of DNA oxidation products, a marker of oxidative stress (Kehe *et al.*, 2009a; Laskin *et al.*, 2010). DNA base oxidation, lipid peroxidation and protein oxidation are all examples of oxidative damage mechanisms (Naghii, 2002; Khansari *et al.*, 2009). Biomarkers of ROS exposure in the skin include increased dermal protein oxidation, formation of DNA oxidation product 8-oxo-2-deoxyguanosine, and 4-hydroxynonenal adducts, a marker of lipid peroxidation (Naghii, 2002). Application of CEES, an SM derivative, to mouse skin has been reported to cause oxidative stress by formation of protein and DNA oxidation products, protein radical adducts, and 4-hydroxynonenal protein adducts (Pal *et al.*, 2009a). CEES-treatment in a human skin construct model has been reported to induce hydrogen peroxide production in the keratinocytes, and carbonyl protein adduct formation (Black *et al.*, 2010b). ROS can also be generated by mitochondria as a byproduct of electron transport (Laskin *et al.*, 2010; Shakarjian *et al.*, 2010). These ROS regulate cell death processes including apoptosis (programmed cell death) and autophagy, a process to eliminate damaged organelles from a cell (Laskin *et al.*, 2010).

SM can inactivate ROS-scavenging antioxidant proteins, i.e. thioredoxin reductase, further contributing to an oxidative state in cells (Laskin *et al.*, 2010;

Poursaleh *et al.*, 2012). Interestingly, thioredoxin reductase is also a mediator of redox cycling, a process responsible for creation of anion radicals from various quinones and flavonoids, which can increase oxidative stress (Jan *et al.*, 2010).

Infiltrating macrophages and neutrophils observed in the skin as a response to SM contribute to oxidative stress by generating ROS during a respiratory burst and releasing nitric oxide (Laskin *et al.*, 2010; Shakarjian *et al.*, 2010). Leukocyte infiltration to the papillary dermis and epidermis has been observed in mice (Wormser *et al.*, 2004). An increase in myeloperoxidase, an enzyme that produces the toxic mediators hypochlorous acid and chloride anion and is an indicator of neutrophil influx, has been reported after vesicant treatment (Laskin *et al.*, 2010; Shakarjian *et al.*, 2010).

3.2 Proinflammatory Cytokines

A number of cytokines have been reported to participate in the recruitment and activation of inflammatory cells at sites of injury (Ricketts *et al.*, 2000; Sabourin *et al.*, 2000; Shakarjian *et al.*, 2010). In earlier studies using the mouse ear vesicant model (MEVM), elevated levels of IL-1 β , IL-6, GM-CSF (granulocyte monocyte-colony stimulating factor) and TNF- α were observed as early as 6 hours post exposure (Ricketts *et al.*, 2000; Sabourin *et al.*, 2000; Wormser *et al.*, 2005). In mouse dorsal skin, increases in IL-1 α , IL-1 β , MCP-1, MIP-2 and TNF- α mRNA were detected (Ricketts *et al.*, 2000; Sabourin *et al.*, 2000; Shakarjian *et al.*, 2010). In normal human epidermal keratinocytes (NHEKs), 100-300 μ M SM stimulated the release of IL-1 β , IL-6, IL-8 and TNF- α (Shakarjian *et al.*, 2010). The detection of elevated levels of signaling molecules controlling cytokine expression, including the transcription factors nuclear factor kappa B (NF- κ B) and activator protein 1 (AP-1), was reported after vesicant exposure (Rebholz *et al.*, 2008; Pal *et al.*, 2009a).

3.3 Pro-Inflammatory Mediators

The pro-inflammatory mediator arachidonic acid, along with products of its metabolism by COX and LOX, have been identified in skin post SM exposure and have been reported to play a role in vesicant-induced cutaneous injury (Wormser *et al.*, 2004; Shakarjian *et al.*, 2010). Cyclooxygenases (COX-1/2) are the rate-limiting enzymes in prostaglandin synthesis from arachidonic acid (Vane, 1998). Arachidonic acid is first oxidized to the hydroperoxy endoperoxide (PGG₂) then reduced to the hydroxy endoperoxide PGH₂. PGH₂ is metabolized to the primary prostanoids PGE₂, PGF_{2α}, PGD₂, PGI₂ AND TXA₂ (Vane, 1998; Williams *et al.*, 1999). COX-1 is constitutive, while COX-2 is inducible (Vane, 1998; Futagami *et al.*, 2002). COX-2 inducers include inflammation-associated cytokines such as IL-1, IL-2 and TNFα, and bacterial lipopolysaccharide (LPS). Both COX isoforms have been detected in keratinocytes, but with differential roles during wound healing and inflammation (Kampfer *et al.*, 2003; Goren *et al.*, 2015). Selective inhibition of COX-1 revealed its necessity for skin wound repair; however, COX-2 expression was associated with impaired re-epithelialization, ECM formation, angiogenesis and myofibroblast differentiation (Futagami *et al.*, 2002; Kampfer *et al.*, 2005). COX-2 has been identified in mouse skin after SM treatment, while in a skin construct model, CEES treatment increased expression of COX-2 mRNA and protein (Nyska *et al.*, 2001; Black *et al.*, 2010b). Treatment with non-steroidal anti-inflammatories (NSAIDs) reduced skin injury, suggesting these mediators contribute to SM toxicity (Babin *et al.*, 2000). In addition, COX-2^(-/-) mice or wild-type mice treated with COX-2 specific inhibitor celecoxib showed markedly reduced ear swelling after treatment with SM (Wormser *et al.*, 2004).

In previous studies by our group, CEES treatment of keratinocytes in a human skin construct model increased mRNA expression of microsomal prostaglandin E synthase-2 (mPGES-2) and prostaglandin D synthase (PGDS), prostanoid synthases

downstream of COX-2 responsible for PGE₂ and PGD₂ generation. PGE₂ is known to mediate skin inflammation and edema (Murakami *et al.*, 2002) and SM has been reported to stimulate PGE₂ production in full-thickness human skin explants and intact mouse skin (Rikimaru *et al.*, 1991; Dachir *et al.*, 2002). CEES treatment also increased expression of 5-lipoxygenase (5-LOX), leukotriene A₄ (LTA₄) hydrolase and LTC₄ synthase, responsible for synthesis of LTB₄ and LTC₄ (Black *et al.*, 2010b). CEES also activated JNK and p38 MAP kinases, regulators of antioxidant enzymes and prostaglandin and leukotriene synthase expression, in keratinocytes (Black *et al.*, 2010b; Zheng *et al.*, 2013). Inhibition of these kinases suppressed expression of GSTA1-2, COX-2, mPGES-2, PGDS, 5-LOX, LTA₄ hydrolase and LTC₄ synthase, as well as PGDS and GSTP1 (Black *et al.*, 2010b). These data showed that the half-mustard CEES modulates expression of enzymes responsible for production of inflammatory mediators, as well as antioxidants.

3.4 Apoptosis & Terminal Differentiation

Blisters formed after SM exposure result from detachment of the epidermis from the dermis at the basal membrane (Rosenthal *et al.*, 1998). Toxicity to basal cells includes apoptosis and induction of terminal differentiation (Rosenthal *et al.*, 1998).

Apoptosis of keratinocytes in the epidermis and dermal appendages is a well-known effect of vesicant exposure, and occurs through both intrinsic and extrinsic pathways (Kehe *et al.*, 2009a; Balszuweit *et al.*, 2014; Joseph *et al.*, 2014). Apoptosis via the intrinsic pathway involves mitochondrial swelling and alkylation of mitochondrial DNA, toxic effects of SM exposure (Ray *et al.*, 1995; Brown and Rice, 1997). Pro-apoptotic signals from Bcl-2 family proteins like Bax and Bak induce mitochondrial membrane permeability and release of apoptotic death promoting factors, including cytochrome *c* (Sourdeval *et al.*, 2006). The pro-apoptotic Bcl-2 member Bad can displace Bax from binding to Bcl-2 and Bcl-x1, promoting apoptosis, an effect prevented

by Bad phosphorylation (Sourdeval *et al.*, 2006). However, SM induces Bad dephosphorylation, promoting apoptosis through the calmodulin pathway (Simbulan-Rosenthal *et al.*, 2006).

Expression of Fas receptor and Fas ligand (FasL), activators of the extrinsic apoptosis pathway, is upregulated after vesicant exposure (Thorburn, 2004; Kehe *et al.*, 2009a). SM exposure leads to stabilization of intracellular p53, increasing Fas receptor and FasL expression in human keratinocytes (Rosenthal *et al.*, 2003). SM also activates caspase-8, recruitment of (Fas associated protein with death domain) FADD and subsequent activation of executioner caspases -3, -6, and -7 (Rosenthal *et al.*, 2003). SM treated keratinocytes also express increased TNF- α , another Fas/TFNR ligand, whose binding to p55 TNF receptor induces apoptosis (Arroyo *et al.*, 2004).

The nuclear protein poly (ADP-ribose) polymerase (PARP) plays a role in vesicant-induced apoptosis (Rosenthal *et al.*, 1998). After low-dose exposure to SM, caspase-3 cleaves the nuclear protein poly (ADP-ribose) polymerase (PARP)-1, which halts PARP activity and ATP consumption (Soldani and Scovassi, 2002). However, high exposure levels of SM induce DNA strand breakage and overactivate PARP, depleting levels of cellular nicotinamide adenine dinucleotide (NAD⁺) (Rosenthal *et al.*, 1998). Increased metabolism to restore NAD⁺ levels decreases intracellular adenosine triphosphate (ATP), and may result in necrotic cell death (Kehe *et al.*, 2009a). PARP activation by lower SM doses can elevate intracellular levels of free Ca²⁺ in keratinocytes, playing a role in apoptosis induction (Rosenthal *et al.*, 1998). One apoptosis mechanism involves protein tyrosine kinases activation by SM, leading to phospholipase C activation, formation of IP3 and Ca²⁺ release (Takata *et al.*, 1995). Another suggested mechanism involves SM-generated ROS, which damage endoplasmic reticulum, mitochondrial, and plasma membrane Ca²⁺ transport systems

(Takata *et al.*, 1995). Perturbation of Ca^{2+} homeostasis and prolonged increase in Ca^{2+} results (Orrenius *et al.*, 1989).

In addition to apoptosis, increased intracellular calcium levels induce terminal differentiation in skin (Li *et al.*, 1995; Bikle *et al.*, 2012; Tu *et al.*, 2012). In NHEK, SM upregulates keratin 1, involucrin and loricrin expression, suggesting induction of premature differentiation (Rosenthal *et al.*, 1998; Popp *et al.*, 2011). In addition, SM exposure increases phosphorylation, nuclear translocation and activity of p38 and ERK1/2 (Popp *et al.*, 2011). While inhibition of p38 downregulates K1 and loricrin, inhibition of ERK1/2 upregulates them, indicating opposing roles for these kinases during differentiation (Popp *et al.*, 2011). These results agree with an earlier study in an impaired wound healing model in mice, where p38 inhibition improved wound contraction, formation of granulation tissue and re-epithelialization (Medicherla *et al.*, 2009). In addition, exposure to SM and CEES has been reported to upregulate both K10, a differentiation marker, and K6, a marker of epithelial wound repair and cell migration (Black *et al.*, 2010a; Chang *et al.*, 2014).

4.0 Endocannabinoid System

4.1 Endocannabinoids

Endocannabinoids act as lipid signaling mediators and are found throughout the body, where they are responsible for diverse biological effects (Maccarrone *et al.*, 2010; Fezza *et al.*, 2014). They are amides, esters and ethers of polyunsaturated fatty acids (PUFAs) (Kendall and Nicolaou, 2013; Fezza *et al.*, 2014). The endocannabinoid system is comprised mainly of the two endocannabinoids, anandamide (AEA) and 2-arachidonoylglycerol (2-AG); two classical cannabinoid (CB) receptors; enzymes responsible for endocannabinoid catabolism: fatty acid amide hydrolase (FAAH) and

monoacylglycerol lipase (MAGL); and synthesis: N-acyltransferase (NAT), N-acylphosphatidylethanolamine-phospholipase D (NAPE-PLD) (Pertwee, 2014).

Anandamide (AEA) and 2-arachidonoyl glycerol (2-AG) are the main endogenous agonists of the cannabinoid receptors. These lipids are not stored in vesicles, but are synthesized on-demand and interact with hydrophobic moieties including phospholipid domains and serum albumin (Nicolussi and Gertsch, 2015). Effects of endocannabinoid signaling mimic pharmacological effects of Δ^9 -tetrahydrocannabinol (THC), the active component of marijuana and hashish, whose benefits include pain relief and reduction of inflammation (Pertwee, 2014; Turcotte *et al.*, 2015). Other *N*-acylethanolamines have been reported to bind and signal through CB receptors: N-palmitoylethanolamine (PEA) and N-oleoylethanolamine (OEA), both of which reduce inflammation and edema in *in vivo* models (Sun *et al.*, 2006; Petrosino *et al.*, 2010). AEA, PEA and OEA also bind to peroxisome proliferator activator receptors (PPARs) (Sun *et al.*, 2006; O'Sullivan and Kendall, 2010).

4.2 Biosynthesis, Transport & Metabolism of Anandamide

AEA and other *N*-acylethanolamines are synthesized from the lipid membrane precursor *N*-acylphosphatidylethanolamines (NAPEs) in response to an increase in intracellular Ca^{2+} concentrations from processes such as cell depolarization, or mobilization of intracellular Ca^{2+} stores (Maccarrone *et al.*, 2010; Fezza *et al.*, 2014). NAPEs are synthesized by Ca^{2+} -dependent or –independent *N*-acyltransferases (NAT), which catalyze the transfer of an acyl moiety from phosphatidylcholine to the head group of phosphatidylethanolamine (Maccarrone *et al.*, 2010; Fezza *et al.*, 2014). Different NAE precursors are generated depending on which fatty acid is transferred to the head group of PE, palmitic acid and arachidonic acid result in PEA and AEA precursors, respectively (Maccarrone *et al.*, 2010; Kendall and Nicolaou, 2013). Several routes of NAE synthesis from NAPEs have been reported. *N*-acylphosphatidylethanolamine

phospholipase D (NAPE-PLD) releases NAE from NAPE. Another mechanism involves phospholipase C (PLC) generation of phospho-*N*-acylethanolamine (P-NAE), with subsequent phosphate group removal by a protein tyrosine phosphatase (i.e. PTPN22). The NAE-synthesis intermediate lyso-NAPE can be generated by elimination of one acyl chain from NAPE by the α/β hydrolase domain 4 (ABDH4). Lyso-NAPE can either be hydrolyzed to NAE by lyso-phospholipase D (lyso-PLD), or to glycerophospho-*N*-acylethanolamine (GP-NAE) by ABDH4. In the case of GP-NAE, glycerophosphodiesterase GDE1 then converts GP-NAE to NAE (Maccarrone *et al.*, 2010; Fezza *et al.*, 2014).

AEA is lipophilic, acting either as an autocrine or paracrine messenger near its site of production (Maccarrone *et al.*, 2010). Binding of AEA triggers activation of non-selective ion channels and protein kinases, and increases in intracellular Ca^{2+} concentration followed by mitochondrial uncoupling and cytochrome c release (Maccarrone *et al.*, 2010; Fonseca *et al.*, 2013). AEA is a partial agonist at both CB receptors (Pertwee *et al.*, 2010; Fonseca *et al.*, 2013). Similar to THC, AEA has lower affinity for CB2 than CB1 (Pertwee *et al.*, 2010; Fonseca *et al.*, 2013). Additional targets of AEA include the intracellular TRPV-1 receptor and the nuclear PPARs (Maccarrone *et al.*, 2010; De Petrocellis *et al.*, 2011). AEA activates CB receptors at concentrations in the low micromolar/nanomolar range, TRPV-1 in the low micromolar and PPARs in the high micromolar ranges (Howlett *et al.*, 2010; Maccarrone *et al.*, 2010; Pertwee *et al.*, 2010; De Petrocellis *et al.*, 2011).

Alternative models for the mechanism of uptake and transport of AEA have been proposed, including passive diffusion assisted by formation of AEA-cholesterol complexes, simple diffusion facilitated by FAAH activity, facilitated transport across the plasma membrane followed by carrier-mediated intracellular transport, and endocytosis involving caveolae (Di Pasquale *et al.*, 2009; Yates and Barker, 2009; Nicolussi and

Gertsch, 2015). Experimental evidence also exists for an anandamide membrane transporter (AMT), however it has not yet been cloned (Nicolussi and Gertsch, 2015). Another hypothesis proposes that adiposomes act as shuttles for AEA transport as well as sites for AEA catabolism (Maccarrone *et al.*, 2010).

After synthesis and transport, AEA is rapidly hydrolyzed into arachidonic acid (AA) and ethanolamine, primarily by the membrane-bound enzyme fatty acid amide hydrolase (FAAH) (Cravatt *et al.*, 2001; Di Marzo and Petrosino, 2007). Elevated brain levels of endogenous AEA, as well as PEA and OEA have been reported in FAAH knockout mice and in mice treated with URB597 or JNJ-40355003, specific FAAH inhibitors (Cravatt *et al.*, 2001; Fegley *et al.*, 2005; Keith *et al.*, 2012).

Two isoforms of FAAH have been identified, FAAH-1 present in both humans and rodents, and FAAH-2, found mainly in higher placental mammals including most primates, but excluding many lower placental mammals including rodents (Wei *et al.*, 2006; Maccarrone *et al.*, 2010; Keith *et al.*, 2012). FAAH-2 shares 20% sequence homology with FAAH-1 and hydrolyzes fatty acid amide substrates at equivalent rates, although FAAH-1 is more active with *N*-acylethanolamine substrates such as AEA (Wei *et al.*, 2006; Keith *et al.*, 2012). AEA can also be metabolized by lysosomal *N*-acylethanolamine-hydrolyzing acid amidase (NAAA), although this enzyme has greater affinity for PEA (Maccarrone *et al.*, 2010; Tai *et al.*, 2012).

AEA can be oxygenated to arachidonic acid by COX-2, LOX and several CYP450 isoforms in a similar mechanism (Maccarrone *et al.*, 2010; Turcotte *et al.*, 2015). COX-2 metabolizes AEA into the prostaglandin ethanolamides (prostamides) PGG₂-EA, PGH₂-EA, PGD₂-EA, PGE₂-EA, PGF_{2α}-EA, and PGI₂-EA (Yu *et al.*, 1997; Kozak *et al.*, 2002; Turcotte *et al.*, 2015). *In vivo*, FAAH knockout mice produce PGD₂-EA, PGE₂-EA, PGF_{2α}-EA after treatment with 50 mg/kg anandamide, the dose required to observe behavioral effects (Weber *et al.*, 2004). PG-EAs are weaker activators of

CB1, CB2 and PG receptors than AEA (Berglund *et al.*, 1999; Woodward *et al.*, 2003). They can directly activate PPAR γ and prostaglandin E₂ receptors, and studies suggest a specific PG-EA receptor (Woodward *et al.*, 2008). PGF_{2 α} -EA has an identical pharmacological profile to the PGF_{2 α} analog bimatoprost, an ocular hypotensive drug used to treat glaucoma, which also exerts hypertrichotic effects in murine hair follicles (Woodward *et al.*, 2003; Woodward *et al.*, 2013; Fezza *et al.*, 2014).

In mammals, arachidonic acid and AEA are metabolized by 5-, 12-, and 15-LOX enzymes (Turcotte *et al.*, 2015). Oxidation of AEA by 12- and 15-LOX leads to the biosynthesis of 12(S)- and 15(S)-hydroperoxyeicosatetraenyl-EA (12- and 15-HpETE-EA), which are then reduced to their hydroxyl derivatives (12- and 15-HETE-EA) (Turcotte *et al.*, 2015). These mediators bind and exert their effects primarily through vanilloid receptors, although 12-HETE-EA binds minimally to CB1 (Turcotte *et al.*, 2015).

CYP450 metabolites of AEA include 20-HETE-EA, and 5,6-, 8,9-, 11,12-, and 14,15-epoxyeicosatetraenoic (EET-EA). EET-EAs and HETE-EAs bind to CB1 and CB2 receptors with different affinities than AEA (Zelasko *et al.*, 2015). 5,6-EET-EA binds to CB2 with 1000-fold greater affinity than AEA and also degrades more slowly, so it may have more potential to react at CB2 (Snider *et al.*, 2009; Zelasko *et al.*, 2015). 5,6-EET-EA binds CB2 with a 300-fold higher affinity than CB1 (8.9 nM vs. 3.2 μ M), indicating that CYP oxidation may play a more prominent role in CB2 activation than AEA (Snider *et al.*, 2009; Zelasko *et al.*, 2015). The 14,15-EET-EA and 20-HETE-EA have shorter half-lives and bind CB1 with a lower affinity than AEA, and may be less potent at this receptor (Sridar *et al.*, 2011; Zelasko *et al.*, 2015).

4.3 Palmitoylethanolamine

PEA is an endogenous anti-inflammatory lipid member of the *N*-acylethanolamine family produced by most mammalian cells (Petrosino *et al.*, 2010). PEA is synthesized from the phospholipid precursor *N*-palmitoyl-

phosphatidylethanolamine and inactivated by both fatty acid amide hydrolase (FAAH) and *N*-acyl-ethanolamine-hydrolyzing acid amidase (NAAA) to palmitic acid and ethanolamine (Petrosino *et al.*, 2010). Several hypotheses have been suggested to explain the anti-inflammatory and analgesic effects of PEA (Petrosino *et al.*, 2010). It may downregulate degranulation of mast cells, directly stimulate CB2 or a CB2-like receptor (Petrosino *et al.*, 2010). Other studies suggest PEA may participate in an entourage effect by enhancing the effects of AEA at CB1, CB2 or TRPV-1 receptors, by either inhibiting FAAH expression or allosterically stimulating TRPV-1 receptors (Di Marzo *et al.*, 2001; Ho *et al.*, 2008). Finally, anti-inflammatory and analgesic effects were observed through PEA binding to PPAR α (LoVerme *et al.*, 2006).

4.4 Endocannabinoid Receptors

CB1 and CB2 are considered the classical CB receptors, both of which bind AEA and 2-AG but with different affinities (Pertwee *et al.*, 2010). Matsuda *et al.* cloned CB1 from rat brain cortex in 1990, and determined it was responsible for the pharmacological effects of Δ^9 -THC, the main psychoactive compound in *cannabis* (Matsuda *et al.*, 1990). Human and rat cDNA CB1 analogs were subsequently cloned, and although the two had different amino acid chain lengths (rat 473 and human 327 amino acids), their sequence homology was 97 – 99% (Howlett, 2002). CB2 was identified in and cloned from human promyelocytic leukemic HL60 cells (Munro *et al.*, 1993). This receptor was only 360 amino acids in length, and had only 40% homology with CB1 (Brown *et al.*, 2013).

Activation of CB receptors inhibits adenylate cyclase activity and activates MAPK by signal transduction through G_{i/o} proteins, as evidenced by their sensitivity to pertussis toxin (Howlett, 2005; Pertwee *et al.*, 2010). In addition, CB receptor signaling can modulate ERK1/2 and PI3K/Akt signaling pathways (Maccarrone *et al.*, 2003; Jia *et al.*, 2006; Ozaita *et al.*, 2007). CB1 is coupled through G_{i/o} proteins to ion channels; positively to A-type and inward rectifying potassium channels, and negatively to N- and

P/Q-type calcium channels (Howlett, 2002; Pertwee, 2005; Pertwee *et al.*, 2010). CB1 can also activate adenylyl cyclase by coupling to G_s proteins; however, the signaling mechanisms have not been fully elucidated and may involve cross talk between CB1 and non-CB receptors, or two subpopulations of CB1, one signaling through $G_{i/o}$ and another through G_s (Calandra *et al.*, 1999; Pertwee *et al.*, 2010). CB2 modulates Ca^{2+} channels less than CB1, but also promotes MAPK activation (Pacher and Mechoulam, 2011).

Four major agonist classes for the CB receptors are: classical CBs, structurally similar to and including Δ^9 -THC and the synthetic (-)-11-hydroxy- Δ^8 -THC-dimethylheptyl (HU-210) (Slipetz *et al.*, 1995; Song and Bonner, 1996); non-classical CBs, including CP55940, a full agonist at both CB receptors (Brown *et al.*, 2013; Deng *et al.*, 2015); aminoalkylindoles, including WIN 55,212-2, a potent and effective agonist at both CB receptors used extensively in CB receptor research; and the endocannabinoids, including AEA and 2-AG (Brown *et al.*, 2013). Synthetic analogs of AEA which selectively activate CB1 include R-(+)-methanandamide-arachidonoyl-2'-chloroethylamide (ACEA) and arachidonoylcyclopropylamide (ACPA); and of 2-AG, noladin ether (Pertwee, 2010). Selective synthetic CB2 activators include JWH-133, a classical (retains natural cannabinoid ring structures and oxygens) CB; HU-308, a non-classical CB and JWH-015 and AM1241, aminoalkylindoles (Pertwee, 2010).

CB1 receptors are abundant in CNS neurons, and can be found in liver, adipose tissue, vascular tissue, cardiomyocytes, reproductive tissue, immune cells, bone and skin (Howlett *et al.*, 2010). CB2 receptors were once thought to be found primarily in the immune system, however later studies revealed possible roles in mobilization of hematopoietic stem and progenitor stem cells; and they have been detected at low levels in bone, myocardium or cardiomyocytes, human vascular smooth muscle cells, activated hepatic stellate cells, mouse and human exo- and endocrine pancreas,

endothelial cells, reproductive organs and cells, the skin and in some human tumors (Pacher and Mechoulam, 2011). They can also be found in some regions of the brain, spinal cord and dorsal root ganglia, neurons of the myenteric and submucosal plexus of the enteric nervous system, and in activated microglia (Pacher and Mechoulam, 2011). CB2 receptor expression can be markedly upregulated in some pathological/disease states, accompanied by increased endocannabinoid levels as part of the inflammatory response (Pacher and Mechoulam, 2011).

4.5 Involvement of Non-Classical Receptors with Endocannabinoid System

a. Peroxisome proliferator-activated Receptor (PPAR α)

PPAR α is a member of the PPAR nuclear receptor family. PPARs form heterodimers with the retinoid X receptor (RXR) then bind the PPAR response element (PPRE), a specific DNA element to activate gene transcription (Straus and Glass, 2007). PPAR α activation regulates the transcription of enzymes controlling β -oxidation, mitochondrial β -oxidation, activation of fatty acids to acyl-CoA derivatives, microsomal ω -oxidation, ketogenesis and lipoprotein metabolism (Sertznig *et al.*, 2008). Active synthesis of cholesterol and fatty acids occurs in the epidermis, and PPAR α activation by these ligands induces keratinocyte differentiation, inhibits inflammation, and improves permeability barrier function (Schmuth *et al.*, 2004). Endogenous PPAR α ligands also include LTB₄ and 8-HETE, the anti-inflammatory omega-3 fatty acids docosahexaenoic acid (DHA) and eicosapentaenoic acid (EPA), along with the endocannabinoids AEA, PEA and OEA (Straus and Glass, 2007; Grygiel-Gorniak, 2014). Synthetic ligands include fibrates (i.e. fenofibrate, clofibrate), gemfibrozil, GW7647, and Wy14643 (Straus and Glass, 2007). PPAR α is also activated by the NSAIDs indomethacin and ibuprofen (Lehmann *et al.*, 1997). PPAR α has been called the PEA receptor; PEA directly activates PPAR α with an EC₅₀ of approximately 3 μ M (Lo Verme *et al.*, 2005). Unlike the

structurally analogous OEA, it does not activate PPAR β/γ . Anti-inflammatory effects of PEA signaling through PPAR α include reduced expression of iNOS, COX-2, and TNF α (Lo Verme *et al.*, 2005; D'Agostino *et al.*, 2009).

In the rodent and human skin, PPAR α is expressed in keratinocytes, dermal cells, sebaceous glands and Langerhans cells (Hanley *et al.*, 1998; Michalik *et al.*, 2001; Dubrac and Schmuth, 2011). Macrophages and T-cells found in skin also express PPAR α (Cunard *et al.*, 2002; Babaev *et al.*, 2007; Dubrac and Schmuth, 2011).

b. Transient receptor potential vanilloid receptor-1 (TRPV-1)

TRPV-1 is a cation channel predominantly expressed in sensory neurons, hepatocytes and pancreatic cells, epithelial, endothelial, and smooth muscle cells, as well as lymphocytes (Brown *et al.*, 2013). In the skin, it is found on human epidermal and hair follicle keratinocytes, dermal mast cells, Langerhans cells and sebocytes (Stander *et al.*, 2005; Biro *et al.*, 2009; Toth *et al.*, 2011a). It was first cloned as a receptor for capsaicin, the vanilloid ingredient in hot chili peppers (Toth *et al.*, 2011a). Its expression is modulated by a number of inflammatory skin conditions, including psoriasis, allergic contact and atopic dermatitis, UV exposure and mastocytosis (Toth *et al.*, 2011a). TRPV-1 is activated by protons (pH<5.9), increased temperatures (T>42°C), and anandamide and some of its analogs (Toth *et al.*, 2011a; Brown *et al.*, 2013).

c. GPR55

Studies have indicated some cannabinoid signaling is mediated neither by CB1 nor CB2, and that other receptors may be involved (Pertwee, 2010; Brown *et al.*, 2013; Yamashita *et al.*, 2013). Several studies have suggested that GPR55, an orphan GPCR sometimes referred to as CB3, may indeed be a cannabinoid receptor (Ryberg *et al.*, 2007; Yamashita *et al.*, 2013). It is widely expressed throughout the human body, and has also been detected in murine epidermis where it supports keratinocyte proliferation

(Andradas *et al.*, 2011; Perez-Gomez *et al.*, 2013). Structurally it is unrelated to either cannabinoid receptor; it has low sequence identity to both CB1 (13.5%) and CB2 (14.4%), and lacks the cannabinoid binding pocket typical to both CB receptors (Petitet *et al.*, 2006). GPR55 is a member of the non-Edg P2Y receptor family, which includes receptors for lysophospholipids (i.e. LPA, lyso-PS). LPI binding rapidly increased both the phosphorylation of ERK and intracellular Ca^{2+} levels, indicating it is an LPI receptor (Andradas *et al.*, 2011; Yamashita *et al.*, 2013). The highest biological activity ($\text{EC}_{50} = 30 \text{ nM}$) was observed with 2-arachidonoyl LPI (Yamashita *et al.*, 2013). GPR55 has been reported to be activated by cannabinoids such as THC, or the endocannabinoids AEA and 2-AG (Yamashita *et al.*, 2013). However, because of conflicting data on its effects in ERK1/2 phosphorylation, GTP γ S binding and calcium mobilization, it has not been included as a member of the cannabinoid receptor family (Brown *et al.*, 2013).

4.6 Fatty Acid Amide Hydrolase (FAAH)

FAAH is a 60kDa integral membrane protein that degrades fatty acid primary amides including AEA, PEA and OEA, and esters (Vacondio *et al.*, 2011). It is a member of the serine hydrolase superfamily, amidase signature family localized to the endoplasmic reticulum (Giang and Cravatt, 1997; Oddi *et al.*, 2005; Seierstad and Breitenbucher, 2008; Ahn *et al.*, 2009). FAAH can hydrolyze both AEA and 2-AG, but the primary inactivator of 2-AG in the brain and periphery is MAGL, a serine hydrolase which hydrolyzes medium- and short-chain fatty acid esters (Turcotte *et al.*, 2015). Recent evidence demonstrates FAAH is a critical regulator of endogenous cannabinoid levels, and that accumulation of AEA through FAAH inhibition can reduce pain and inflammation (Pertwee, 2014). FAAH is expressed in murine and human keratinocytes and fibroblasts (Maccarrone *et al.*, 2003; Palumbo-Zerr *et al.*, 2012). Thus, this enzyme could be utilized as a therapeutic target for treatment of pain, inflammation and skin pathologies.

Structurally, FAAH is made up of channels and cavities that are involved in both substrate and inhibitor binding (Mor *et al.*, 2004; Seierstad and Breitenbucher, 2008; Ahn *et al.*, 2009). Unlike other serine hydrolases, FAAH possesses an unusual catalytic triad, Ser241-Ser217-Lys142, that is distinct from other serine hydrolases which have a characteristic His-Ser-Asp (Seierstad and Breitenbucher, 2008; Ahn *et al.*, 2009). Three major enzyme structures are the membrane access channel connecting an opening located at the membrane-anchoring side of the enzyme to the active site; the cytosolic port, which may permit hydrophilic products to exit the active site for release to the cytosol; and the acyl chain-binding pocket, which participates in catalysis by interacting with the substrate acyl chain (Mor *et al.*, 2004; Ahn *et al.*, 2009).

Catalysis begins with nucleophilic attack of the catalytic Ser241 on the carbonyl group of the substrate, which causes formation of a tetrahedral intermediate (Otrubova *et al.*, 2011). Upon collapse of the intermediate, the amine and the enzyme-bound acyl intermediate are released. Lys142 mediates the deprotonation of Ser241 by acting as a general base-acid, followed by the protonation of the leaving group which is first bound, then released, by Ser217 (Otrubova *et al.*, 2011). Water mediates the termination of the reaction through deacylation of the enzyme-bound acyl intermediate. The free fatty acid is released, leaving the active enzyme free to bind another substrate (Otrubova *et al.*, 2011).

4.7 FAAH Inhibition

Several classes of FAAH inhibitors have been reported. Reversible inhibitors (such as α -ketoheterocycles) are more selective for FAAH in comparison with other mammalian serine hydrolases, but tend to produce only brief increases in AEA concentrations *in vivo* (Lichtman *et al.*, 2004; Otrubova *et al.*, 2011). Since *in vivo* concentrations of reversible FAAH inhibitors may be reduced by their rapid metabolism, a substantial reduction (>85%) of FAAH activity is necessary to maintain elevated levels

(Fegley *et al.*, 2005). In addition, FAAH inhibition leads to an increase in levels of *N*-acylethanolamine substrates which can compete with the inhibitor, reducing its effectiveness and potency (Ahn *et al.*, 2009).

Earlier carbamate-based FAAH inhibitors, URB524 and later URB597 were *O*-aryl carbamates derived from a known AChE inhibitor (Mor *et al.*, 2004; Otrubova *et al.*, 2014). Results of kinetics studies showed these carbamates were non-competitive and nondialyzable, suggesting an irreversible, covalent modification of the enzyme (Otrubova *et al.*, 2011). The activated carbamate carbonyl contributed to inhibitor effectiveness (Mor *et al.*, 2004; Otrubova *et al.*, 2011). Subsequent QSAR studies revealed that compound activity was inversely correlated with phenol leaving group lipophilicity, and that the carbamate bound to Ser241 in the active site (Alexander and Cravatt, 2005). The endogenous cannabinoid AEA and many FAAH inhibitors reported in the literature including ureas and carbamates are amides or amide analogs, however, other compounds, including ketones, aldehydes, phenols (Propofol) and esters have been studied (Seierstad and Breitenbucher, 2008).

Studies combining the use of both FAAH and COX-2 inhibitors suggest that dual-action FAAH/COX-2 inhibition may reduce pain and inflammation activity without the undesirable side effects associated with NSAIDs (Bertolacci 2013; Cipriano 2013; Grim 2014). NSAIDs are also known to be weak inhibitors of FAAH (Ibuprofen $IC_{50}=130\text{ }\mu\text{M}$; Indomethacin $IC_{50}=45\mu\text{M}$, pH 7.2) and the inhibitory potency of both compounds for FAAH is increased at an acidic pH ((*R*)-ibuprofen $IC_{50}=55\text{ }\mu\text{M}$; indomethacin $IC_{50}=17\text{ }\mu\text{M}$, pH 6.0) (Fowler *et al.*, 2003; Holt *et al.*, 2007). It has been suggested that the non-ionized form of acidic NSAIDs is responsible for FAAH inhibition, and this may affect binding (Holt *et al.*, 2001; Fowler *et al.*, 2003). A more recent study showed that carprofen, an ibuprofen analog, did not bind FAAH in the active site core but to residues at the entrance of the membrane access channel, and that IC_{50} values were reduced at

pH 6.0 (Bertolacci *et al.*, 2013). Preincubation with URB597, a carbamate known to bind within the inner core of the substrate binding cavity did not affect carprofen binding, further suggestive of an alternate binding site (Bertolacci *et al.*, 2013).

4.8 Endocannabinoid System Role in Skin Inflammation

a. FAAH

Recent studies suggest FAAH can be targeted to treat inflammatory conditions. Elevated levels of AEA and 2-AG have been measured in rheumatoid arthritis and osteoarthritis patients, suggesting these anti-inflammatory endocannabinoids are released to protect degrading arthritic connective tissues (Richardson *et al.*, 2008). In gastrointestinal models, FAAH knockouts or WT mice treated with URB597 showed reduced levels of MPO activity, ulceration and edema after treatment with DNBS/TNBS or oral DSS (Massa *et al.*, 2004; Storr *et al.*, 2008).

FAAH has also been reported to modulate inflammatory activity in murine skin models. The carrageenan inflammation model uses an intraplantar injection of λ -carrageenan in the rodent hind paw to elicit local edema and hyperalgesic responses to thermal and tactile stimuli. FAAH (-/-) mice and mice treated with FAAH inhibitors display elevated levels of AEA and other bioactive fatty acid amides, along with reduced edema and inflammation compared to controls (Cravatt *et al.*, 2004). The response in FAAH (-/-) mice was unaffected by CB1 or CB2 receptor antagonists, suggesting it may be attributed to PEA (Wise *et al.*, 2008). FAAH inhibition by URB597 reduced paw edema through a CB2-dependent mechanism (Holt *et al.*, 2005).

The Complete Freund's Adjuvant (CFA) rodent inflammation model uses an antigen solution of inactivated, dried *mycobacterium* emulsified in saline, which is injected into a murine hind paw (Billiau and Matthys, 2001; Fehrenbacher *et al.*, 2012). Injection causes a strong immune response, including granulomas, tissue lesions and inflammatory pain resembling arthritis (Schlosburg *et al.*, 2009). Methanandamide, an

AEA analog resistant to FAAH activity reduced mechanical allodynia, an effect blocked by the CB1 antagonist AM251 (Potenzieri *et al.*, 2008). URB597 treatment suppressed both thermal and mechanical threshold sensitivity, both effects reversed by CB1 and CB2 antagonists (Jayamanne *et al.*, 2006).

Genetic deletion of FAAH was also effective against inflammation due to allergic contact dermatitis. Repeated exposure of mice to the contact allergen 2,4-dinitrofluorobenzene (DNFB) produces swelling of the ear pinnae. FAAH (-/-) mice displayed a significantly less swelling than wild-type controls after DNFB application. Increased AEA levels and expression of CB2 mRNA were reported after repeated DNFB treatments, while CB1 and CB2 compromised mice displayed a significant increase in ear swelling (Karsak 2007).

More recently, Olah *et al.* reported that TLR-2 activation by lipoteichoic acid (LTA) increased FAAH activity in NHEK and human immortalized HPV-KER cells, and that the carbamate FAAH inhibitors URB597, WOBE440 and WOBE479 prevented upregulation of the pro-inflammatory cytokines IL-1 α , IL-1 β , IL-6 and IL-8. Combined antagonism of both CB receptors abolished the effects of the FAAH inhibitors, suggesting the anti-inflammatory effects were due to signaling through these receptors. Using an NC/Tnd mouse model of atopic dermatitis, they showed that topically applied FAAH inhibitors reduced ear swelling in the ears of antigen-exposed mice (Olah *et al.*, 2016).

b. CB1 Receptor

CB1 receptors participate in the regulation of inflammatory responses and barrier repair in skin (Karsak *et al.*, 2007; Gaffal *et al.*, 2013). CB1(-/-) mice with skin disrupted by tape-stripping displayed delayed barrier recovery and decreased expression of filaggrin, loricrin and involucrin, markers of terminal differentiation, in both control and tape-stripped animals (Roelandt *et al.*, 2012). In a mouse model of dinitrofluorobenzene

(DNFB) induced contact hypersensitivity, CB1(-/-) mice exhibited a greatly increased inflammatory response, including elevated expression of CXCL10 and CCL8 (Gaffal *et al.*, 2013). These proinflammatory chemokines regulate recruitment of effector T cells and myeloid immune cells, respectively, and are associated with Th-2-type allergic inflammatory responses (Karsak *et al.*, 2007; Gaffal *et al.*, 2013). CB1(-/-) mice also displayed a time-dependent, significant increase in proliferation of epidermal keratinocytes and epidermal thickness and after exposure to DNFB (Karsak *et al.*, 2007; Gaffal *et al.*, 2013). In a model of fluorescein isothiocyanate (FITC)-induced atopic-like dermatitis, CB1 deletion resulted in increased ear swelling after FITC challenge. In addition, mRNA expression of filaggrin, loricrin, and keratin 10 in the epidermis were significantly reduced in CB1(-/-) mice (Gaffal *et al.*, 2014). Increased mRNA levels of IL-4, CCL8 and eosinophil peroxidase (EPO) were observed (Gaffal *et al.*, 2014).

Activation of CB1 in HaCaT and NHEK keratinocytes by AEA inhibited the formation of cornified envelopes, a key indicator of keratinocyte differentiation (Maccarrone *et al.*, 2003; Paradisi *et al.*, 2008). AEA treatment also reduced expression of differentiation-associated transglutaminase 5, keratin 1 and keratin 10 genes (Paradisi *et al.*, 2008). Treatment of differentiating keratinocytes with ACEA, a selective agonist of CB1, led to a significant decrease in K10 expression and increase of DNA-methyltransferase (DNMT) activity, indicating induction of K10 expression by AEA may be regulated by DNA methylation (Paradisi *et al.*, 2008). AEA was found to activate CB1 signaling through p38 and p42/p44 MAPK pathways (Bouaboula *et al.*, 1995; Lui *et al.*, 2000). Selective inhibitors of p38 MAPK restored K10 expression fully, while preventing the AEA-dependent increase in DNMT in AEA-treated differentiating keratinocytes (Paradisi *et al.*, 2008). A selective inhibitor of p44/p42 MAPK had a lesser, though significant effect (Paradisi *et al.*, 2008), suggesting CB1 signaling through the p38 MAPK pathway had a significant effect on gene and protein expression of differentiation-related markers and

that the anti-differentiating effect of AEA is CB1-dependent (Maccarrone *et al.*, 2003; Paradisi *et al.*, 2008).

c. CB2 Receptor

CB2 receptors are expressed in human and murine keratinocytes (Karsak *et al.*, 2007; Zhang *et al.*, 2010; Gaffal *et al.*, 2013) and immune cells (macrophages, monocytes, NK cells, neutrophils and B and T cells) (Galiegue *et al.*, 1995; Klein *et al.*, 2003). Human immortalized SZ95 sebocytes mainly express CB2 receptor, and studies by Dobrosi *et al.* suggest CB2 is expressed in undifferentiated epithelial cells of the sebaceous gland. AEA and 2-AG treatment increased lipid production and induced cell death primarily by apoptosis, and involving the MAPK pathway. Endocannabinoids upregulated key lipid synthesis genes (PPARs and their target genes), an effect which was suppressed in cells with RNAi knockdown of CB2 or treatment with AM-630, a CB2-specific antagonist (Dobrosi *et al.*, 2008).

Recent studies have described CB2 involvement in inflammatory responses and fibrotic tissue injury repair, however the role of CB2 in skin inflammation is controversial (Kupczyk *et al.*, 2009; Zheng *et al.*, 2012). Exacerbated chronic allergic inflammation was observed in CB1/2^(-/-) mice injected i.p. with the CB2 receptor antagonist SR144528 (Karsak *et al.*, 2007). In contrast, oral or topical administration of SR144528 reduced acute skin inflammatory responses. Oka *et al.* observed CB2 activation during inflammation. Treatment with a selective CB2 receptor antagonist blocked ear swelling, reduced leukotriene B₄ production and neutrophil infiltration in the mouse ear. Application of the endocannabinoid 2-AG produced swelling in the mouse ear in an NO-mediated reaction (Oka *et al.*, 2005). In a DNFB allergic inflammation model, Ueda *et al.* reported administration of the selective CB2 receptor inverse antagonist JTE-907 and the CB2 receptor antagonist SR144528 suppressed allergic inflammation (Ueda *et al.*, 2005).

d. PPAR α

PPAR α is expressed in both murine and human keratinocytes, and is activated by the endocannabinoids AEA, OEA and PEA (Fu *et al.*, 2003; LoVerme *et al.*, 2006; Sun *et al.*, 2006). In particular, PPAR α activation by PEA has been shown to reduce inflammation in murine models of atopic and allergic dermatitis (LoVerme *et al.*, 2006; D'Agostino *et al.*, 2007; Chiba *et al.*, 2012). PPAR α reduces inflammation through induction of anti-inflammatory proteins such as I κ B α , which binds to NF- κ B and prevents its translocation into the nucleus and subsequent transcription of pro-inflammatory mediators such as TNF α , iNOS, IL-1, COX-2 (Sheu *et al.*, 2002; Dubrac and Schmuth, 2011). In both *in vitro* and *in vivo* models, PPAR α ligands stimulate keratinocyte differentiation and suppress proliferation (Hanley *et al.*, 1998; Sheu *et al.*, 2002).

4.9 Endocannabinoid System in Wound Healing

Recent studies suggest signaling through CB1 receptor is involved in wound healing in some tissues (Wright *et al.*, 2005; Kozono *et al.*, 2010; Ramot *et al.*, 2013). Upregulation of CB1/CB2 expression was reported in fibroblasts and macrophage-like cells in granulation tissue in a rat wound-healing model. In human periodontitis patients, AEA levels increased in gingival crevicular fluid post periodontal surgery. In a model of periodontal healing, AM250 & AM630, selective antagonists of CB1 and CB2 respectively, attenuated proliferation of human gingival fibroblasts (HGFs) induced by AEA *in vitro* (Kozono *et al.*, 2010). A CB1/CB2 agonist induced phosphorylation of ERK (1/2), p38 MAPK, and Akt in HGFs. Inhibitors of MAP kinase kinase (MEK or MAPKK), p38 MAPK, and phosphoinositol 3-kinase (PI3-K) significantly suppressed wound closure in an *in vitro* scratch assay (Kozono *et al.*, 2010).

Wound closure by cannabinoids was enhanced alone or in combination with lysophosphatidic acid (LPA) in a model of inflammatory bowel disease (IBD) (Wright *et al.*, 2005). LPA enhanced epithelial wound healing in the colon by increasing cell

migration and in a rat colitis model, animals showed reduced weight loss, mucosal inflammation and necrosis (Sturm *et al.*, 1999). The CB1-specific agonist ACPA induced wound closure in HT29 and DLD1 colonic epithelial cells. The effect was reversed by the CB1 antagonist AM251, and the CB2-specific agonist JWH133 had no effect on wound closure. AEA, the endocannabinoid noladin ether (NE) and the CB1/2 agonist WIN 55,212-2 induced ERK 1-2 phosphorylation in primary colonic epithelial cells. Pretreatment with AM251 abolished the effect, showing ERK phosphorylation was CB1-dependent. Pertussis toxin inhibited both spontaneous and ACPA-induced wound closure, suggesting the mechanism involved coupling of CB1 and G_i proteins. When LPA was combined with AEA, NE and ACPA, wound closure increased. The effect was not only blocked by addition of AM251 to the ACPA treatment, but also in spontaneous wound closure (Wright *et al.*, 2005). Taken together, these data suggest the endocannabinoid system plays a role in the wound healing process.

SUMMARY AND RATIONALE

Endocannabinoids including *N*-arachidonylethanolamine (anandamide, AEA) and 2-arachidonoyl glycerol (2-AG), along with the *N*-acylethanolamines palmitoylethanolamine (PEA) and oleoylethanolamine (OEA), are important endogenous fatty acid signaling molecules involved in regulating skin homeostasis and inflammation (Biro *et al.*, 2009; Kupczyk *et al.*, 2009). These lipid-derived mediators function by binding to cannabinoid receptors and other lipid signaling molecules, including the peroxisome proliferator-activated receptor alpha (PPAR α), a nuclear receptor important in regulating lipid catabolism and inflammatory responses (Di Marzo *et al.*, 2001; O'Sullivan and Kendall, 2010; Dubrac and Schmuth, 2011; Kendall and Nicolaou, 2013). Two primary endocannabinoid receptors, cannabinoid receptor 1 (CB1) and cannabinoid receptor 2 (CB2), have been identified in the skin (Kupczyk *et al.*, 2009; Pertwee, 2014). Binding of AEA to keratinocyte CB1 has been shown to regulate growth, differentiation and apoptosis (Maccarrone *et al.*, 2003; Paradisi *et al.*, 2008). CB2 is expressed in keratinocytes, hair follicles and sebaceous glands (Stander *et al.*, 2005; Karsak *et al.*, 2007; Telek *et al.*, 2007; Dobrosi *et al.*, 2008; Zheng *et al.*, 2012). It is also found in skin mast cells, macrophages, neutrophils, NK cells, and B and T cells (Galiegue *et al.*, 1995; Stander *et al.*, 2005; Zheng *et al.*, 2012; Gui *et al.*, 2015). Endocannabinoid signaling through CB2 upregulates genes for lipid synthesis, and immune cell signaling and migration (Kishimoto *et al.*, 2005; Ueda *et al.*, 2005; Oka *et al.*, 2006; Dobrosi *et al.*, 2008). PPAR α has been identified in rodent and human keratinocytes, in sebaceous glands and in T-cells, where it is thought to play a role in wound re-epithelialization, sebocyte differentiation, and the resolution of inflammation (Michalik *et al.*, 2001; Di-Poi *et al.*, 2004; Dubrac and Schmuth, 2011).

Inhibition of FAAH increases levels of endocannabinoids (Pertwee, 2014).

Alterations in expression and/or activity of FAAH, as well as CB1, CB2 and PPAR α have

been linked to a number of skin diseases in animal models including allergic contact dermatitis, acute and chronic contact dermatitis, dermal fibrosis and skin tumor induction (Biro *et al.*, 2009; Kendall and Nicolaou, 2013). In human skin, endocannabinoids have shown promise in treating pruritus secondary to cholestatic liver disease, histamine-induced dermatitis, allergic contact dermatitis and xerosis (Neff *et al.*, 2002; Dvorak *et al.*, 2003; Paus *et al.*, 2006; Lambert, 2007).

Sulfur mustard (SM, bis[2-chloroethyl] sulfide) and nitrogen mustard (NM, methylbis(2-chloroethyl)amine) are bifunctional alkylating agents first synthesized for chemical warfare and are considered high priority chemical threats (Wattana and Bey, 2009). Depending on the dose and timing of exposure, mustards induce inflammation, epidermal and dermal injury, blistering and scarring (Graham *et al.*, 2009; Shakarjian *et al.*, 2010; Joseph *et al.*, 2014). Wound healing can ensue, although repair depends on the individual and extent of injury (Graham *et al.*, 2005; Ghabili *et al.*, 2010). Delayed wound healing is also a characteristic of mustard-induced injury.

Arachidonic acid, a product of FAAH degradation of anandamide, is a pro-inflammatory mediator which plays a role in the inflammatory response in skin conditions such as atopic dermatitis, psoriasis, and after doses of UVA irradiation (Hawk *et al.*, 1983; Ruzicka *et al.*, 1986; Fogh *et al.*, 1989). Topical application of AA to mouse ear skin causes an intense, acute inflammatory response, inducing synthesis of PGE₂, LTC₄ and LTD₄, and can be measured as an increase in ear thickness (Chang *et al.*, 1986). The inflammatory response can be attenuated by application of lipoxygenase and cyclooxygenase inhibitors (Opas *et al.*, 1985; Chang *et al.*, 1986). AA, PGE₂, LTC₄ and D₄ are produced as a result of SM exposure and play a role in the vesicant-induced inflammatory response (Dachir *et al.*, 2002; Black *et al.*, 2010b).

As endocannabinoids can modulate keratinocyte growth and differentiation, and inhibition of FAAH plays a role in the attenuation various inflammatory conditions, the

present studies were aimed at determining if NM and SM exposure are associated with alterations in expression of proteins of the endocannabinoid system.

The central hypothesis of this dissertation is that the endocannabinoid system is present in mouse skin and dermal appendages, and expression of endocannabinoid proteins is modulated by vesicant exposure. Upregulation of FAAH, an endocannabinoid-degrading enzyme, contributes to chemically-induced skin inflammation, thus FAAH inhibition is a potential countermeasure to vesicant-induced inflammation and injury. To test this hypothesis, three specific aims were proposed:

Specific Aim 1. Characterize the expression of FAAH, CB1, CB2 and PPAR α in mouse skin and dermal appendages. To characterize the constitutive expression of these proteins in mouse skin, we used immunohistochemistry on dorsal skin sections taken from CD-1 treated with NM, and from SKH1-Hr hairless mice treated with SM. Paraffin-embedded skin sections (6 μ m) mounted on glass slides were stained with antibodies to FAAH, CB1, CB2 and PPAR α to evaluate constitutive levels of expression in the epidermis, dermis and dermal appendages.

Specific Aim 2. Determine if vesicant treatment modulates expression of FAAH, CB1, CB1 and/or PPAR α . Similarly, dorsal skin sections from both CD-1 mice treated with NM and SKH-1hr hairless mice treated with SM were evaluated for changes in endocannabinoid protein expression using immunohistochemistry. Differences in staining location and intensity in vesicant-treated mouse skin verses untreated mouse skin indicated changes in endocannabinoid protein expression.

Specific Aim 3. Determine whether inhibition of FAAH suppresses the inflammatory response to 12-O-tetradecanoylphorbol-13 acetate (TPA) or 2-chloroethyl ethyl sulfide (CEES) exposure in mouse skin. We first used structure/activity relationships to predict which compounds in our chemical library had

the ability to inhibit FAAH. The candidates were screened for FAAH activity *in vitro* using an inhibition assay. For *in vivo* studies, the compounds were applied to the ears of CD-1 mice, followed by either TPA or CEES, and assessed for anti-inflammatory activity.

Taken together, the results of these experiments showed that the endocannabinoid system is a target for vesicants in the skin, and that treatment with FAAH inhibitors shows promise as a countermeasure to vesicant-induced injury.

PART 1: Specific Aims 1 & 2.

Endocannabinoids including AEA and 2-AG, as well as related *N*-acylethanolamines, have been identified in the epidermis and dermis of both murine and human skin (Kupczyk *et al.*, 2009; Kendall and Nicolaou, 2013; Maccarrone *et al.*, 2015). They are thought to be important in regulating cell growth and differentiation, as well as in controlling skin inflammation (Maccarrone *et al.*, 2003; Biro *et al.*, 2009; Kupczyk *et al.*, 2009). Endocannabinoids have also been detected in human skin suction blister fluid, presumably generated in response to trauma where they likely function to suppress inflammation and promote wound healing (Kendall *et al.*, 2015). As NM and SM are skin blistering agents, endocannabinoids are also likely to be generated in vesicant-induced blisters.

Mouse models are used extensively by our group and others to evaluate the effects of vesicants on the skin. Encouraged by preliminary results showing the effectiveness of candidate FAAH inhibitors in the MEVM, we moved forward to characterize the endocannabinoid system in mouse skin. Studies on the endocannabinoid system by our lab are ongoing, necessitating a foundation for new ideas and projects. Thus, the first two aims of this project were to first characterize the expression of FAAH, CB1, CB2 and PPAR α in mouse skin and dermal appendages, then determine if vesicant treatment modulates expression of FAAH, CB1, CB1 and/or PPAR α .

1. EXPERIMENTS

a. Animals

i. Mouse Strains

Two strains of mice, CD-1 and SKH1-Hr hairless mice were used in our studies. The CD-1 mouse is inexpensive, readily available, polymorphic at a significant number of loci and has a genetic history of similar complexity to a human founder population (genetically diverse) (Aldinger *et al.*, 2009). Because of these characteristics, they are often used in toxicology and cancer research (Cui *et al.*, 1993; Chia *et al.*, 2005; Aldinger *et al.*, 2009). Another advantage is that their light skin color offers a better background on which to observe injury and inflammatory changes.

SKH1-Hr hairless mice are an outbred, albino strain also frequently used in skin research (Benavides *et al.*, 2009). The mutant allele is *hairless* (Hr^{hr}) and the mutation is autosomal recessive (Potter *et al.*, 2001). *Hr* is located at the 70 Mb position of chromosome 14, and encodes a transcriptional co-repressor protein binding to thyroid hormone-, vitamin D- and retinoic acid receptor-related orphan receptors (Potter *et al.*, 2001; Benavides *et al.*, 2009). At birth, *Hr* mRNA is normally expressed in the suprabasal layers of the interfollicular epidermis, and in the hair follicle infundibulum in a hair-cycle dependent manner (Panteleyev *et al.*, 2000). The first coat develops normally, but by 2 weeks after birth they begin losing hair. Hair loss starts at the eyelids and proceeds caudally until approximately 3 weeks of age, when they are nearly hairless (Benavides *et al.*, 2009). At 5 weeks, a second wave of growth begins with development of only a few abnormal tylotrich follicles and vibrissae, which are repeatedly shed (Benavides *et al.*, 2009). Histologically, there are two characteristic structures observed, utriculi and dermal cysts (Panteleyev *et al.*, 1998). A utriculus is a flask-shaped structure connected to the skin surface, lined with hyperkeratotic epithelium. The dermal cysts are lined with keratinized epithelium and found deep in the dermis (Panteleyev *et*

al., 1998). In addition to these structures, differences from wild type mice include enlarged sebaceous glands and dermal granulomas (Benavides *et al.*, 2009). Hair follicle structure abnormalities show during the first catagen stage, and the entire regression process is dysregulated (Panteleyev *et al.*, 1998). Despite these differences, there are advantages to using this model. Depilation is unnecessary before application of toxic or therapeutic agents and processes associated with wound healing and inflammation are readily observed. The hairless mouse model has been used successfully by our group and others in previous studies using chemical vesicants (Joseph *et al.*, 2011; Clery-Barraud *et al.*, 2013; Jain *et al.*, 2014; Tewari-Singh *et al.*, 2014).

b. Chemical Treatments

i. Nitrogen Mustard Application to Mouse Dorsal Skin:

All animals received humane care in compliance with institutional guidelines as outlined in the National Institute of Health's *Guide for Care and Use of Laboratory Animals*. For NM experiments, female CD-1 mice, 8-10 weeks of age (Charles River Laboratories) were used. Mice were anesthetized by intraperitoneal injection of ketamine (80 mg/kg, Ketathesia, Henry Schein Animal Health, Dublin, OH) and xylazine (12 mg/kg, Anased, Henry Schein Animal Health) and the hair on the dorsal lumbar region shaved. Two six-millimeter diameter glass microfiber filters (GE Healthcare Life Sciences, Buckinghamshire, UK) were placed on the shaved dorsal lumbar skin, on either side of the spine. Twenty μ moles of freshly prepared NM (20 μ l of a 1 M solution prepared in 20% water and 80% acetone (v/v) (Sigma, St. Louis, MO) or control solvent was applied directly on the glass microfiber filters which were then covered with Parafilm® M (Bemis NA, Neenah, WI). The filters were removed from the skin after 6 min. Mice were euthanized 1, 2, 3, 4 and 5 days post NM exposure and 12 mm full

thickness skin punch biopsies of exposed areas immediately collected, trimmed, and stored at 4°C in ice cold phosphate buffered saline (PBS) containing 2% paraformaldehyde/3% sucrose. After 24 h, skin samples were rinsed in ice-cold PBS containing 3% sucrose, transferred to ethanol (50%), and paraffin embedded. Skin sections (6 µm) were prepared and stained with hematoxylin and eosin (H&E) for analysis (Goode Histolabs, New Brunswick, NJ).

ii. Sulfur Mustard Application to Mouse Dorsal Skin:

For SM experiments, male CRL: SKH1-Hr hairless mice, 5 weeks of age (Charles River Laboratories, Wilmington, MA) were used. Animals were exposed to SM on the dorsal skin using a vapor cup model as previously described (Joseph *et al.*, 2014). Mice were euthanized 1, 3, 7, 14 and 21 days post-exposure and full thickness skin punch biopsies of exposed areas prepared for immunohistochemistry as described below. All experiments with SM were performed at MRIGlobal (Kansas City, MO). The efficacy of candidate FAAH inhibitors was studied in the mouse ear vesicant model (MEVM) as previously described (Babin *et al.*, 2000; Casillas *et al.*, 2000; Young *et al.*, 2012). The sulfur mustard analog 2-chloroethyl ethyl sulfide (65 µmoles) was used to induce inflammation. To evaluate each compound, ears (3–4 mice per group) were treated with 20 µL of vehicle control (methylene chloride or acetone) or the test compound (1.5 µmol) in 20 µL of the appropriate vehicle. After 5 h, mice were euthanized and ear punches (6 mm in diameter) were taken and weighed. Once the raw data were obtained, masses of ear punches were averaged and the percent reduction of vesicant-induced edema and inflammation was calculated using a previously described method (Casillas *et al.*, 2000).

iii. CEES and TPA Applications to Mouse Ear (Mouse Ear Vesicant Model):

MEVM experiments were performed in collaboration with the laboratory of Mou-Tuan Huang Ph.D., Rutgers Department of Chemical Biology at Rutgers University in Piscataway, NJ. In studies using the MEVM, an irritant is applied topically to the mouse ear, and after a period of time edema is induced, increasing the weight of the ear. Application of anti-inflammatory agents can reduce or suppress irritant-induced increases in ear weight (Babin *et al.*, 2000; Casillas *et al.*, 2000).

CEES (2-chloroethyl ethyl sulfide) is a potent skin vesicant and inflammatory agent structurally related to sulfur mustard, used in earlier MEVM experiments to screen for anti-inflammatory agents (Casillas *et al.*, 2000). In this assay, female CD-1 mice (4-5 weeks of age, 6-10 animals/group) were treated on the inner surface of the right ear with CEES (2.5 mg/mL) in methylene chloride or 20 microliters of methylene chloride (control). Test compounds (1-2 micromoles) were applied to the ears as the inflammatory agent. Animals were sacrificed after 6 hours and 6 mm diameter ear punch biopsies taken and weighed. Anti-inflammatory activities of NDH compounds were determined by the percent inhibition of CEES-induced edema as percent reduction in ear weight (% REW) compared to controls:

$$\% \text{ REW} = \frac{\text{CEES (cpd + CEES) exposed ear weight (right ear)} - \text{Vehicle control ear weight (left ear)}}{\text{Vehicle control ear weight (left ear)}} \times 100$$

TPA, also known as phorbol ester or 12-O-tetradecanoylphorbol-13 acetate, is a topical inflammatory agent. Test compounds (1-2 micromoles) and TPA (1.5 micromoles) were applied to the inner surface of the right ears of female CD-1 mice (4-5 weeks of age, 6-10 animals/group). Animals were sacrificed after 6 hours and 6mm-diameter ear punch biopsies were taken and weighed. Anti-inflammatory activity was

determined by relative percent inhibition of edema induced by TPA using the equation above substituting TPA results for CEES.

c. Immunohistochemistry

Tissue sections were deparaffinized and blocked at room temperature with 1% BSA for 1 h for FAAH, 25% normal goat serum for 2 h for CB2 and PPAR α , or 25% normal goat serum in 1% BSA for 2 h for CB1. Tissue sections were then incubated overnight at 4°C with rabbit affinity purified polyclonal antibodies against FAAH (1:250; Cayman Chemical, Ann Arbor, MI), CB1 receptor (1:250; Cayman Chemical), CB2 receptor (1:250; Cayman Chemical), PPAR α (1:250; Cayman Chemical), IgG control antibody or blocking peptide controls (Cayman Chemical, 1:1 FAAH amino acids 561-579, CLRFMREVEQLMTPQKQPS, 1:10 CB1 receptor amino acids 461-472 MSVSTDTSAEAL, 1:1 CB2 receptor amino acids 20-33 NPMKDYMILSGPQK, 1:1 PPAR α : amino acids 22-36 PLSEEFLQEMGNIQE). This was followed by incubation with biotinylated goat anti-rabbit secondary antibody (1:200; Vector Laboratories, Burlingame, CA) for 30 min at room temperature; binding was visualized using 3,3'-diaminobenzidine (Vector Laboratories).

2. RESULTS

a. NITROGEN MUSTARD

NM-induced alterations in mouse skin and dermal appendages.

Morphological changes in the skin and dermal appendages of CD-1 mice were characterized following NM exposure. Control skin contained a thin layer of differentiating epidermal cells, as well as developed dermal appendages including prominent sebaceous glands and hair follicles within the papillary dermis (Fig.3). Within 1 day of NM exposure, alterations in dorsal skin structures were evident. The dermal-epidermal junction was disorganized with aplastic nuclei within the basal layer. Edema was apparent in the dermis, along with increased numbers of inflammatory cells. By days 2-3 days post exposure, increased edema and inflammatory cell infiltrates were noted in the papillary dermis. Thickening of the epidermis was evident with areas of parakeratosis. Pyknosis and karyolysis were observed in the disorganized basal keratinocytes within the wound region and a developing eschar was present. Deteriorating sebaceous glands and hair follicles within the edematous dermis were evident within the wound site. Extending beneath the eschar, a hyperplastic neoepidermis was observed, while the stratum corneum appeared to wall off the eschar. By 4-5 days post NM, hyperplastic epidermis was noted beneath the eschar, sitting on compacted papillary and reticular dermis. Although separation was observed between the dermis and epidermis, this appeared to be an embedding artifact. At the wound margins, the epidermis was organized into a basal layer covered by a suprabasal layer with basophilic staining granules. Remnants of pilosebaceous units were observed within the epidermis and in the compacted dermis. After 5 days, the intact hyperplastic epidermis extended across the wound bed. Both the stratum spinosum and stratum granulosum were well-developed, while the stratum basale was disorganized with cellular vacuoles, karyolytic and pyknotic nuclei. Parakeratosis was evident within a well-

developed stratum corneum. Also of note was the development of rete at the dermal/epidermal junction.

Effects of NM on expression of cannabinoid receptors and PPAR α in mouse skin.

Skin from control CD-1 mice expressed low constitutive levels of CB1 and CB2 throughout the epidermis and dermal appendages (Figs. 4 and 5). Expression of these receptors was noted in sebaceous glands and outer root sheaths of hair follicles. Following NM exposure, CB1 was upregulated in the epidermis, pilosebaceous units and inflammatory cells within the dermis, a response noted after 1-3 days (Fig. 4). Increased CB2 was evident by 2-3 days post NM in the hyperplastic epidermis and degenerating pilosebaceous units (Fig. 5). After 4-5 days, there was an overall decrease in expression of CB1 and CB2 in the hyperplastic epidermis (Figs. 4 and 5 and not shown). CB1 was primarily expressed in basal keratinocytes while CB2 was expressed in both basal and suprabasal keratinocytes. Of note, increased CB2 was evident in the uppermost layers of the stratum granulosum directly below the stratum corneum. A marked increase in CB1 was evident in keratinocytes in the basal and spinous layers. Anti-CB1 and anti-CB2 antibody binding was inhibited by their respective blocking peptides indicating that antibody binding was specific for these receptors (Fig. 6 and not shown).

Low constitutive levels of PPAR α were expressed throughout the epidermis, the outer root sheath of hair follicles, and in sebaceous glands in control skin (Fig. 7 and not shown). One to three days post NM exposure, increased PPAR α expression was evident in the epidermis and sebaceous glands as well as inflammatory cells within the dermis (Fig. 7). Nuclear localization of PPAR α was evident in sebocytes one day post-NM, while increased PPAR α 2-5 days post-NM was largely cytoplasmic. PPAR α expression was upregulated throughout the hyperplastic epidermis after 3 days post SM and NM. Four days post NM, marked increases in PPAR α expression were observed

within the stratum granulosum, stratum spinosum and in the stratum basale (Fig. 7). Five days post NM, PPAR α was upregulated in the stratum basale and stratum spinosum with decreased PPAR α expression in the stratum granulosum (Fig. 7). PPAR α was also localized in remnants hair follicle outer root sheaths and within dystrophic sebaceous glands. PPAR α was also highly expressed in the stratum corneum and within areas of parakeratosis. Anti-PPAR α antibody binding was inhibited using a PPAR α -specific blocking peptide demonstrating that antibody binding was specific for PPAR α (Fig. 6).

Effects of NM on expression of FAAH in mouse skin.

Low levels of FAAH were expressed in the epidermis, the outer root sheath of hair follicles, and in sebaceous glands (Fig. 8). Within 1-3 days post NM, an increase in FAAH expression was evident throughout the epidermis and hyperplastic neoepidermis at the wound edge, in the isthmus and outer root sheath of hair follicles, and in inflammatory cells in the dermis and hypodermis (Fig. 8 and not shown). After 4-5 days post NM, FAAH was differentially expressed in the hyperplastic epidermis during wound healing. FAAH was primarily localized in the granular layer of the epidermis directly below the stratum corneum. Anti-FAAH antibody binding was inhibited by a blocking peptide, indicating that antibody binding was specific for FAAH (Fig. 6).

b. SULFUR MUSTARD

SM-induced alterations in mouse skin and dermal appendages.

In recent studies, we characterized morphological changes in the skin and dermal appendages of SKH-1 hairless mice 1, 3, 5, 7, 14, and 21 days post NM exposure. Throughout the 21 days the epidermis of control mice was 3-5 layers thick, with a thin stratum corneum and a well-demarcated dermal/epidermal junction (Fig. 9).

Prominent pilosebaceous units were scattered throughout a fibrous collagen dermis, where cysts were also observed. A hypodermal layer consisting of adipocytes, capillaries was evident beneath the dermis. 1-3 days post SM-treatment, changes were evident in both epidermis and dermis (Fig. 9). The suprabasal layers of the epidermis had degraded, and the remaining basal layer keratinocytes were vacuolated with loss of nuclear structures. Edema and hemorrhage were apparent in the dermis, with shrinking pilosebaceous units and infiltrating inflammatory cells at the dermal/epidermal junction, and in the hypodermis. With time, the dermal/epidermal boundary became indistinguishable and the dermal collagen compact. At 3 days, an eschar had formed over the wound region while the thickened hypodermis extended upward beneath the wound. A thick layer of inflammatory cells had organized along the boundary of the eschar and dermis, and degraded sebaceous glands were evident within the eschar. By days 5-7 the eschar had separated from the wounded skin (Fig. 9 and not shown). The wound region was covered by a thin layer of neoepidermis with hyperplastic stratum corneum. Vestiges of pilosebaceous units were observed within the dermis, while inflammatory cells were noted at the dermal/hypodermal region. Fourteen days post-SM a thickened layer of hyperplastic neoepidermis was evident which extended into the papillary dermis, forming rete ridges (Fig. 9). The suprabasal neoepidermis contained several layers of basophilic staining granules. Remnants of hair follicles formed lamellated keratin structures in the dermis. By day 21 post SM, a thick stratum corneum with parakeratosis was evident. Rete ridges were not evident at this time.

Effects of SM on expression of cannabinoid receptors and PPAR α in mouse skin.

Skin from control SKH-1 mice expressed low constitutive levels of CB1 and CB2 throughout the epidermis and dermal appendages (Figs. 10 and 11). One day post SM, an increase in the cannabinoid receptors was evident in hair follicles while increases in CB1 and CB2 were evident in neoepidermis 3-7 days post SM (Figs. 10 and 11). CB1

and CB2 were also expressed in hyperplastic epidermis 14-21 days post SM; increased expression of CB2 was noted in suprabasal layers of the epidermis. In control SKH mouse skin, low constitutive levels of PPAR α were expressed throughout the epidermis, the outer root sheath of hair follicles, and in sebaceous glands (Fig. 12). One to three days post SM, increased PPAR α was evident in the epidermis and sebaceous glands (Fig. 12). PPAR α expression was upregulated throughout the hyperplastic epidermis by 7 days post SM. At later times, 14-21 days post SM, PPAR α was upregulated in the stratum basale and stratum spinosum with decreased PPAR α expression in the stratum granulosum (Fig. 12). In addition, PPAR α was localized in remnants of the hair follicle outer root sheaths. Interestingly, PPAR α was also highly expressed in the stratum corneum and within areas of parakeratosis.

Effects of SM on expression of FAAH in mouse skin.

In skin from control SKH-1 mice, low levels of FAAH were expressed in suprabasal layers of the epidermis, the outer root sheath of hair follicles, and in sebaceous glands (Fig. 13). Within 1 day post SM, an increase in FAAH was evident in the epidermis and sebaceous glands. By three days, FAAH was expressed in the hyperplastic neoepidermis at the wound edge (Fig. 13). FAAH expression was also upregulated in the hyperplastic epidermis 7 days post SM, increased FAAH was expressed in basal cells and proliferating cells above the basal cell layer. A decrease in FAAH expression was noted in the hyperplastic epidermis during wound healing, 14-21 days post SM. At this time, FAAH was expressed in differentiated layers of the epidermis, low levels of FAAH were expressed in proliferating basal cells (Fig. 13).

3. DISCUSSION

The first two aims of this project were to first characterize expression of FAAH, CB1, CB2 and PPAR α in normal mouse skin, and second to determine if these proteins were modulated by vesicant exposure in mouse skin. In control mouse skin, FAAH and CB receptors were expressed at relatively low levels throughout the epidermis, in dermal appendages, and in cells in the dermis. Marked increases in expression of these proteins were observed within one day following NM and SM exposure. These increases preceded frank tissue injury indicating that factors regulating ECS protein expression are independent of products released from degraded and necrotic tissue. These mediators may be tissue-derived, or from infiltrating leukocytes following vesicant-induced inflammation. In this regard, lipid mediators, growth factors, and pro-inflammatory cytokines including PGE₂, IL-1 β , IL-6 and TNF α have been reported to upregulate expression of FAAH and the CB receptors in different cell types and may function to increase endocannabinoid proteins in the skin (Karaliota *et al.*, 2009; Rettori *et al.*, 2012; Tomar *et al.*, 2015). Earlier studies have shown that SM induces differentiation of human keratinocytes (Rosenthal *et al.*, 1998; Popp *et al.*, 2011); changes in endocannabinoid protein expression and differentiation of keratinocytes may be due in part to vesicant treatment. These data are consistent with findings that FAAH activity and expression increases in human keratinocytes induced to differentiate *in vitro* and that treatment of keratinocytes with AEA inhibits keratinocyte differentiation (Maccarrone *et al.*, 2003).

FAAH is expressed in both interfollicular and follicular compartments of the control skin, suggesting it has a function in maintaining both epidermal and follicular homeostasis. Increased expression following vesicant exposure indicates that FAAH may reduce anti-inflammatory endocannabinoid levels, contributing to an increase in

inflammation and injury (Biro *et al.*, 2009). These data are supported by our findings that FAAH inhibitors reduce inflammation and edema in the MEVM.

In both NM and SM-exposed mouse skin, a dramatic upregulation of FAAH expression was noted throughout the epidermis and pilosebaceous units within 24 hours. Increased FAAH expression would result in reduced endocannabinoid levels and increased levels of arachidonic acid. Oxidation of arachidonic acid by COX-2 contributes to the inflammatory process by generating prostaglandins, reported to function as a pro-inflammatory mediators in SM-induced injury (Wormser *et al.*, 2004; Joseph *et al.*, 2011). Previous studies by our group and others showed increased COX-2 expression in basal and suprabasal keratinocytes as early as 1 day post SM-exposure (Joseph *et al.*, 2011; Dachir *et al.*, 2012). The observed upregulation of FAAH and increase in AA would contribute to the increase in PGE₂ and other pro-inflammatory prostaglandins reported in vesicant-induced injured skin. In addition to contributing to the inflammatory response, PGE₂ has been reported to increase keratinocyte proliferation and play a role in the hyperplastic response to epidermal inflammation, which could suggest a role in the increased differentiation reported in SM-induced injury (Rys-Sikora *et al.*, 2000; Ansari *et al.*, 2008). By day 3 post-SM and -NM, increased epidermal thickness was observed along with high FAAH expression. FAAH expression in the epidermis and hair follicles became more pronounced in the differentiating, suprabasal layers and outer root sheath during days 4-5 in the NM-treated animals, and by day 5 in the SM-treated. The catabolism of AEA, along with an increase in PGE₂ resulting in increased differentiation may be responsible for the epidermal hyperplasia observed from days 2-5.

Increased expression of FAAH is prolonged (up to 21 days post-SM exposure), thus, it is likely that the ECS is important in repair processes. FAAH expression in the hyperplastic basal and spinous keratinocytes of SM-treated mouse skin increased

sharply in the basal epidermis on day 7, decreasing by day 14 and remained at a low level through day 21. Upregulated FAAH would presumably increase the concentration of PGE₂ and other prostaglandins in the epidermis. However, in contrast to the early inflammatory stage when PGE₂ promotes redness, edema and pain, during the proliferative stage it contributes to healing by inducing granulation tissue formation at the wound site, stimulating angiogenesis and fibroblast mitogenesis, proliferation and migration (Laulederkind *et al.*, 2002; Kampfer *et al.*, 2003; Goren *et al.*, 2015). Thus, the role of the endocannabinoid system may change during the course of the inflammatory response, modulating pro-inflammatory effects early, followed later by resolution of inflammation and wound healing.

A question arises as to the role of CB receptor expression during wound repair post vesicant exposure. Upregulated CB1 and CB2 expression was observed throughout the epidermis during days 1-3 in the SM- and NM-exposed skin. At later times points after NM- and SM-induced injury (3-4 days), during the wound repair process, endocannabinoid proteins were expressed in the hyperplastic epidermis. However, by day 5, differential expression of CB receptors was apparent; CB1 was predominantly localized in basal and suprabasal keratinocytes, while CB2 was largely expressed in suprabasal cells. Differential expression of cannabinoid receptors in basal and suprabasal keratinocytes suggests that they may perform distinct functions in the skin during the wound healing process. For example, basal cell CB1 may be important in regulating endocannabinoid-mediated keratinocyte proliferation, while suprabasal cell CB2 may regulate keratinocyte differentiation. Increased CB2 expression in the upper granular layers in the SM-treated skin continued 14-21 days. Absence of CB2 at the SG/SC border has been associated with accelerated terminal differentiation (Roelandt *et al.*, 2012); the increased CB2 expression could suggest an adaptive role in controlling the vesicant-induced hyperplasia during the wound healing process.

PPAR α expression increased markedly after 24 hours and remained elevated days 1-3 in both NM- and SM-treated skin, in agreement with previous studies supporting a role for PPAR α early in the inflammatory process (Michalik *et al.*, 2001; Dubrac and Schmuth, 2011). Interestingly, marked upregulation of epidermal PPAR α was observed on day 4, especially in suprabasal epidermal layers and stratum corneum, suggesting PPAR α is important in epidermal differentiation (Sertznig *et al.*, 2008). By day 5, there was an overall decrease in expression observed in the skin of NM-treated animals, although levels remained elevated compared to controls. At 7 days, expression was observed primarily in the basal, spinous epidermal layers in the SM-treated mice, which persisted through day 21. Basal and spinous epidermal lipids include unsaturated fatty acids, which may be targets of lipid peroxidation by vesicants. Unsaturated lipids possessing two or more double bonds interspersed with methylene (-CH₂-) units are subject to lipid peroxidation by vesicant-generated free radicals. Oxidated lipids are known to be potent PPAR α activators. Upregulated PPAR α has been reported to activate catalase activity, which would provide protection against the increased hydrogen peroxide generated by vesicants and may play a role in the observed upregulation of catalase post-vesicant exposure. Given that the effects of vesicant induced-injury at the dermal/epidermal junction are not immediate but occur over time, the persistent, elevated expression of PPAR α observed in the basal and lower suprabasal regions may be a protective response resulting from the prolonged oxidative effects of vesicant exposure. Unlike AEA or 2-AG, which have unsaturated lipid chains vulnerable to lipid peroxidation, PEA possesses a saturated side chain. Since saturated lipids are less likely to oxidize than polyunsaturated lipids (Hogg and Kalyanaraman, 1999), PEA may be less vulnerable to peroxidation, and could play a greater role in suppressing vesicant-induced inflammation than AEA or 2-AG.

Sebocytes from control and mustard-treated mouse skin were found to express FAAH, cannabinoid receptors and PPAR α . These data are consistent with earlier studies showing constitutive endocannabinoid protein expression in sebaceous glands of dogs, mice and humans (Stander *et al.*, 2005; Campora *et al.*, 2012; Zheng *et al.*, 2012). These findings indicate that, as in other skin cell types, endocannabinoid proteins function in maintaining homeostasis (Dobrosi *et al.*, 2008; Toth *et al.*, 2011e). Mature, differentiated sebocytes produce sebum, while proliferating cells replenish terminally differentiated cells that have undergone apoptosis (Zouboulis, 2004; Schneider and Paus, 2010). Following NM- or SM-induced injury, FAAH and CB2 were homogeneously distributed in the sebaceous glands, while CB1 and PPAR α were most upregulated in flattened, proliferating cells near the distal end of the sebaceous gland and in nucleated sebocytes. These data suggest that FAAH and CB2 are important in controlling sebocyte growth and differentiation, while CB1 and PPAR α signaling regulates proliferation. As observed in keratinocytes, 1-3 days post NM or SM, there was a marked increase in expression of these proteins. As endocannabinoids control sebocyte function, regulating growth, differentiation and sebum biosynthesis, these changes may be important in protecting the skin following injury (Dobrosi *et al.*, 2008). Conversely, excessive sebum production may contribute to cytotoxicity. Sebocyte lipids and lipid-derived products can undergo peroxidation reactions which generate cytotoxic mediators (Zouboulis, 2004; Tochio *et al.*, 2009). These lipid peroxides can also stimulate keratinocytes to produce pro-inflammatory mediators including prostaglandins, IL-1 α and IL-6, as well as antioxidants such as heme oxygenase-1, catalase and glutathione S-transferase (Ottaviani *et al.*, 2006; Zhou *et al.*, 2013; Zouboulis *et al.*, 2014). PPAR α ligands have been reported to inhibit sebaceous gland lipogenesis (Downie *et al.*, 2004) and this may be important in regulating sebocyte function following injury.

Of interest were our findings that NM- and SM-induced tissue injury and repair as well as changes in the endocannabinoids were generally similar on days 1-5, despite the fact that two different strains of mice and different model exposure systems were used. For example, in both NM- and SM-treated groups, FAAH was upregulated in the epidermis and pilosebaceous units to a similar degree within 24 hours. By day 3, hyperplastic epidermis and degrading pilosebaceous units at the wound edge in both models expressed FAAH. On day 5, FAAH was predominantly expressed in the upper suprabasal epidermal layers of both groups. Similarly, CB receptor expression in both models was observed in similar regions of the skin and at comparable levels at each time point. PPAR α showed some differences; at day 5 in the SM-treated skin the level of expression was lower and more uniform, however this may be due to differences in wound severity. The SM-induced wound appears less severe and the epidermal hyperplasia less than we observed in the NM-treated animal.

We also noted that inflammatory cells accumulating at the wound site following NM- or SM-induced injury upregulate CB1. Innate immune cells in the skin have been reported to express various endocannabinoid proteins (Stander *et al.*, 2005; Sugawara *et al.*, 2012; Chiurchiu *et al.*, 2014). Both pro- and anti-inflammatory effects of endocannabinoids have been described in neutrophils and macrophages (Lenglet *et al.*, 2013; Tomar *et al.*, 2015). It is likely that the early appearance of these cells in the wound site (1-3 days) following injury contributes to inflammation and tissue damage, whereas at later stages they contribute to the resolution of inflammation, tissue remodeling and wound healing (Daley *et al.*, 2010). Expression of the endocannabinoid system in these cells suggests that endocannabinoid signaling may contribute to the functional activity of these immune cells.

Figure 3. Structural changes in mouse skin following NM exposure. Histological sections, prepared after exposure to control (CTL) or 1, 2, 3, 4, and 5 days after exposure to NM, were stained with H&E. One representative section from 3 mice/treatment group is shown (original magnification, x400; Bar, 50 μ m). Epidermis (E), dermis (D), eschar (ES), hair follicles (H), areas of parakeratosis (PK), sebaceous glands (S). Solid arrow indicates basal layer with pyknotic nuclei. Asterisk indicates inflammatory infiltrate within eschar.

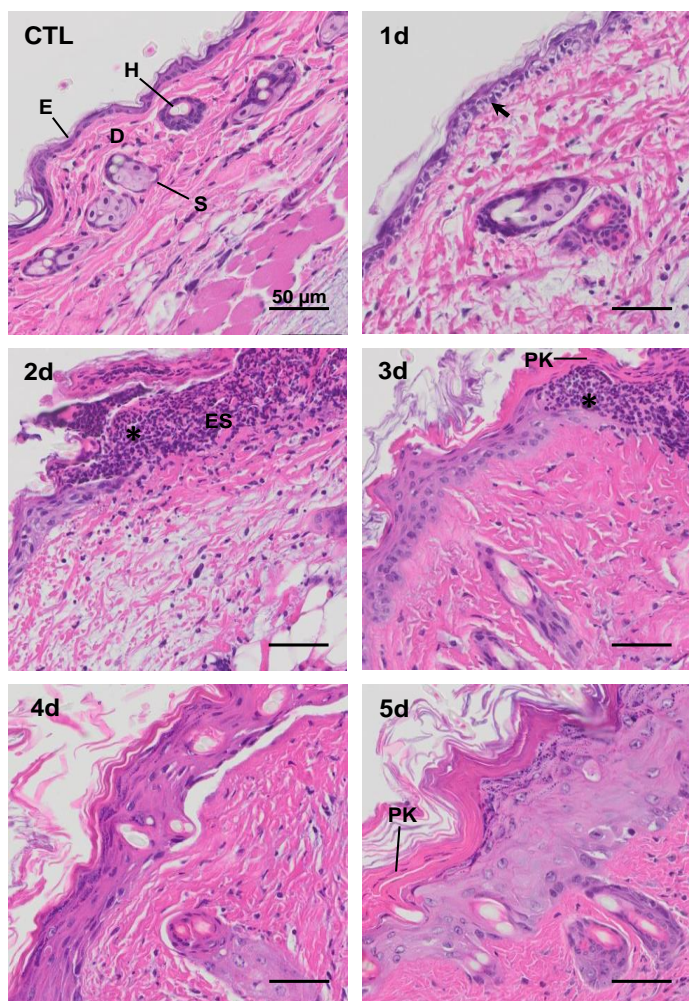


Figure 4. Effects of nitrogen mustard on CB1 receptor expression. Histological sections, prepared after exposure to control (CTL) or 1, 2, 3, 4, and 5 days after exposure to NM, were stained with an antibody to CB1 receptor. One representative section from 3 mice/treatment group is shown. Antibody binding was visualized using a Vectastain Elite ABC kit (original magnification, x 400; Bar, 50 μ m). Epidermis (E), dermis (D), hair follicles (H), sebaceous glands (S), eschar (ES). Solid arrow indicates epidermal expression of CB1 receptor; open arrow indicates CB1 expression in hair follicle; arrowhead indicates CB1 expression in sebaceous glands; asterisk indicates inflammatory infiltrate within the eschar.

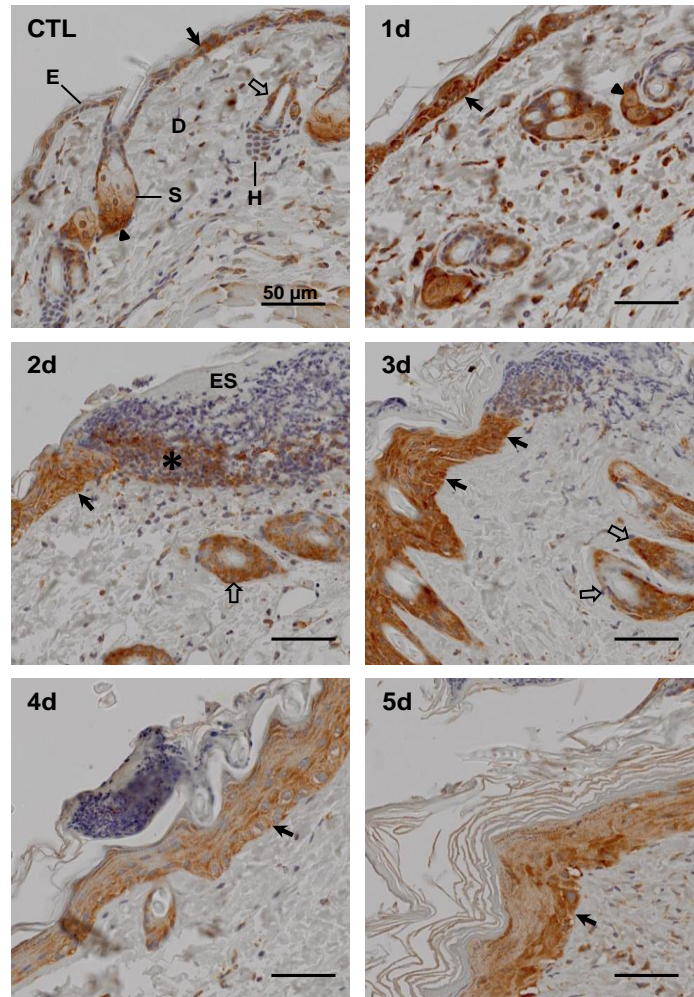


Figure 5. Effects of nitrogen mustard on CB2 receptor expression. Histological sections, prepared after exposure of mice to control (CTL) or 1, 2, 3, 4, and 5 days after exposure to NM, were stained with an antibody to CB2 receptor. One representative section from 3 mice/treatment group is shown. Antibody binding was visualized using a Vectastain Elite ABC kit (original magnification, x 400; Bar, 50 μ m). Epidermis (E), dermis (D), hair follicles (H), sebaceous glands (S), eschar (ES). Solid arrow indicates epidermal expression of CB2 receptor; open arrow indicates CB2 expression in hair follicle; arrowhead indicates CB2 expression in sebaceous glands.

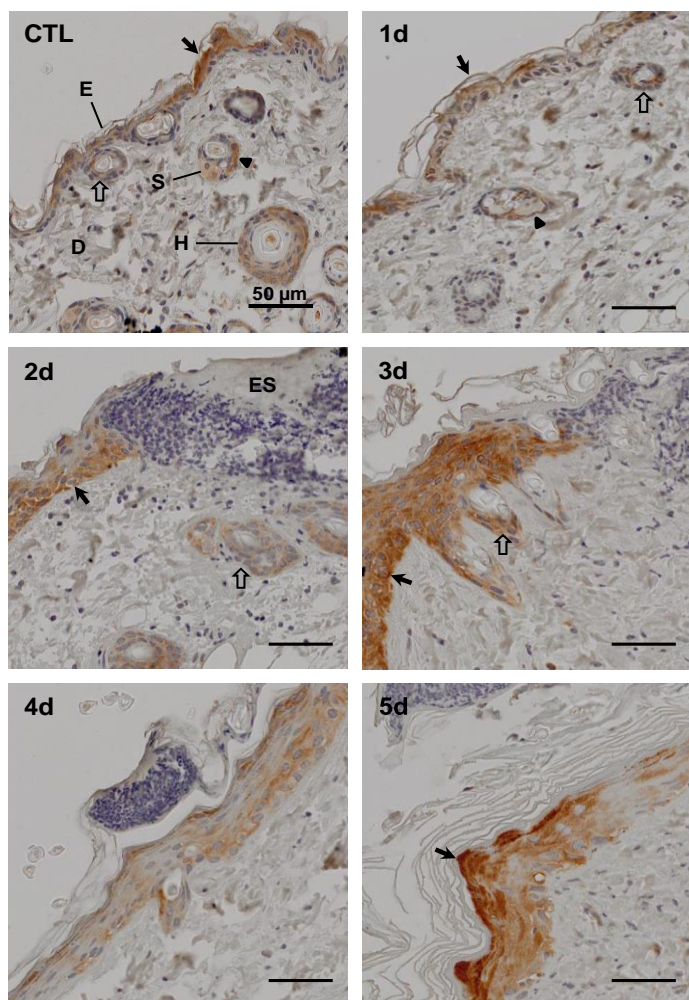


Figure 6. Effects of blocking peptides on FAAH, CB1, CB2, and PPAR α antibody binding to tissue sections. Left panels: histological sections prepared 3 days after exposure to NM were stained with antibodies to CB1 (a), CB2 (c), PPAR α (e), or FAAH (g). Right panels: histological sections treated with antibodies and respective blocking peptides to CB1 (b), CB2 (d), PPAR α (f), and FAAH (h). One representative section from 3 mice/treatment group is shown. Antibody binding was visualized using a Vectastain Elite ABC kit (original magnification, x 400; Bar, 50 μ m).

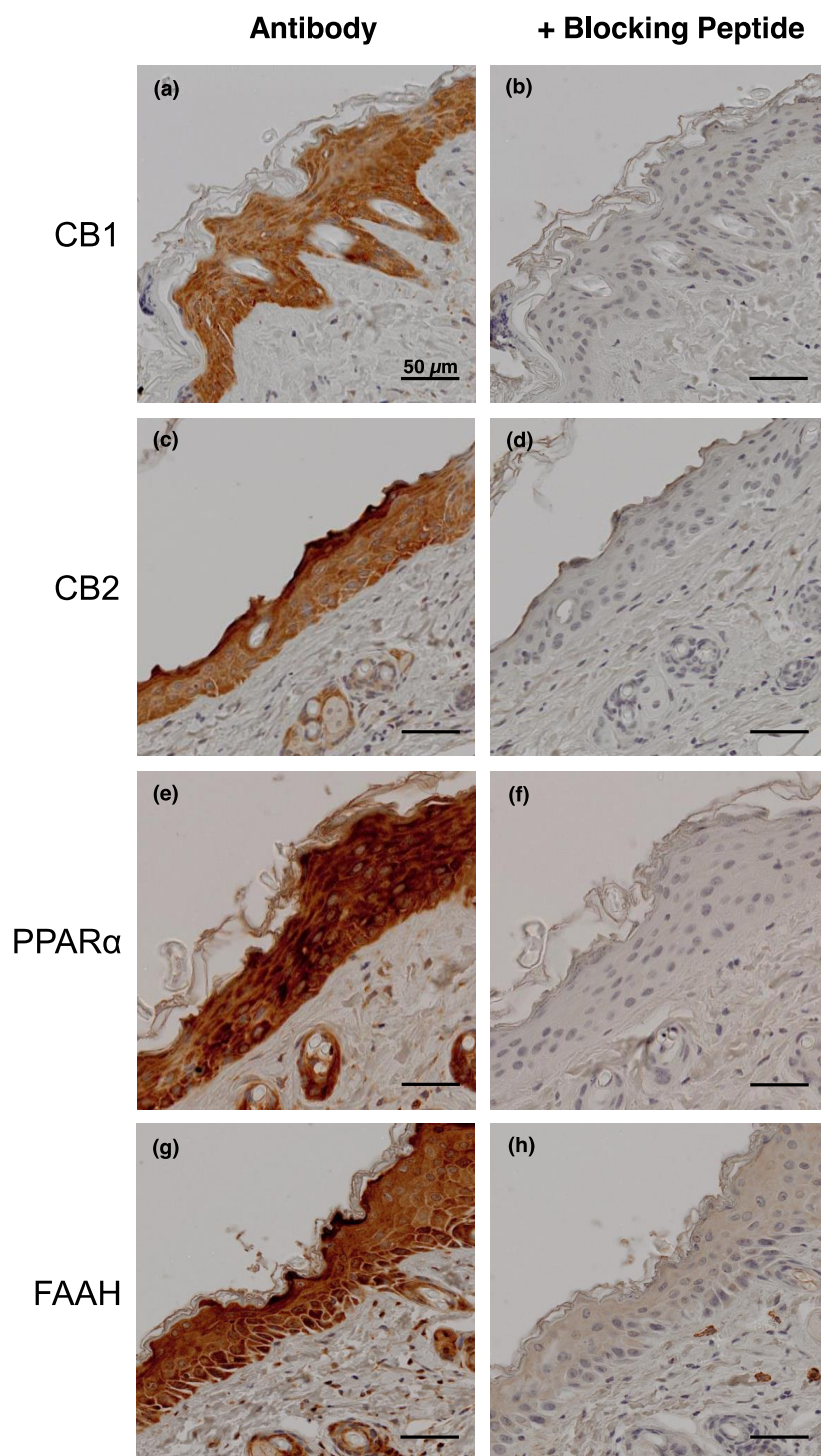


Figure 7. Effects of nitrogen mustard on PPAR α expression. Histological sections, prepared after exposure of mice to control (CTL) or 1, 2, 3, 4, and 5 days after exposure of mice to NM, were stained with antibody to peroxisome proliferator receptor alpha (PPAR α). One representative section from 3 mice/treatment group is shown. Antibody binding was visualized using a Vectastain Elite ABC kit (original magnification, x 400; Bar, 50 μ m). Epidermis (E), dermis (D), hair follicles (H), sebaceous glands (S), eschar (ES), parakeratosis (PK). Solid arrow indicates epidermal expression of PPAR α ; open arrow indicates PPAR α expression in hair follicle; arrowhead indicates PPAR α expression in sebaceous glands; asterisk indicates inflammatory infiltrate within the eschar.

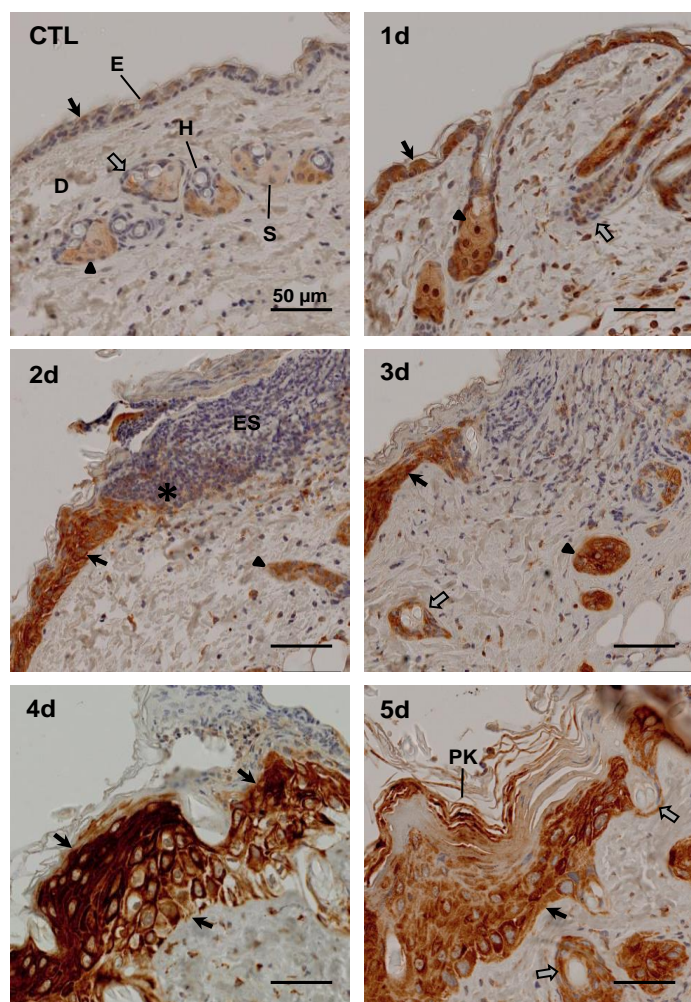


Figure 8. Effects of nitrogen mustard on FAAH expression. Histological sections, prepared after exposure of mice to control (CTL) or 1, 2, 3, 4, and 5 days after exposure of mice to NM, were stained with antibody to fatty acid amide hydrolase (FAAH). Antibody binding was visualized using a Vectastain Elite ABC kit. One representative section from 3 mice/treatment group is shown (original magnification, x 400; Bar, 50 μ m). Epidermis (E), dermis (D), hair follicles (H), sebaceous glands (S), eschar (ES). Solid arrow indicates epidermal expression of FAAH; open arrow indicates FAAH expression in hair follicle; arrowhead indicates FAAH expression in sebaceous glands.

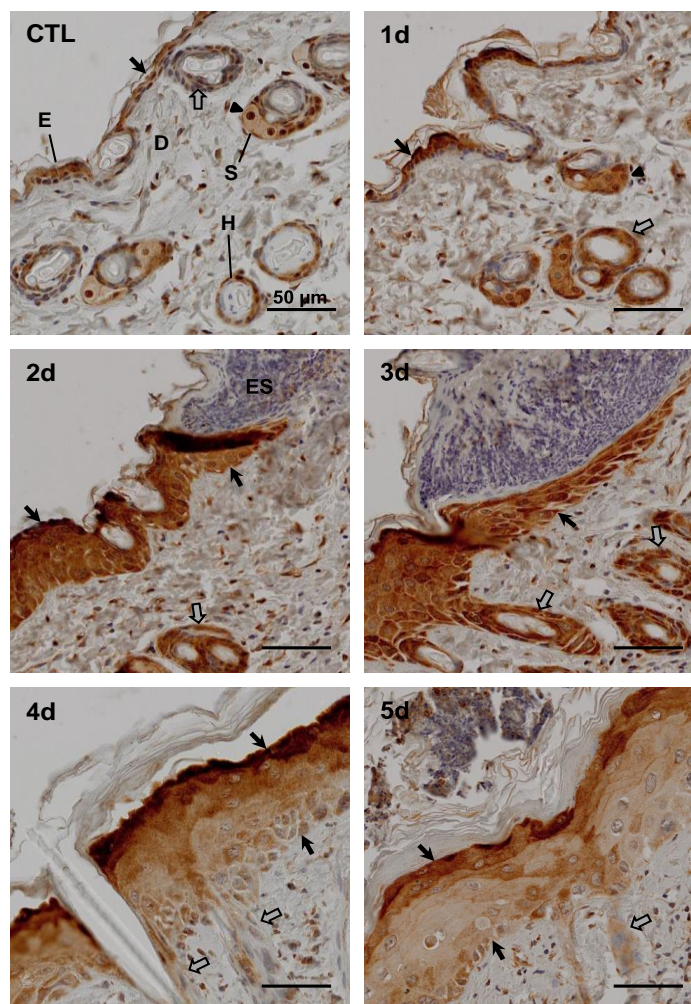


Figure 9. Structural changes in mouse skin following SM exposure. Histological sections, prepared after exposure to control (CTL) or 1, 3, 7, 14 and 21 days after exposure of mice to SM, were stained with H&E. One representative section from 3 mice/treatment group is shown (original magnification, x400; Bar, 50 μ m). Epidermis (E), dermis (D), eschar (ES), hair follicles (H), parakeratosis (PK), sebaceous glands (S). Solid arrow indicates basal layer with pyknotic nuclei. Asterisk indicates inflammatory infiltrate within eschar.

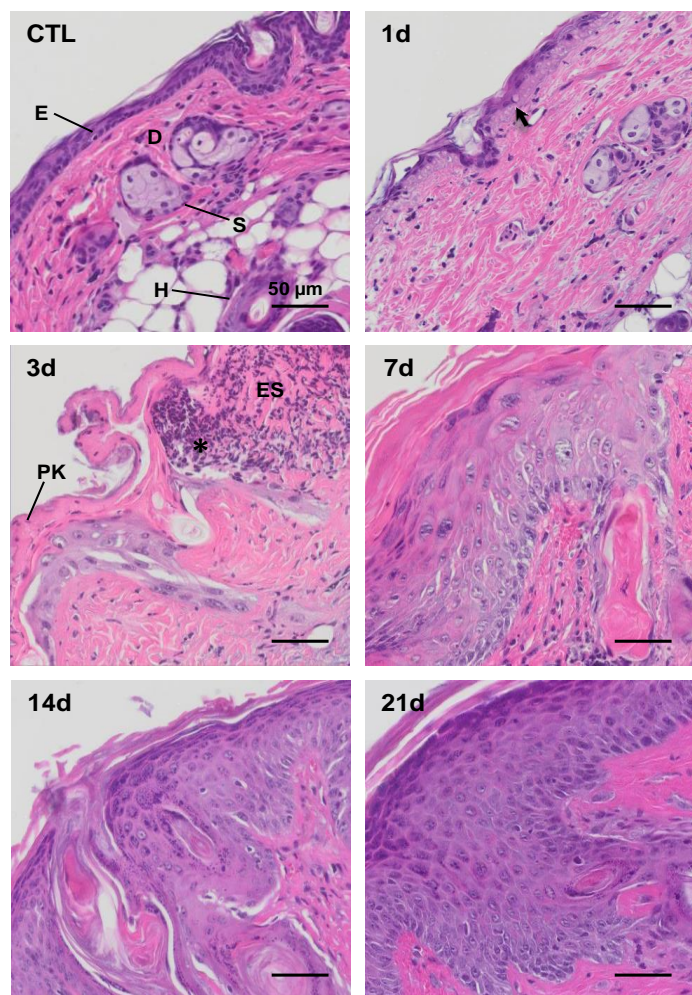


Figure 10. Effects of sulfur mustard on CB1 receptor expression. Histological sections, prepared after exposure to control (CTL) or 1, 3, 7, 14 and 21 days after exposure of mice SM, were stained with antibody to CB1 receptor. One representative section from 3 mice/treatment group is shown. Antibody binding was visualized using a Vectastain Elite ABC kit (original magnification, x 400; Bar, 50 μ m). Epidermis (E), dermis (D), hair follicles (H), sebaceous glands (S), eschar (ES). Solid arrow indicates epidermal expression of CB1 receptor; open arrow indicates CB1 expression in hair follicle; arrowhead indicates CB1 expression in sebaceous glands; asterisk indicates inflammatory infiltrate within the eschar.

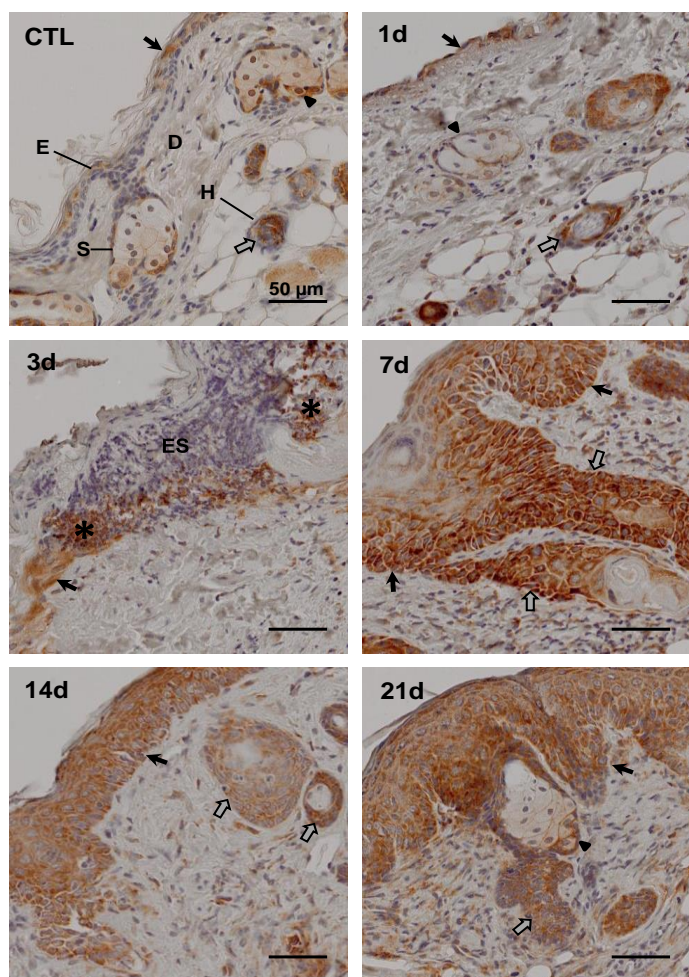


Figure 11. Effects of sulfur mustard on CB2 receptor expression. Histological sections, prepared after exposure to control (CTL) or 1, 3, 7, 14 and 21 days after exposure of mice to SM, were stained with an antibody to CB2 receptor. One representative section from 3 mice/treatment group is shown. Antibody binding was visualized using a Vectastain Elite ABC kit (original magnification, x 400; Bar, 50 μ m). Epidermis (E), dermis (D), hair follicles (H), sebaceous glands (S), eschar (ES). Solid arrow indicates epidermal expression of CB2 receptor; open arrow indicates CB2 expression in hair follicle; arrowhead indicates CB2 expression in sebaceous glands.

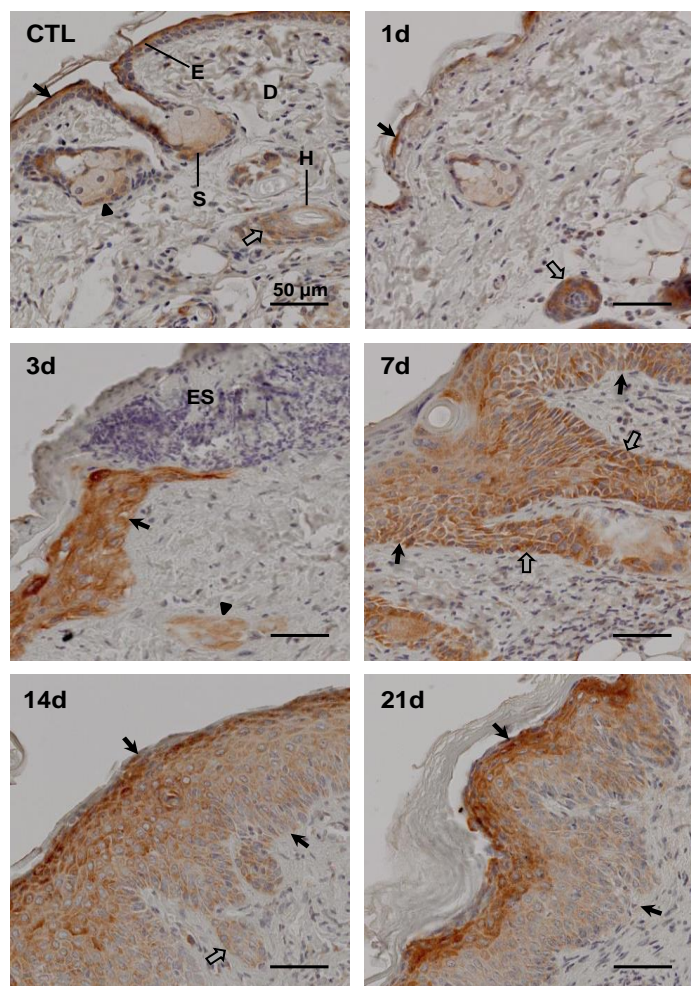


Figure 12. Effects of sulfur mustard on PPAR α expression. Histological sections, prepared after exposure to control (CTL) or 1, 3, 7, 14 and 21 days after exposure of mice to SM, were stained with antibody to PPAR α . One representative section from 3 mice/treatment group is shown. Antibody binding was visualized using a Vectastain Elite ABC kit (original magnification, x 400; Bar, 50 μ m). Epidermis (E), dermis (D), hair follicles (H), sebaceous glands (S), eschar (ES), parakeratosis (PK). Solid arrow indicates epidermal expression of PPAR α ; open arrow indicates PPAR α expression in hair follicle; arrowhead indicates PPAR α expression in sebaceous glands.

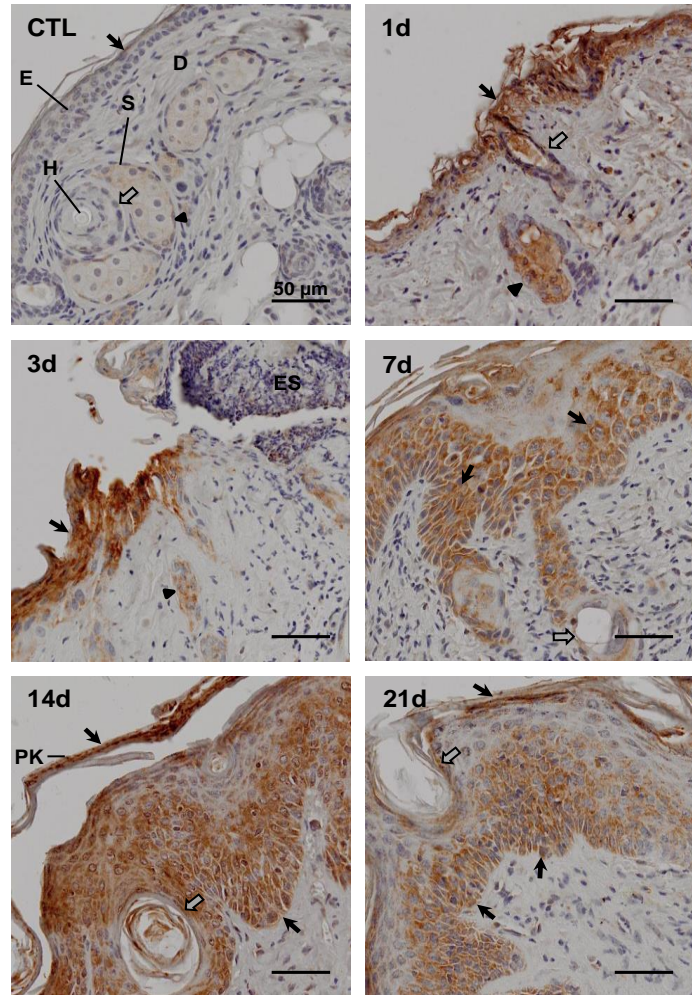
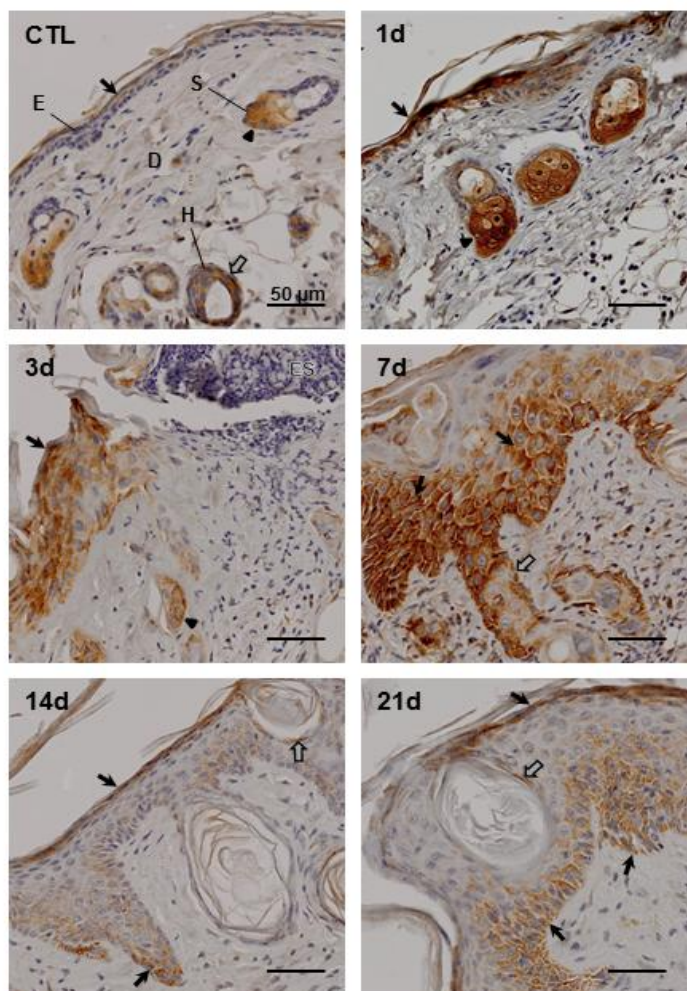


Figure 13. Effects of sulfur mustard on FAAH expression. Histological sections, prepared after exposure to control (CTL) or 1, 3, 7, 14 and 21 days after exposure of mice to SM, were stained with antibody to fatty acid amide hydrolase (FAAH). Antibody binding was visualized using a Vectastain Elite ABC kit. One representative section from 3 mice/treatment group is shown (original magnification, x 400; Bar, 50 μ m). Epidermis (E), dermis (D), hair follicles (H), sebaceous glands (S), eschar (ES). Solid arrow indicates epidermal expression of FAAH; open arrow indicates FAAH expression in hair follicle; arrowhead indicates FAAH expression in sebaceous glands.



PART 2: Specific Aim 3.

The third aim was to determine whether inhibition of FAAH suppresses the inflammatory response to CEES or TPA exposure in mouse skin, and which classes of inhibitors were most effective. Our group synthesized several classes of candidate therapeutics by combining vanillyl alcohols and amides to various alkyl and aryl/ring groups or NSAIDs using a carbamate linker (Classes I-IV). Carbamates are derivatives of carbamic acid, effective as FAAH inhibitors with anti-inflammatory and anti-nociceptive properties *in vivo* (Kathuria *et al.*, 2003; Alexander and Cravatt, 2005). Vanilloids, analogs of capsaicin that bind and block TRPV1 receptors, have also successfully reduced pain and inflammation in animal models (Janusz *et al.*, 1993; Walpole *et al.*, 1993; Szallasi *et al.*, 2007). Combining both moieties as described above generated pharmacologically active compounds that were effective as FAAH inhibitors and potent suppressors of inflammation in the MEVM. Additional bifunctional compounds were prepared by conjugating NSAIDs and AChEIs using carbamate or carbamate ester linkers. Given that NSAIDs and AChEIs individually inhibit the serine hydrolases FAAH and acetylcholinesterase, we assayed these bifunctional compounds for FAAH inhibitory activity as well as inhibition of inflammation in the MEVM.

1. EXPERIMENTS

a. FAAH Inhibitor Assays

The preparation of the candidate anti-inflammatories was done by the Heindel lab and described elsewhere (Laskin, 2012; Laskin, 2013). A fluorescent FAAH Inhibitor Screening Assay Kit (Cayman Chemical Co., Ann Arbor, MI) was used to evaluate the ability of these compounds to inhibit FAAH activity (Ramarao *et al.*, 2005; Wang *et al.*, 2006). Assays were run in triplicate according to the manufacturer's instructions using 96-well plates (Greiner Bio-One, Monroe, NC). Changes in fluorescence were monitored using a SpectraMax M5 microplate reader (Molecular Devices, Sunnyvale, CA) with excitation and emission wavelengths set at 340nm and 450nm, respectively. The calculated log n-octanol/water partition coefficient (cLogP), $P = (\text{amount of cpd. dissolved in octanol} / \text{amount of cpd. dissolved in water})$ was used as a measure of hydrophobicity; the greater the cLogP the more hydrophobic the compound. cLogP values were determined using ChemBioDraw Ultra 12.0 (CambridgeSoft, Perkin Elmer Informatics, Waltham, MA). The IC_{50} , or half maximal inhibitory concentration of each chemical was calculated GraphPad Prism 6.0 (GraphPad Software, San Diego, CA) and are $n=1$; means \pm S.E.M., $n=3$, where applicable.

b. COX-1 & COX-2 inhibitor assays

Compounds containing indomethacin, ibuprofen or naproxen, all well known COX inhibitors, were also assayed for COX activity. Activities of COX-1(purified bovine) or COX-2 (human recombinant) were determined using a COX Colorimetric Inhibitor Screening Assay Kit (Cayman Chemical, Ann Arbor Michigan, USA). All test compounds were dissolved in methanol. Assays were run in duplicate using 96-well plates as per manufacturer's instructions. Change in absorbance was measured in a Perkin-Elmer

HTS 7000 Plus spectrophotometer set at a wavelength of 590 nm. IC_{50} values were calculated using GraphPad PRISM 6.0 (GraphPad Software, San Diego, CA).

c. Acetylcholinesterase inhibitor assay

Candidate anti-inflammatories containing AChEI moieties were assayed for acetylcholinesterase inhibition activity. Cholinesterase inhibition was assayed spectrophotometrically at 412 nm according to the method of Ellman (Ellman *et al.*, 1961). Assays were performed in duplicate using polystyrene 96-well plates (Corning 96-well flat transparent). A solution of 200 μ L of 0.5 mM 5'5-dithio-bis-(2-nitrobenzoic acid) (DTNB) in 100 mM sodium phosphate buffer (pH 8), 30 μ L of inhibitor stock solution prepared in methanol, 50 μ L of 3 mM acetylthiocholine (ATChI), and 20 μ L of 1.25 u/mL of AChE prepared in phosphate buffer 100 mM pH 8 and 20 mM pH 7 buffer, respectively. Immediately after the enzyme was added, the absorption signal was measured at 30 s intervals over 5 min at 25°C in a Tecan's Infinite 200 multimode microplate reader. Percentage inhibition was calculated relative to a methanol control. The background signal was measured in wells containing all of the reagents except for AChE. IC_{50} values were calculated using GraphPad Prism 6.0 (GraphPad Software, San Diego, CA).

2. RESULTS

Effects of FAAH Inhibitors on Skin Inflammation using the MEVM

Compounds are grouped by class and substituent type (Fig. 14), and are listed in order of increasing activity as inhibitors of FAAH. Also included for each class of compounds are the calculated log n-octanol/water partition coefficient (cLogP), $P = (\text{amount of cpd. dissolved in octanol} / \text{amount of cpd. dissolved in water})$ as a measure of a chemical's hydrophilicity or hydrophobicity. Compound cLogP is calculated by first breaking the neutral molecule into smaller chemical fragments, then assessing the bonding environment of each individual fragment and summing the effects of the relationships between each (Hansch *et al.*, 2003). The higher the cLogP, the more hydrophobic the chemical. Since chemical hydrophobicity has been correlated with FAAH inhibitor potency, we included compound cLogP values in our comparison of inhibitor effectiveness. For comparison, anandamide, the primary substrate for FAAH, is highly lipophilic (cLogP=6.3) (Tian *et al.*, 2005).

To assess *in vivo* anti-inflammatory activity, we used the mouse ear vesicant model (MEVM) as described in the Experiments section. The skin inflammatory response to vesicant exposure includes dermal edema, blood vessel congestion, hemorrhage and inflammatory cell infiltration. Increases in ear weight due to inflammation, primarily from edema and swelling, were observed in positive controls. To quantify a compound's ability to suppress inflammation, the weight of chemical-treated ears was compared to the weight of CEES- or TPA-treated ears from positive controls. Values are expressed as percent reduction in ear weight compared to controls (%REW).

a. Class I -Vanillyl alcohol carbamates

The vanillyl alcohol carbamates are 3-methoxy-4-hydroxybenzyl alcohol (vanillyl alcohol) derivatives with an amide conjugated to the alcohol oxygen (Fig. 15). During

synthesis, a carboxylic acid is attached to the phenolic 4-hydroxyl forming an ester to protect against condensation, provide stability, and direct the reaction to form the carbonate. The protective moiety is subsequently hydrolyzed in polar solution. In these studies, we examined the effects of two substituent subclasses conjugated to the carbamate amide nitrogen: cyclic (aryl, cyclohexyl, or heterocyclic rings - Table 1) and alkyl (linear, branched alkanes or alkene - Table 2).

In the cyclic subclass, the phenethyl 4453 was the most effective FAAH inhibitor (14 μM), followed by 2-phenoxyethyl 4452 (31 μM) and cyclohexylmethyl 4455 (93 μM) (Fig. 16). 4464, a hydrophilic morpholinethyl derivative, had minimal effect as an FAAH inhibitor (>800 μM). 4453 was the most active in suppressing CEES-induced increases in ear weight (80%), followed by 4452 (51%) and 4455 (40%). 4464 had little effect in the MEVM, only inhibiting ear swelling by 4%.

Alkyl compounds contained alkane substituents ranging from C_4 (butyl) to C_{12} (dodecyl) (Table 2). 4439, where $\text{R}=\text{C}_{12}$, showed optimal FAAH inhibitory activity within the subclass (9 μM). 4435 ($\text{R}=\text{C}_{10}$) was less effective (62 μM), followed by 4440 ($\text{R}=\text{C}_{10}$), which inhibited FAAH with an IC_{50} of 104 μM . The C_4 compound 4405 was least effective as an inhibitor of FAAH (338 μM) (Fig. 17, Table 2). FAAH inhibitory potency for compounds within the alkyl subclass was correlated with increased lipophilicity and chain length: 4439 (C_{12}) > 4435 (C_{10}) > 4440 (C_7) > 4405 (C_4) (Table 2). The alkyl R-group subclass was less effective overall in the MEVM, but more active against TPA (20-77%) than CEES (7-47%). No obvious correlations were observed between CEES- or TPA-induced inhibition of inflammation and FAAH inhibition, or alkyl chain length. The butyl compound 4405, although the least potent against FAAH, prevented TPA-induced edema by 77%.

b. Class II-Hydroxamates

The hydroxamate class is comprised of two subclasses, N-hydroxylated vanilloid fatty carbamates [(4-hydroxy-3-methoxybenzyl) carbamate] and N-hydroxylated vanilloid fatty amines [(4-hydroxy-3-methoxybenzyl) amine] (Figure 18). As a class, the hydroxamates moderately to weakly inhibited FAAH ($IC_{50}=10\ \mu\text{M}$ -1.56 mM), but were effective in the MEVM against CEES- and TPA-induced edema (mean inhibition of edema: CEES $49 \pm 8.3\%$; TPA $34 \pm 4\%$) (Figure 19, Table 3).

The carbamate subclass showed greater efficacy as FAAH inhibitors, but FAAH inhibitor effectiveness and hydrophobicity did not directly correlate with anti-inflammatory effects (Table 3). 4493, the most effective FAAH inhibitor in this group ($IC_{50}=10\ \mu\text{M}$), was moderately hydrophobic ($c\text{LogP}=2.27$), and effective against CEES (42%). The least effective compound, 4492 ($IC_{50} > 1\text{mM}$) was the least hydrophobic ($c\text{LogP}=0.97$), but was highly effective against CEES-induced inflammation (80%).

Two amines in this class were screened for FAAH inhibitory activity: 4474 (undecenoyl), an 11-carbon alkene with a double bond between C_{10} - C_{11} ; and 4475 (2-hexyldecanoyl), containing a branched alkyl group conjugated to the amide carbonyl (Table 3). 4474 was a weak FAAH inhibitor ($IC_{50}=163\ \mu\text{M}$); 4475 showed little inhibitory activity ($IC_{50}=1.56\text{ mM}$) (Fig. 19). In the MEVM, 4474 was screened against both CEES and TPA, reducing edema by 45% and 26%, respectively. 4475 was screened against TPA, reducing inflammation by 26% compared to positive controls.

However, some correlation was noted between the hydroxamates ability to inhibit FAAH and R-group structure and lipophilicity (Table 3). Incorporation of the O-phenoxy R-group into the hydroxamate structure increased FAAH inhibitor potency. The C_{11} compound containing a C_{10} - C_{11} double bond was less effective than compounds with saturated C_{12} and C_8 R-substituents. Shortening the chain length to C_6 or increasing the

length to C₁₆ further diminished inhibitor effectiveness. Finally, addition of a branched alkyl R-group to the vanillyl amide greatly reduced potency, as did shortening the alkyl chain below C₆. Interestingly, hydroxamates at the upper and lower extremes of cLogP values were moderate to poor FAAH inhibitors.

c. Class III-Vanillyl fatty amides and carbamates

Class III agents are analogs of the hydroxamates lacking an N-hydroxyl group (Figure 20). Vanillyl amide and amide carbamate R-substituents are analogous to those used in Class II compounds. Class III compounds were slightly less hydrophobic than their hydroxamate congeners (*i.e.* cLogP 4369=2.16 vs. cLogP 4493=2.27), but were effective both as FAAH inhibitors and in the MEVM (IC₅₀=3.5 ± 1.8 µM-300 µM; mean inhibition of edema for CEES: 76 ± 4%; TPA: 67 ± 8.0%) (Table 4). Interestingly, 4360, the most hydrophobic (cLogP=8.73) compound in the class, was the least effective as both an FAAH inhibitor (NA), and anti-inflammatory against CEES induced-inflammation (0%), but was active against TPA-induced inflammation (56%).

Two vanillyl amides were assayed for FAAH inhibition activity: 4380 (undecenoyl) and 4379 (2-hexyldecanoyl) (Table 4). Both R-groups are analogous to those presented in their Class II counterparts. The straight-chain undecenoyl substituent was a moderately potent FAAH inhibitor (IC₅₀=65 µM); addition of the branched R-substituent reduced FAAH inhibitory potency to an IC₅₀ of 300 µM. 4380 was very effective in the MEVM against both CEES- (75%) and TPA- (91%) induced edema. The 2-hexyldecanoyl inhibitor was ineffective against CEES, but showed good activity against TPA (76%).

Compounds with carbamate linkage were more effective FAAH inhibitors (Table 4). The O-phenoxy group enhanced FAAH inhibitor potency, resulting in the lowest IC₅₀

of the class (3.5 μM). Addition of an octyl R-group to the carbamate oxygen slightly reduced inhibitory activity ($\text{IC}_{50}=17 \mu\text{M}$). Lauryl, hexyl, and methoxyethyl substituents resulted in compounds that were very similar in potency ($\text{IC}_{50}=43\text{-}66\mu\text{M}$), while the hydrophobic C_{16} cetyl compound was inactive against FAAH. As with the Class II agents, no direct correlations were observed between FAAH inhibition, suppression of inflammation in the MEVM and hydrophobicity.

Interesting comparisons between the Class II and Class III compounds with analogous R-groups were observed. Varying compound R-substituents affected FAAH inhibitor potency less in Class II than in Class III compounds. Only one Class II compound showed an IC_{50} in FAAH assays as greater than 300 μM while three Class III inhibitor IC_{50} s that were greater than 300 μM , two were over 1 mM. Both the Class II and Class III compounds with an O-phenoxy group on the amide carbonyl were the most effective FAAH inhibitors (Tables 3 and 4). The vanillyl amide 4369 was a slightly more effective FAAH inhibitor than the hydroxamate 4493 (Table 5), but much more effective against CEES in the MEVM. Interestingly, in both classes, compounds at the extremes of hydrophilicity and hydrophobicity were less effective FAAH inhibitors, and less effective in the MEVM against both CEES and TPA with the exception of 4492. FAAH IC_{50} values for alkyl Class II and Class III agents were greater than IC_{50} s in the O-phenoxy compounds, but less than the 2-hexyldecanoyl compounds.

d. Class IV-Olvanil-NSAID

NSAIDs including ibuprofen and indomethacin (Fig. 21), and olvanil, a structural analog of capsaicin, have been reported to inhibit FAAH (Holt *et al.*, 2007; Bertolacci *et al.*, 2013). Increased COX-2 metabolism of AEA in FAAH (-/-) mice has been observed, and given that COX-2 is upregulated during inflammation, a dual-action inhibitor

containing an FAAH inhibitor and an NSAID would be a desirable candidate to treat inflammatory conditions (Weber *et al.*, 2004; Jhaveri *et al.*, 2008). The olvanil-NSAIDs are a combination of these two groups, comprised of an NSAID conjugated to a vanillyl amide carbamate and an O-phenoxy attached to the amide carbonyl (Figs. 22 and 23). Compounds were screened for FAAH, COX-1, COX-2 and AChE inhibition *in vitro*, and against CEES- and TPA-induced inflammation in the MEVM (Table 6). The olvanil-NSAIDs were potent FAAH inhibitors, and effective against CEES- and TPA-induced inflammation in the MEVM. Class IV compounds inhibited FAAH with a similar potency to URB597, a well-studied FAAH inhibitor with carbamate linkage (Table 6, Fig. 24). Compound 4369, the vanilloid without an NSAID group and the most hydrophilic, was less potent as an FAAH inhibitor and less effective at inhibiting TPA-induced inflammation (46%). All three Class IV compounds were effective against CEES-induced inflammation; 4369 > (76%) > 4495 (58%) > 4496 (23%) (Table 6). 4495 and 4496 were exceptionally potent against TPA (82% and 97%, respectively). 4369 and 4495 were inactive against COX-1, while 4496 showed weak inhibitory activity ($IC_{50}=170\pm2.2\ \mu\text{M}$). The three compounds differed in COX-2 inhibitory effectiveness (4369, NA; 4495 $IC_{50}=238\pm0.16\ \mu\text{M}$; 4496 $IC_{50}=0.11\pm0.01\ \mu\text{M}$). Pharmacological characterization has shown URB597 has no significant inhibitory activity against either COX isoform or AChE (Piomelli *et al.*, 2006). 4495 and 4496 were effective against AChE ($4.5\pm1.04\ \mu\text{M}$ and $0.63\pm0.03\ \mu\text{M}$, respectively), 4369 did not inhibit AChE.

Ibuprofen and indomethacin were weakly effective against FAAH in our assay; the indomethacin IC_{50} for FAAH inhibition was greater than $500\ \mu\text{M}$, while ibuprofen had little inhibitory effect below an IC_{50} of $1.0\ \text{mM}$ (Table 7, Fig. 25). Previous studies have reported modest FAAH inhibitory activity for these chemicals at lower pH levels (6.0 - 7.5) (Holt *et al.*, 2001; Fowler *et al.*, 2003; Bertolacci *et al.*, 2013), so the alkaline pH

conditions of our assay (pH 9.0) may have affected NSAID potency. NSAID IC_{50} values for COX-1 and COX-2 inhibition were: ibuprofen, NA and $0.11 \pm 0.25 \mu M$; indomethacin, $0.415 \pm 0.02 \mu M$, $6.49 \pm 0.07 \mu M$, respectively. Indomethacin was inactive in the AChE assay and ibuprofen was not tested.

The O-phenoxy leaving group increased both FAAH inhibitor potency and inflammation suppression in the MEVM (Table 8). Compound 4497, a vanillyl amide with an O-phenoxy group on the amide carbonyl actively inhibited FAAH ($IC_{50} = 0.64 \pm 0.3 \mu M$), and was effective in suppressing both CEES- and TPA-induced inflammation (63% and 97%, respectively). 4500, a compound of similar structure to 4497 but with the phenyl bound directly to the amide carbonyl and no oxygen atom, was ineffective as a FAAH inhibitor ($IC_{50} > 1 mM$) and against CEES-induced inflammation, and only moderately effective against TPA (Table 8, Fig. 26). Further structural comparisons between the O-phenoxy compounds revealed that addition of a second amide carbonyl group to the vanillyl amide structure of 4369 greatly reduced inhibitor effectiveness (FAAH $IC_{50} > 1 mM$), but did not affect its anti-inflammatory activity in the MEVM against CEES or TPA (Table 8, Fig. 27).

e. Class V(a) and V(b) - NSAID-AChEI conjugates

Anti-inflammatories combining an NSAID and a reversible acetylcholinesterase inhibitor have proved effective in treating vesicant-induced inflammation (Amitai *et al.*, 2006). BChE, AChE and FAAH are serine hydrolases targeted by organophosphate agents, and recent studies indicate AEA, PEA and OEA are either uncompetitive or noncompetitive inhibitors of BChE (Quistad *et al.*, 2001; Romani *et al.*, 2011). Given the interactions between endocannabinoids and the cholinergic system and the effects of both on inflammation, we screened the NSAID-AChEI compounds for FAAH inhibition. Compounds were chosen from two subclasses (Fig. 28): one comprised of a choline

bioisostere (X=C) linked to indomethacin by an ester carbonate (4338) (Figure 29); and two comprised of galantamine directly linked to an NSAID by an ester, the NSAID conjugate either (4461) naproxen or (4462) indomethacin (Fig. 30) (Laskin, 2012). Compounds were also screened for AChE, COX-1, COX-2 inhibition, and for suppression of inflammation in the MEVM. Results are presented in Table 9, and Figures 31 and 32.

Results varied for the carbonate-ester 4338. Initial assays showed it was the most effective against FAAH ($IC_{50}=0.82\ \mu M$), however due to solubility difficulties subsequent assays were inconclusive (Table 9, Fig. 31). The two galantamine esters were moderately active against FAAH, 4461 more potent than 4462 (Table 9). FAAH inhibitory effectiveness was negatively correlated with COX-1 inhibition; no obvious correlations between FAAH inhibition and the other endpoints were observed. Interestingly, the indomethacin-choline bioisostere conjugate 4338 was more active against COX-2 than COX-1, while 4462, comprised of indomethacin and galantamine, showed more activity against COX-1. Compound AChEI activity from greatest to least was 4462 > 4338 > 4461; the two indomethacin conjugates more effective than naproxen-galantamine. All three effectively reduced CEES- and TPA-induced edema and inflammation by between 58% and 97% (Table 9).

3. DISCUSSION

The third aim of these studies was to assay FAAH inhibitors as suppressants of vesicant-induced injury in the MEVM. FAAH is inhibited by classical serine hydrolase inhibitors including various amides, ketones, and carbamate derivatives possessing lipophilic components and highly electrophilic carbonyls (Lodola *et al.*, 2011; Otrubova *et al.*, 2011). It is also inactivated by organophosphate pesticides, some of which are AChE and BuChE inhibitors, for example chlorpyrifos oxon, paraoxon; oleyl-, dodecyl- and octyl-benzodioxaphosphorin (BDPO) oxides; and the phosphonofluoridates – methyl arachidonoyl phosphonofluoridate (MAPF) and ethyl octylphosphonofluoridate (EOPF) (Quistad *et al.*, 2001). Using pharmaceutical agents from the classes described below, our group designed and synthesized bifunctional compounds as topical anti-inflammatories to suppress vesicant-induced edema.

Various pharmacological agents have been efficacious in protecting against or reducing SM-induced skin injury in animal models (Sabourin *et al.*, 2000). Some of the agents decreasing the inflammatory response to SM include vanilloids (octyl homovanillamide or olvanil derivatives), NSAIDs (indomethacin, celecoxib), antioxidants (*N*-acetyl cysteine, vitamin E, sulforaphane) and anticholinesterase inhibitors (galantamine, diclofenac) (Casillas *et al.*, 2000; Sabourin *et al.*, 2000; Han *et al.*, 2004; Paromov *et al.*, 2007; Black *et al.*, 2010b). Several of these agents were studied by our group in the MEVM for effectiveness against CEES.

Pretreatment with vanilloids prior to SM exposure significantly reduced edema, inhibited leukocyte migration and downregulated mRNA expression of the proinflammatory cytokines IL-1 β and IL-6 (Babin *et al.*, 2000; Sabourin *et al.*, 2000). Vanilloids modulate skin inflammation by disrupting release of neuropeptides (Substance P and neurokinin A) from skin sensory fibers, blocking their vasodilative activity, possibly

by binding to TRPV-1 receptors (Szallasi *et al.*, 2007). They are analogs of capsaicin, a compound originally isolated from hot chili peppers.

NSAIDs celecoxib and indomethacin were assayed in the MEVM against CEES, and found to reduce inflammation and edema (Casillas *et al.*, 2000; Wormser *et al.*, 2004). Arachidonic acid and its proinflammatory COX-2 and LOX metabolites are reported to play a role in vesicant-induced edema, possibly by increasing capillary permeability to allow influx of kinins, complement and fibrin into the dermis (Rikimaru *et al.*, 1991; Black *et al.*, 2010b).

a. Class I – Vanillyl alcohol carbamates

Several of the vanillyl alcohol carbamates (4439, 4452 and 4453) were effective inhibitors of FAAH activity, and also inhibited inflammation in the MEVM. Vanillyl amine (*i.e.*, 3-hydroxy-4-methoxybenzylamine or vanillyl amine) and vanillyl alcohol (*i.e.*, 3-hydroxy-4-methoxybenzyl alcohol or vanillyl alcohol) are well-known elements in anti-inflammatory compounds (Pal *et al.*, 2009c; Tomohiro *et al.*, 2013). Vanillyl alcohol itself is a natural anti-inflammatory found in ginger and in a wide variety of other botanicals used as an additive in foods, pharmaceuticals, and cosmetics (Jung *et al.*, 2008; Khallouki *et al.*, 2011; Tai *et al.*, 2011; Raffai *et al.*, 2015). Most of the reported candidate FAAH inhibitors have been carbamates and amides of vanillyl amine; few studies have been performed using vanillyl alcohols in conjugate systems (Costa *et al.*, 2010; Malek *et al.*, 2015). The vanillyl alcohol carbamates (4452, 4453, 4455, and 4464) were all synthesized from vanillyl alcohol with the lipophilic (fatty amine) side chain derived from phenethyl, phenoxyethyl, cyclohexylmethyl, and morpholinylethyl (Laskin, 2013). Varying the hydrocarbon amine side chain allows manipulation of overall molecular lipophilicity. In addition, acetylating the para-phenol hydroxyl on the vanilloid

greatly increases shelf life of these inhibitors while having no effect on their biological activity.

Three channels connecting the catalytic site of FAAH to the enzyme's periphery have been reported: a membrane access channel (MAC), leading to a protein surface opening at the membrane bilayer; an acyl-chain binding pocket (ABP); and a cytosolic port (CP) (Mor *et al.*, 2004; Min *et al.*, 2011). The CP is theorized allow entry of water molecules leading to the catalytic center and exit of polar reaction products while the MAC and ABP create a wide channel that is mainly hydrophobic on one side and somewhat polar on the other (Min *et al.*, 2011). The carbamates evaluated in our study clearly show the importance of the hydrophobic-hydrophilic balance for inhibitor activity.

Of the vanillyl alcohol derivatives, compound 4439 was not only the most lipophilic, but also the best FAAH inhibitor and an effective inflammation suppressant in the MEVM, while the water soluble 4464 was ineffective. Other groups have reported that an aryl moiety proximal to the carbonyl site contributes to FAAH inhibitory activity and in one study, inhibitor activity was related experimentally to electron density in the aryl ring, further supporting its importance in site-binding (Keith *et al.*, 2012; Keith *et al.*, 2014). The weak activity against FAAH found in our non-arylated compounds (4455 and 4464) may be due to the lack of an essential planar phenyl ring in their molecular structures.

Another factor influencing the potency of FAAH inhibitors and their anti-inflammatory effects is the length of the alkane R-group. Previous studies using vanillylamine amides showed that the anti-inflammatory potency of these compounds increased with increasing chain length, with an optimum of 8-12 carbons (Janusz *et al.*, 1993; Walpole *et al.*, 1993). Overall size and hydrophobicity contributed more to efficacy than addition of unsaturation or branched-chain elements. Increasing the side chains to greater than 12 carbons showed a progressive reduction in activity, while increasing the

number of carbons from C₂-C₈ improved efficacy (Janusz *et al.*, 1993; Walpole *et al.*, 1993). FAAH inhibitory activity appears to follow a similar trend; Boger *et al.* reported an optimum fatty acid chain length of 8-12 carbons (Boger *et al.*, 2000; Otrubova *et al.*, 2011). Our results for the class I inhibitors were similar as shown in Table 2, in order of increasing IC₅₀: dodecyl>decyl>heptyl>butyl.

b. Class II – Hydroxamates and Class III – Vanillyl Amides

The Class II compounds are vanillyl amides and with a hydroxyl group on the amide nitrogen, and R-substituents conjugated to the amide carbonyl carbon. The analogous Class III compounds differ only by lack of the hydroxyl group. O-conjugation creates a carbamate compound. Because these two classes are similar, we compared FAAH inhibitory and inflammation suppression ability between compounds with the same substituents.

A few trends were immediately visible, one, that the vanillyl amide inhibitors were more effective as a class than the hydroxamates against FAAH. If the proposed mechanism of catalysis is correct, the vanillyl amide portion of the molecule would remain bound in the active site, and the substituents would act as leaving groups. It is possible that the nucleophilic hydroxyl oxygen interferes with catalysis, perhaps slightly destabilizing the acyl enzyme intermediate by bridging to the proton on the hydroxyl, and affecting donation of electrons to the leaving group. It may also react with water molecules positioned in the active site as “guides” to position the reactive nucleophile to approach at an optimal angle, then the nucleophile to attack the reactive carbonyl at an optimal angle for catalytic efficiency (Mileni *et al.*, 2010). The Class III compounds are only slightly more hydrophobic than their Class II counterparts, so hydrophobicity or “fattiness” would not play a significant role in differences in FAAH activity.

The first three compounds in each class were comparable; the O-phenoxy substituent compounds the most potent in both classes, followed by the octyl and dodecyl/lauryl compounds, which were moderately effective. All three are carbamates with IC_{50} s in the low micromolar range, all below 75 micromolar. The R-groups conferred slightly different potencies depending on class: in Class II the dodecyl substituent compound was slightly more effective, in Class III the octyl. The linear dodecyl/lauryl and octyl substituents fell within the optimal 8-12 carbon range for inhibitory effectiveness.

Interestingly, R-groups on the next two inhibitors in each class are similar, one an undecanoyl and the other a hexyl. Again, the R-groups conferred different potencies depending on class; in Class II the undecanoyl was more effective, while in Class III the hexyl. A notable increase in IC_{50} s occurred within this group of Class II compounds compared to the previous group of three inhibitors, IC_{50} s for both the undecanoyl and hexyl increased to over 100 micromolar. This increase was not apparent in the Class III chemicals, whose IC_{50} s remained below 75 micromolar. In these classes of compounds, the substituent is the leaving group. Since the effect of substituent type on FAAH inhibition is following a general trend in both compound classes, it's possible the hydroxyl may have an effect on formation and release of the leaving group. Hydrophobicity as measured by cLogP may only play a small role in inhibitory activity here, given the wide range of cLogP values calculated for all compounds from both classes discussed thus far. The effects are more likely due to how the molecular regions of the compound interact with residues inside the active site to position and then react with the molecule.

Hydrophobicity may play a greater role in the potency of the last three compounds listed in both groups. All are at the extremes of hydrophobicity/hydrophilicity: the hydrophilic Met substituent compounds below 1.0, then

the hydrophobic 2-hexyldecanoyl at 7.32 and 7.59; and cetyl at 8.73 and 8.77. Too much “fattiness” would interfere with binding to hydrophilic residues within the active site, too little would have the opposite effect, both greatly reducing potency. Surprisingly, the Met compound in the Class III group showed moderate inhibitory activity, while the Class II compound with this substituent was practically inactive as an FAAH inhibitor. Activity of the Class III 2-hexyldecanoyl substituent compound was low compared to the other members of its class, but was much greater than its Class II analog. Although these compounds are amides instead of carbamates, removing the hydroxyl group again improved FAAH inhibitory potency.

We found no obvious correlations in our study between FAAH inhibition, anti-inflammatory activity and lipophilicity in the hydroxamate compounds. However, these hydroxamates are potent chelating agents which form tight, colored complexes with iron, zinc, and other metal ions. A correlation between our hydroxamates and inhibition of ADAM17 (MMP-linked enzyme with a metal ion) has been observed in the healing of mustard induced injury in the rabbit cornea (Gordon, 2013). Some metal ions such as Hg^{2+} , Cu^{2+} , and Co^{2+} were reported to potently inhibit an amide hydrolase while others (Mg^{2+} and Mn^{2+}) greatly increased enzymatic activity (Shen *et al.*, 2012). The enzyme was inhibited by up to 20-30% by chelating agents such as EDTA and 1,10-phenanthroline. Thus, the lack of an obvious correlation between anti-inflammatory activity and FAAH inhibition may be partially due to the activities of chelating agents and exogenous metal ions involved in amidase hydrolysis, and the fact that these hydroxamates may act on other targets (ADAM17 and/or MMPs) to inhibit CEES-induced inflammation *in vivo*.

c. Class IV – Olvanil-NSAID

Dual inhibition of COX-2 and FAAH has been suggested to suppress inflammation by preventing the cyclooxygenation of both AEA and AA and the subsequent formation of prostamides and prostaglandins, as well as allowing the increase of anti-inflammatory endocannabinoids such as AEA (Favia *et al.*, 2012; Grim *et al.*, 2014). Additional benefits might include reduction of NSAID-produced gastric damage and other unwanted side effects characteristic of NSAIDs (Cipriano *et al.*, 2013). Compounds 4369 and 4495 showed low inhibitory activity toward COX-2 ($238 \pm 0.16 \mu\text{M}$ and NA), but 4496 inhibited COX-2 with an IC_{50} of $110 \pm 0.01 \text{ nM}$, suggesting this molecule could function as a dual FAAH-COX-2 inhibitor. Although 4496 was slightly less effective against FAAH than 4495, the combined effect of inhibiting both enzymes may make it a more desirable candidate as an anti-inflammatory drug. Both 4495 and 4496 inhibited AChE ($4.5 \pm 1.04 \mu\text{M}$ and $0.63 \pm 0.03 \mu\text{M}$, respectively). AChE is produced by keratinocytes during inflammation, and may modulate epidermal differentiation, proliferation and apoptosis (Grando, 1997). AChE inhibition has previously been proven effective in suppressing vesicant-induced inflammation and may play a role in the potency of these compounds in the MEVM.

The NSAID-olvanils were our most potent FAAH inhibitors, and among the most effective in the MEVM in protecting from chemical-induced inflammation. The vanillyl alcohol compound 4369 possessed moderate FAAH inhibitory activity (in the low micromolar range), and some effectiveness in the MEVM. Attaching the NSAID moiety to the vanillyl alcohol resulted in a compound with increased hydrophobicity, a property correlated with effective FAAH inhibition. An additional benefit of conjugating the two molecules is the addition of an amide to the NSAID providing not only an amide bond, the preferred substrate of FAAH, but also a carbonyl for nucleophilic attack and

carbamoylation by S241, an important hydrolysis step. In addition, the vanillyl alcohol phenoxy is a stable leaving group, increasing efficiency of hydrolysis.

Additional structural modifications were performed to the vanillyl amide to enhance inhibitor potency. Compound 4497, consisting of the vanillyl amide with the O-phenoxy and an additional carbonyl, but no NSAID substituent, potently inhibited FAAH and was effective against both CEES and TPA in the MEVM (Table 8). The importance of the O-phenoxy leaving group is evident when 4497 is compared to 4500, the same compound without the O-phenoxy. Not only was 4500 inactive as an FAAH inhibitor, but was also inactive against CEES. It was 56% active against TPA.

4369, the olvanil portion of the olvanil-NSAIDs, effectively both inhibited FAAH and suppressed CEES- and TPA-induced inflammation. Adding an amide resulted in an increase in IC₅₀ to over 1.0 mM, but in this case the compound retained its anti-inflammatory effectiveness against both CEES- and TPA-induced edema (Table 8).

d. Class V(a) and V(b) – Ester carbonates and Galantamine esters

Although most of the FAAH inhibitors studied to date are analogs of AEA, amides, ureas and carbamates, an amide moiety is not always necessary for inhibition (Seierstad and Breitenbucher, 2008). In addition, FAAH is inactivated by organophosphate pesticides, serine hydrolase inhibitors which also inhibit acetylcholinesterase and butyrylcholinesterase (Quistad *et al.*, 2001).

Keratinocytes possess a functional cholinergic system and produce acetylcholine (AChE) during inflammation (Grando, 1997; Amitai *et al.*, 2006). Nicotinic AChRs are coupled to regulation of Ca²⁺ flux and intracellular metabolism, controlling adhesion and motility (Nguyen *et al.*, 2000). Both muscarinic and nicotinic agonists were reported to protect keratinocytes against acantholysis (loss of intracellular connections, *i.e.* desmosomes) induced by the autoimmune blistering disease pemphigus vulgaris (PV).

Treatment with and AChEI and NSAID conjugate (DICLO-PD) was reported to decrease SM-induced vacuoles, edema and epidermal necrosis (Amitai *et al.*, 2006). Taken together, these results suggest a role for AChE inhibition in the treatment of vesicant-induced injury.

Recent studies by our group agree with earlier work by Amatai et al, who reported that conjugates of NSAID-acetylcholinesterase inhibitor could suppress SM-induced inflammation (Young *et al.*, 2010; Young *et al.*, 2012). Bifunctional compounds tested by the Amitai group consisted of either ibuprofen or diclofenac conjugated to the AChEI pyridostigmine by an octyl or decyl hydrocarbon chain spacer. Prodrug compounds developed by our group are comprised of either a choline bioisostere and NSAID conjugated by an ester-carbonate linker; a choline bioisostere conjugated to an NSAID by an ester; or an AChEI conjugated to an NSAID by an ester (Young *et al.*, 2012). Serine hydrolases typically metabolize esters at greater rates than amides, but the unusual catalytic triad of FAAH allows for hydrolysis of both amides and esters at similar rates (McKinney and Cravatt, 2003). Given that FAAH has esterase activity which could activate these prodrugs, and that some organophosphate pesticides and related compounds which inhibit AChE also inhibit FAAH, we assayed these chemicals for FAAH inhibitory activity.

Compounds from all three groups were highly potent suppressers of CEES-induced inflammation in mouse skin. 4462, a conjugate of indomethacin and the anti-cholinergic galantamine, displayed significant inhibition against CEES and TPA, >75% suppression observed in both assays. The compound was moderately effective against FAAH; although galantamine is not known to inhibit FAAH, indomethacin has moderate FAAH inhibitory activity. The anti-cholinergic activity observed was expected in 4462 due to the galantamine component. 4462 potently inhibited COX-1 versus COX-2, possibly due to the indomethacin conjugate, which although is classified as a non-

selective COX inhibitor is generally more effective against COX-1 (Mitchell *et al.*, 1993; Blanco *et al.*, 1999). 4461, a conjugate of S-naproxen and galantamine, significantly inhibited CEES- and TPA-induced inflammation, > 88% suppression of inflammation for both agents. This compound was moderately effective against FAAH and AChE, but potent against COX-2, suggesting COX-2 inhibition plays a major role in its anti-inflammatory activity. 4338, a conjugate of indomethacin and the anti-cholinergic 3,3-dimethyl butyl carbonate, potently suppressed inflammation and injury in the MEVM. Low micromolar IC₅₀s for both COX-2 and AChE indicates that dual inhibition of these enzymes could be responsible for its effectiveness.

FAAH inhibition may be in part responsible for the demonstrated pharmacological anti-inflammatory activity of these esters. The galantamine conjugates retained some inhibitory effect for FAAH, but were much more effective against AChE or COX-2. FAAH inhibition is not their primary mechanism of inflammation suppression, but may play a role. Although the IC₅₀ results indicated 4338 was a potent FAAH inhibitor, it is very hydrophobic (cLogP=7.87) and was difficult to solubilize. A manual curve fit indicated an IC₅₀ of approximately 500 μ M versus the 0.82 μ M calculated by GraphPad. The higher value may be more representative given the results obtained from similarly hydrophobic compounds in our FAAH assay. In addition, the compound's relative insolubility may have affected assay performance. Additional assays using an alternate solvent or a lower stock concentration may improve results.

These data show that FAAH inhibitors are effective suppressants of inflammation *in vivo*. Further experiments on these compounds would be necessary to confirm and statistically strengthen the data. Since some of these agents were effective against more than one target, confirmation of their mechanism(s) of action would be crucial, especially for activity against AChE. Irreversible AChE inhibitors are associated with toxic effects and would not be useful as a pharmaceutical treatment for vesicant

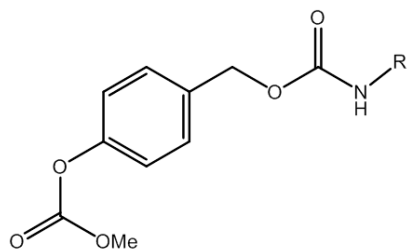
exposure (Colovic *et al.*, 2013). Few irreversible AChEIs are used as therapeutic agents, for example, two organophosphate compounds are used to treat glaucoma (diisopropyl fluorophosphate, echothiophate), one for Alzheimer's or Parkinson's disease (trichlorfon) (Cummings *et al.*, 2001; Rhee *et al.*, 2001). In the case of organophosphate-derived compounds, the AChE/OP carbamate complex is stable, and OPs phosphorylate the AChE active site serine irreversibly. Carbamates form a less stable bond with the active site serine residue and the carbamyl moiety is readily hydrolyzed, so they are considered reversible (Darvesh *et al.*, 2008; Colovic *et al.*, 2013). Examples of carbamate therapeutic compounds are physostigmine (myasthenia gravis), rivastigmine (Alzheimer's Disease), pyridostigmine (Colovic *et al.*, 2013).

Further characterization of the candidate FAAH inhibitors would also include kinetics studies to identify compound mechanism of inhibition, for example, whether it is competitive, non-competitive or un-competitive. Non-competitive results may indicate slow-reversible or irreversible inhibition, desirable qualities for FAAH inhibitors since FAAH hydrolysis quickly eliminates endocannabinoids *in vivo*, so should be confirmed.

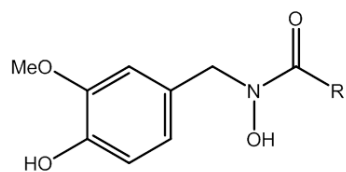
These studies have only begun to characterize the effects of our large library of candidate anti-inflammatories on the endocannabinoid system, and their suitability as treatments for NM- or SM-induced inflammation. New compound classes remain to be tested which may provide additional insights on endocannabinoid function in the skin during the inflammatory response, and result in therapeutics for use against chemical-induced skin injury.

Figure 14. General structures of FAAH inhibitors. Four classes of FAAH inhibitors are shown: Class I, vanillyl alcohol carbamates; Class II, hydroxamates; Class III, vanillyl amides and vanillyl amide carbamates; Class IV, olvanil-NSAIDs. Structures were drawn using ChemDraw Professional, Version 15.0.

Class I-Vanillyl alcohol

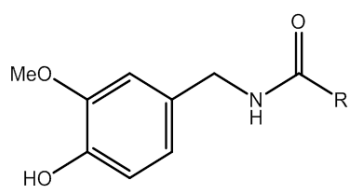


Class II-Hydroxamate



Vanillyl carbamate: R=O-
 Vanillyl amide: R=N-

Class III-Vanillyl amide



Vanilloid carbamate: R=O-
 Vanilloid amide: R=C-

Class IV-Olvanil-NSAID

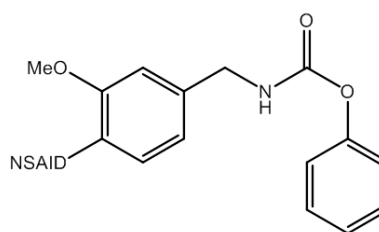
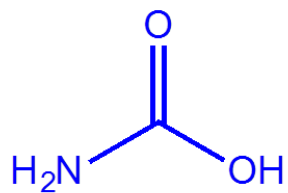
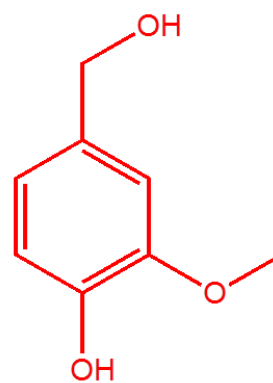


Figure 15. Chemical components of vanillyl alcohol carbamates. Precursor structures of vanillyl alcohol carbamates are shown. For synthesis, the 4-hydroxyl of the vanillyl alcohol is first protected with a carboxylic acid to form an ester, preventing its condensation during the addition of the carbamate to the vanillyl alcohol. The ester is then hydrolyzed in polar solution. R-groups are conjugated to the amide nitrogen. Structures were drawn using ChemDraw Professional, Version 15.0.



carbamate



vanillyl alcohol

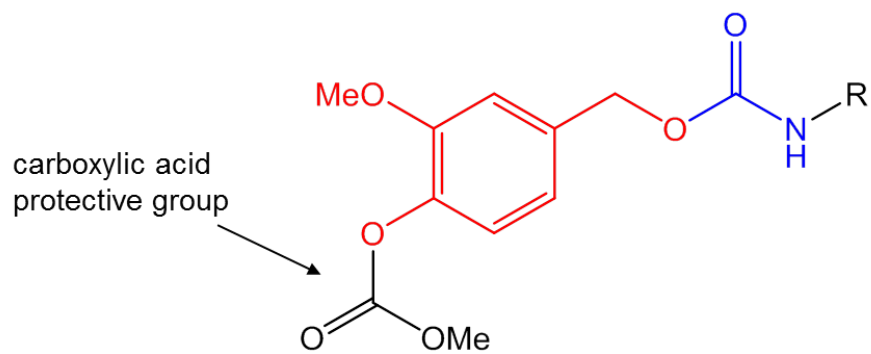
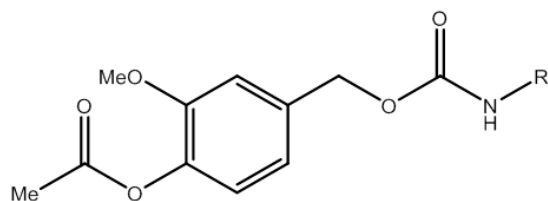


Table 1. Ability of vanillyl alcohol carbamates with N-conjugated ring R-groups to inhibit FAAH enzyme activity and suppress inflammation in the mouse ear vesicant model (MEVM). *In vitro* compound activities are expressed as IC₅₀s, the inhibitor concentration necessary to reduce enzyme activity by half. FAAH hydrolyzes AEA and other *N*-acylethanolamines; AEA to AA and ethanolamine. Compounds are listed in order of increasing FAAH IC₅₀. FAAH IC₅₀ data were calculated using GraphPad Prism 6.0, n=1. CEES data are percent inhibition of inflammatory response by each NDH compound compared to positive controls, n=3. The cLogP is the calculated logarithm of the partition coefficient between n-octanol and water and is used as a measure of compound hydrophilicity. A high cLogP indicates low hydrophilicity. The cLogP for each compound was determined using ChemBioDraw Ultra 12.0 software.



Compound	Name	R	FAAH IC ₅₀ (μM)	CEES % Inhib.	cLogP
4453	Phenethyl		14	80	2.80
4452	2-Phenoxyethyl		31	51	2.64
4455	Cyclohexylmethyl		93	40	3.35
4464	Morpholinethyl		>800	4	1.04

Figure 16. Activity of vanillyl alcohol carbamates with N-conjugated ring R-groups as inhibitors of FAAH enzyme activity. Effects of increasing inhibitor concentrations on FAAH activity. IC₅₀ curves were drawn using GraphPad Prism 6.0. Data are n = 1.

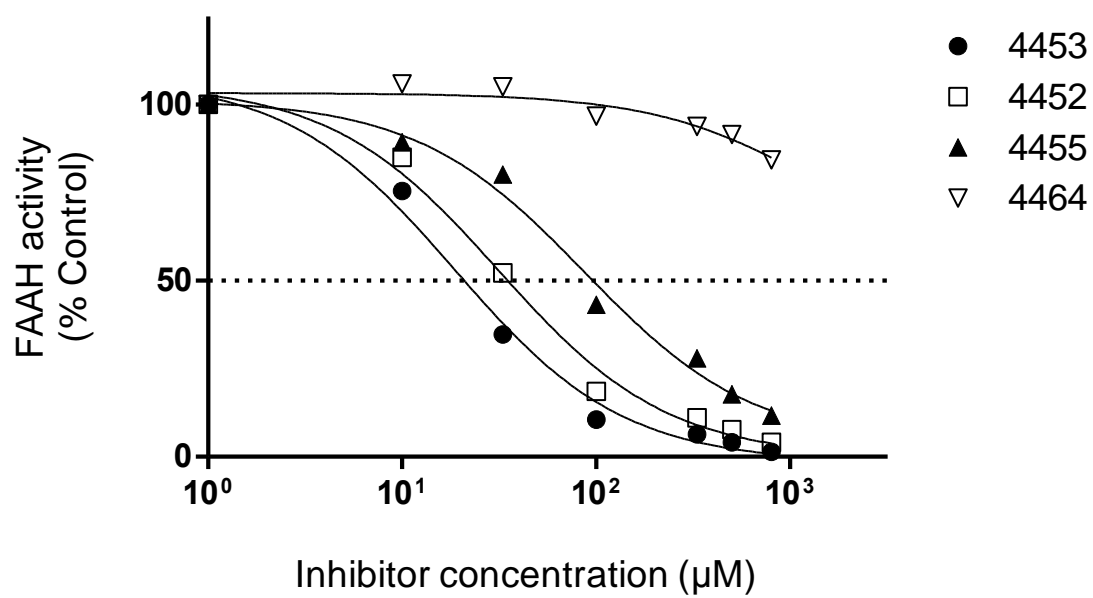


Table 2. Ability of vanillyl alcohol carbamates with C₄-C₁₂ alkane R-groups to inhibit FAAH enzyme and suppress inflammation in the mouse ear vesicant model (MEVM). *In vitro* compound activities are expressed as IC₅₀s, the inhibitor concentration necessary to reduce enzyme activity by half. FAAH hydrolyzes AEA and other *N*-acylethanolamines; AEA to AA and ethanolamine. Compounds are listed in order of increasing FAAH IC₅₀. FAAH IC₅₀ data were calculated using GraphPad Prism 6.0; n=1. CEES and TPA data are percent inhibition of inflammatory response by each NDH compound compared to positive controls treated with CEES or TPA alone, n=3. The cLogP is the calculated logarithm of the partition coefficient between n-octanol and water and is used as a measure of compound hydrophilicity. A high cLogP indicates low hydrophilicity. The cLogP for each compound was determined using ChemBioDraw Ultra 12.0 software.

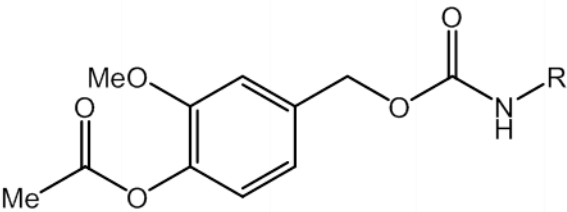
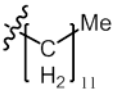
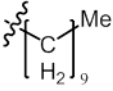
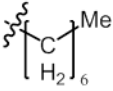
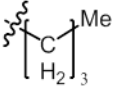
						
Compound	R	FAAH IC ₅₀ (μM)	CEES % Inhib.	TPA % Inhib.	cLogP	Carbon chain length
4439		9	7	57	6.52	12
4435		62	47	20	5.46	10
4440		104	18	58	3.87	7
4405		338	31	77	2.29	4

Figure 17. Ability of vanillyl alcohol carbamates with N-conjugated alkane R-groups to inhibit FAAH. Effects of increasing chain length of alkane R-groups on inhibition of FAAH enzyme activity. IC_{50} curves were drawn using GraphPad Prism 6.0. Data are n=1.

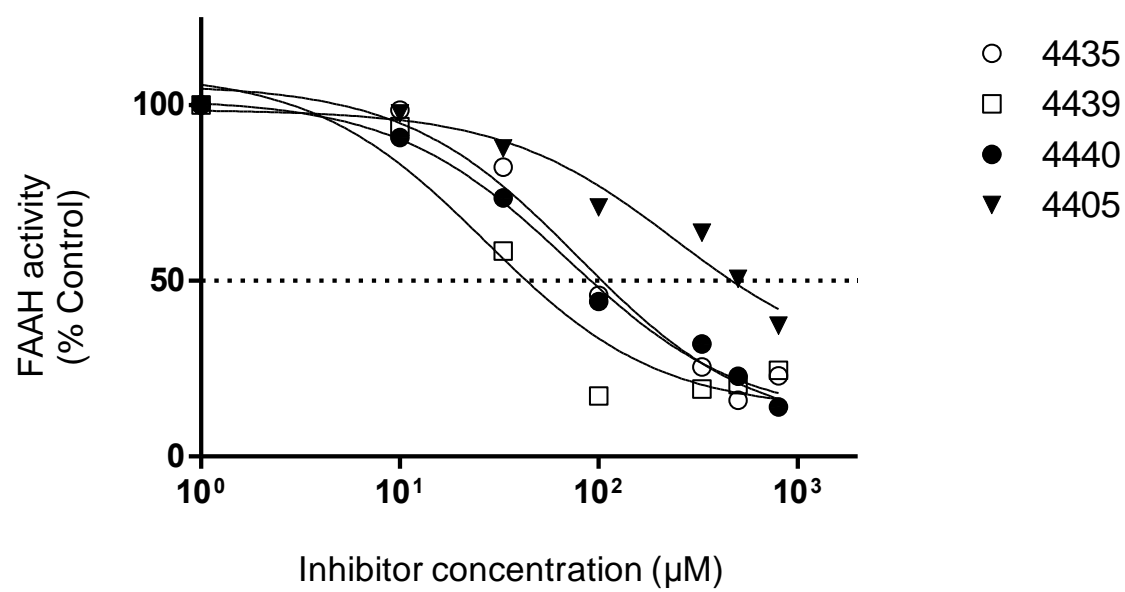
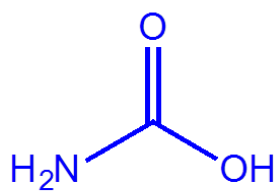
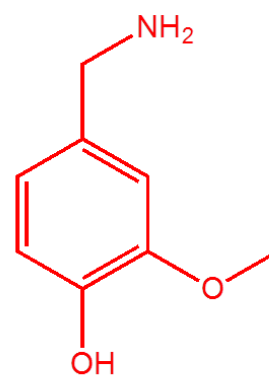


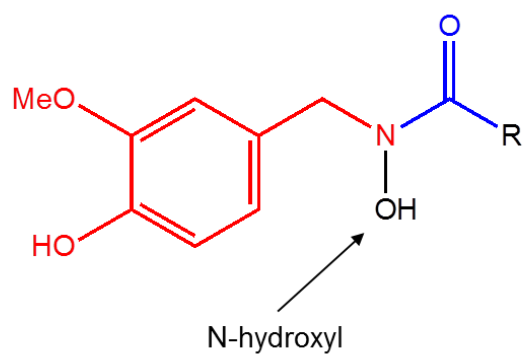
Figure 18. Chemical components of Class II hydroxamate compounds. A carbamate and a hydroxyl group are conjugated to the vanillyl amine nitrogen. R-groups are conjugated to the amide carbonyl. Structures were drawn using ChemDraw Professional, Version 15.0.



carbamate



vanillyl amine



Vanilloid carbamate: R=O-
 Vanilloid amine: R=N-

Table 3. Ability of hydroxamates to inhibit FAAH and suppress inflammation in the mouse ear vesicant model (MEVM). *In vitro* compound activities are expressed as IC₅₀s, the inhibitor concentration necessary to reduce enzyme activity by half. FAAH hydrolyzes AEA and other *N*-acylethanolamines; AEA to AA and ethanolamine. Compounds are listed in order of increasing FAAH IC₅₀. FAAH IC₅₀ data were calculated using GraphPad Prism 6.0, n=1. CEES and TPA data are percent inhibition of inflammatory response by each compound compared to positive controls treated with CEES and TPA alone, n=3. The cLogP is the calculated logarithm of the partition coefficient between n-octanol and water and is used as a measure of compound hydrophilicity. A high cLogP indicates low hydrophilicity. The cLogP for each compound was determined using ChemBioDraw Ultra 12.0 software. n.d., not determined.

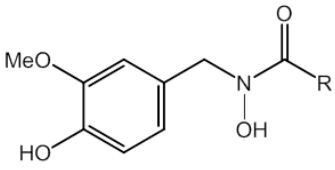
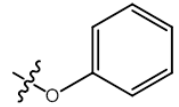
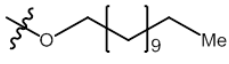
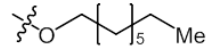
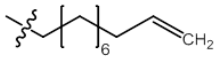
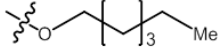
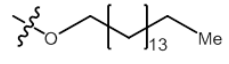
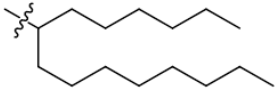
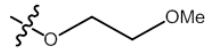
					
Compound	R	FAAH IC ₅₀ (μM)	CEES % Inh.	TPA % Inh.	cLogP
4493		10	42	n.d.	2.27
4488		67	48	n.d.	6.66
4489		73	69	n.d.	4.54
4474		163	45	26	4.69
4490		247	50	39	3.48
4487		337	11	n.d.	8.77
4475		1560	n.d.	37	7.59
4492		>1000	80	n.d.	0.97

Figure 19. Activity of the hydroxamate class of compounds as inhibitors of FAAH enzyme activity. Effects of varying hydroxamate R-substituents on FAAH activity. IC_{50} curves were drawn using GraphPad Prism 6.0. Data are n=1.

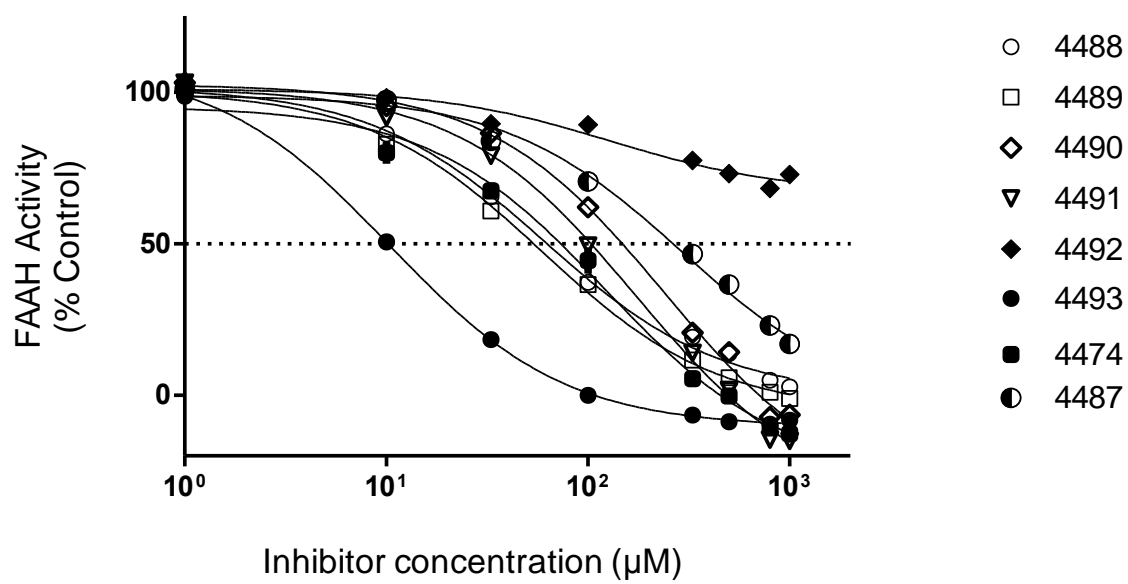
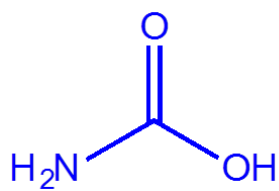
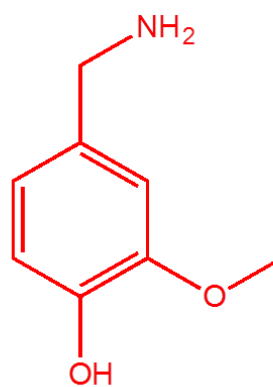


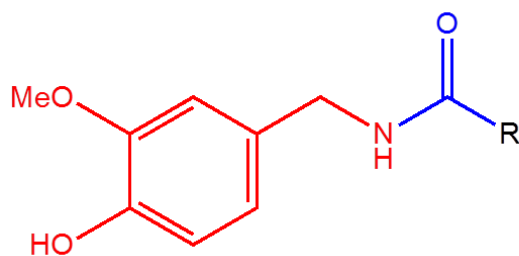
Figure 20. Chemical components of Class III compounds. Class III compounds are vanillyl amines with a carbamate attached at the amine nitrogen, and R-substituents conjugated to the amide carbonyl. This class lacks the N-hydroxyl group. Structures were drawn using ChemDraw Professional, Version 15.0.



carbamate



vanillyl amine



Vanillyl carbamate: R=O-
 Vanillyl amide: R=C-

Table 4. Activity of vanillyl amides and vanillyl amide carbamates as FAAH enzyme inhibitors and suppressors of inflammation in the mouse ear vesicant model (MEVM). *In vitro* compound activities are expressed as IC₅₀s, the inhibitor concentration necessary to reduce enzyme activity by half. FAAH hydrolyzes AEA and other *N*-acylethanolamines; AEA to AA and ethanolamine. Compounds are listed in order of increasing FAAH IC₅₀. FAAH IC₅₀ data were calculated using GraphPad Prism 6.0, n=1; 4369 n=3; mean \pm S.E.M. CEES and TPA data are percent inhibition of inflammatory response by each compound compared to positive controls treated with CEES or TPA alone, n=3. The cLogP is the calculated logarithm of the partition coefficient between n-octanol and water and is used as a measure of compound hydrophilicity. A high cLogP indicates low hydrophilicity. The cLogP for each compound was determined using ChemBioDraw Ultra 12.0 software. NA, not active; n.d., not determined.

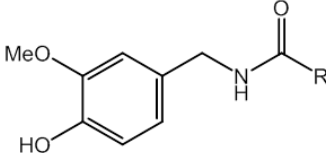
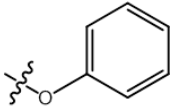

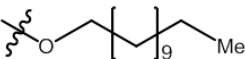
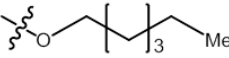
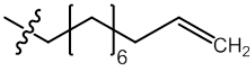
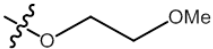
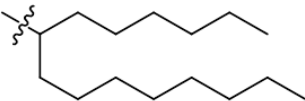
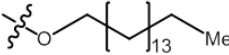
					
Compound	R	FAAH IC ₅₀ (μM)	CEES % Inh.	TPA % Inh.	cLogP
4369		2.2 ± 0.4	76	87	2.16
4366		17	64	28	4.50
4362		43	89	84	6.61
4367		54	76	71	3.44
4380		65	75	91	4.41
4364		66	4	44	0.94
4379		300	NA	76	7.32
4360		NA	NA	56	8.73

Table 5. Comparison of the activity of phenyl- and phenyl hydroxyl carbamates (hydroxamates) as inhibitors of inflammation in the mouse ear vesicant model (MEVM). *In vitro* compound activities are expressed as IC₅₀s, the inhibitor concentration necessary to reduce enzyme activity by half. FAAH hydrolyzes AEA and other *N*-acylethanolamines; AEA to AA and ethanolamine. Compounds are listed in order of increasing FAAH IC₅₀. FAAH IC₅₀ data were calculated using GraphPad Prism 6.0, n=1; 4369 n=3; mean ± S.E.M. CEES and TPA data are percent inhibition of inflammatory response by each compound compared to positive controls treated with CEES and TPA alone, n=3. The cLogP is the calculated logarithm of the partition coefficient between *n*-octanol and water and is used as a measure of compound hydrophilicity. A high cLogP indicates low hydrophilicity. The cLogP for each compound was determined using ChemBioDraw Ultra 12.0 software. n.d., not determined.

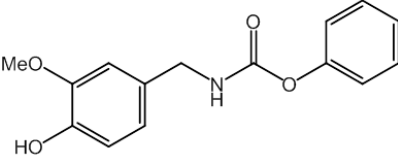
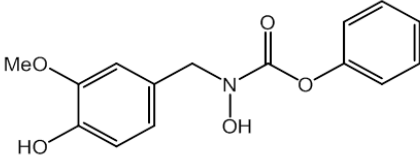
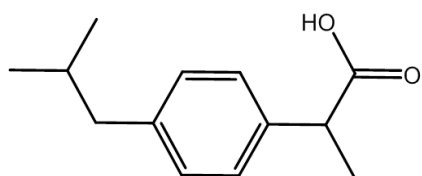
Compound	Structure	FAAH IC ₅₀ (μM)	CEES % Inhib.	TPA % Inhib.	cLogP
4369		2.2 ± 0.4	76	87	2.16
4493		10	42.5	n.d.	2.27

Figure 21. Structures of conjugate NSAID substituents. Ibuprofen and indomethacin molecules are shown. Structures were drawn using ChemDraw Professional, Version 15.0.

Ibuprofen



Indomethacin

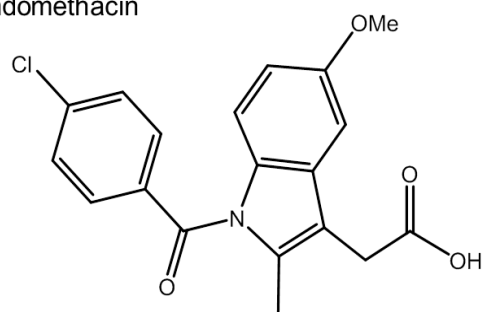
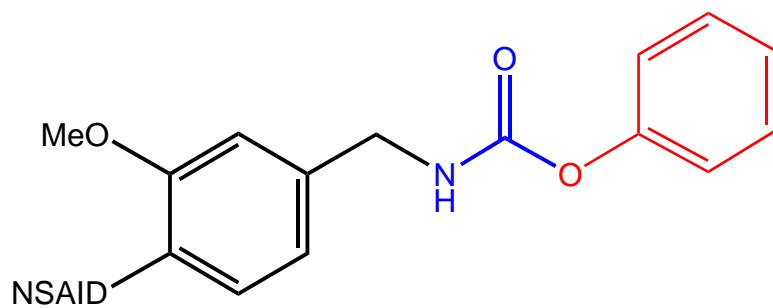
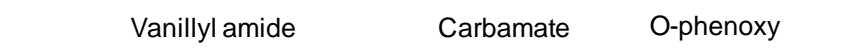


Figure 22. General structure of Olvanil-NSAIDs. Compound is broken into three basic components, the vanillyl amide (black), carbamate linkage (blue) and O-phenoxy leaving group (red). Structures were drawn using ChemDraw Professional, Version 15.0.



NSAID = ibuprofen or indomethacin

Figure 23. Comparison of Olvanil-NSAID and URB597 structures. The Olvanil-NSAID is broken into three components, vanillyl amide (black), carbamate linkage (blue) and O-phenoxy leaving group (red). The carbamate linkage in URB597 is shown in blue. Structures were drawn using ChemDraw Professional, Version 15.0.

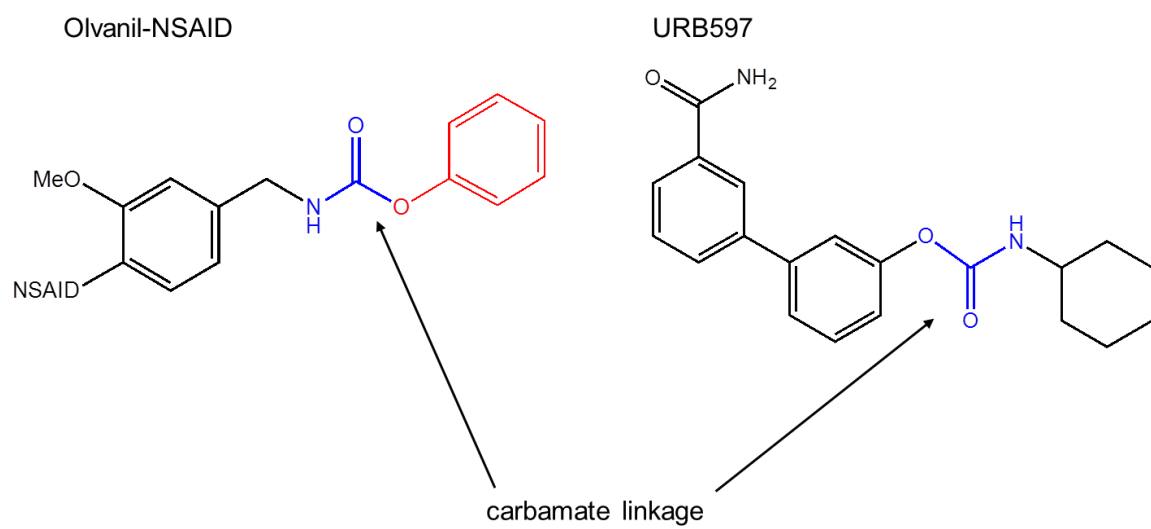


Table 6. Activities of 4369, olvanil-NSAIDs and URB597 as FAAH, COX-1, COX-2 and AChE enzyme inhibitors and suppressors of inflammation in the mouse ear vesicant model (MEVM). *In vitro* compound activities are expressed as IC₅₀s, the inhibitor concentration necessary to reduce enzyme activity by half. FAAH hydrolyzes AEA and other *N*-acylethanolamines; AEA to AA and ethanolamine. COX-1 (constitutive) and COX-2 (inducible) convert AA to PGH₂, which can be further metabolized to pro-inflammatory prostaglandins. AChE is a serine hydrolase inhibited by organophosphate compounds also reported to inhibit FAAH. Compounds are listed in order of increasing FAAH IC₅₀. IC₅₀s were calculated using GraphPad Prism 6.0, n=3, mean ± S.E.M. COX and AChE: n=3, mean ± S.E.M. CEES and TPA data are percent inhibition of inflammatory response by each compound compared to positive controls, n=3. The cLogP is the calculated logarithm of the partition coefficient between n-octanol and water and is used as a measure of compound hydrophilicity. A high cLogP indicates low hydrophilicity. The cLogP for each compound was determined using ChemBioDraw Ultra 12.0 software. n.d., not determined; NA, not active; **NSI, no significant inhibition.

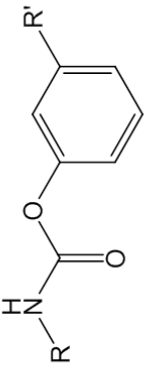
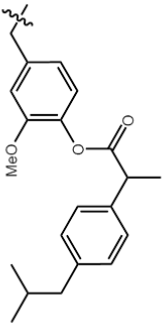
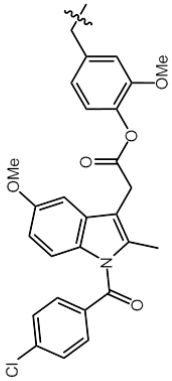
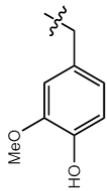
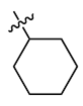
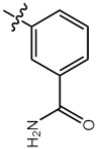
									
Compound	R	R'	FAAH IC ₅₀ (μM)	COX-1 IC ₅₀ (μM)	COX-2 IC ₅₀ (μM)	AChe IC ₅₀ (μM)	CEES % Inh.	TPA % Inh.	CLogP
4495		H	0.034 ± 0.01	NA	238 ± 0.16	4.5 ± 1.04	58	82	6.18
4496		H	0.371 ± 0.13	170 ± 2.2	0.11 ± 0.01	0.63 ± 0.03	23	97	6.68
4369		H	2.2 ± 0.4	NA	NA	n.d.	76	46	2.16
URB597			0.041 ± 0.01	NSI**	NSI**	NSI**	n.d.	n.d.	3.70

Figure 24. Activities of the Olvanil-NSAID compounds and URB597 as inhibitors of FAAH enzyme activity. Effects of varying NSAID substituents on FAAH activity, and comparison to activity of URB597. IC₅₀ curves were drawn using GraphPad Prism 6.0. Data are n=3; means \pm S.E.M.

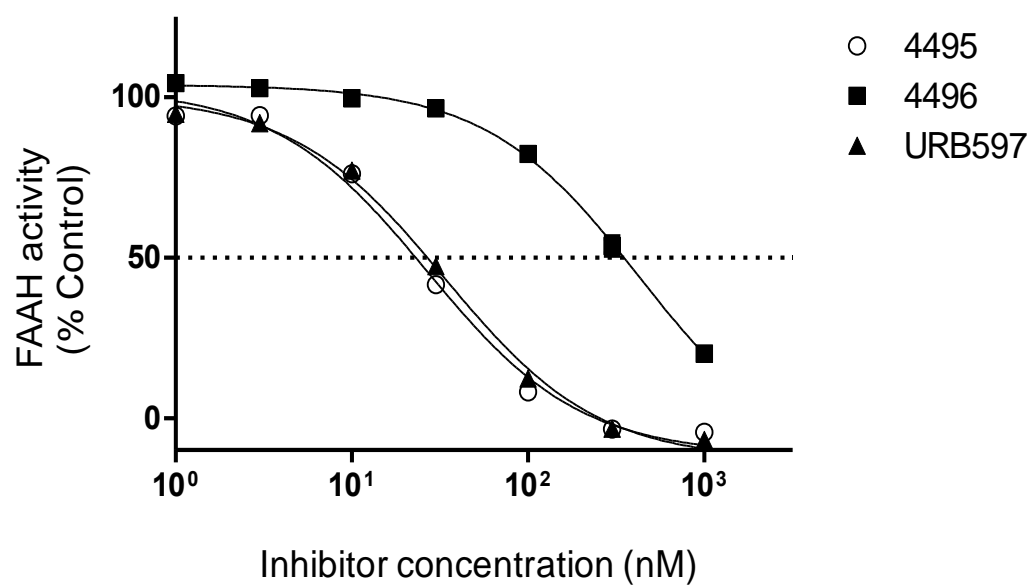


Table 7. Activities of indomethacin and ibuprofen as FAAH, COX-1, COX-2 enzyme inhibitors, and suppressors of inflammation in the mouse ear vesicant model (MEVM).

In vitro compound activities are expressed as IC₅₀s, the inhibitor concentration necessary to reduce enzyme activity by half. FAAH hydrolyzes AEA and other *N*-acylethanolamines; AEA to AA and ethanolamine. Compounds are listed in order of increasing FAAH IC₅₀. COX-1 (constitutive) and COX-2 (inducible) convert AA to PGH₂, which can be further metabolized to pro-inflammatory prostaglandins. AChE is a serine hydrolase inhibited by organophosphate compounds also reported to inhibit FAAH. IC₅₀ data were calculated using GraphPad Prism 6.0; FAAH: n=1; COX and AChE: n=3 ± S.E.M. CEES and TPA data are percent inhibition of inflammatory response by each compound compared to positive controls, n=3. The cLogP is the calculated logarithm of the partition coefficient between n-octanol and water and is used as a measure of compound hydrophilicity. A high cLogP indicates low hydrophilicity. The cLogP for each compound was determined using ChemBioDraw Ultra 12.0 software. n.d., not determined; NA, not active.

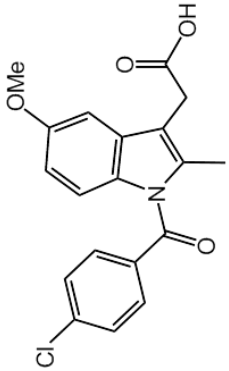
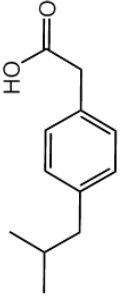
Compound	Name	Structure	FAAH IC ₅₀ (μM)	COX-1 IC ₅₀ (μM)	COX-2 IC ₅₀ (μM)	AChE % Inh.	CEES % Inh.	TPA % Inh.	cLogP
4382	Indomethacin		>500	0.415 ±0.02	6.49 ±0.07	NA	50	90	4.18
4433	Ibuprofen		>1000	NA	0.11 ±0.25	n.d.	NA	NA	3.68

Figure 25. Activities of the NSAIDs ibuprofen and indomethacin as inhibitors of FAAH enzyme activity. Effects increasing concentrations of ibuprofen and indomethacin on FAAH activity. IC_{50} curves were drawn using GraphPad Prism 6.0. Data are n=2.

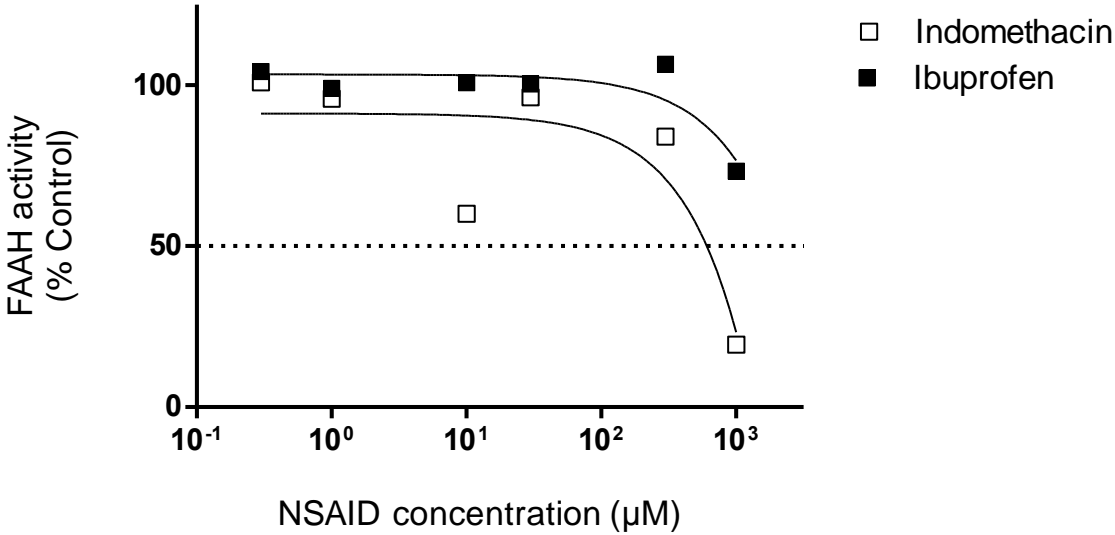
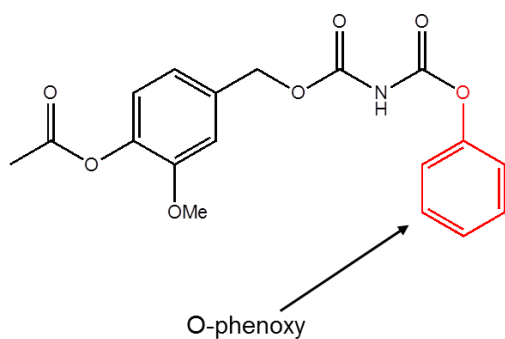


Table 8. Activities of the vanillyl amide compounds as FAAH enzyme inhibitors and suppressors of inflammation in the mouse ear vesicant model (MEVM). *In vitro* compound activities are expressed as IC₅₀s, the inhibitor concentration necessary to reduce enzyme activity by half. FAAH hydrolyzes AEA and other *N*-acylethanolamines; AEA to AA and ethanolamine. Compounds are listed in order of increasing FAAH IC₅₀. FAAH IC₅₀ data were calculated using GraphPad Prism 6.0, n=3, mean ± S.E.M. CEES and TPA data are percent inhibition of inflammatory response by each compound compared to positive controls, n=3. The cLogP is the calculated logarithm of the partition coefficient between n-octanol and water and is used as a measure of compound hydrophilicity. A high cLogP indicates low hydrophilicity. The cLogP for each compound was determined using ChemBioDraw Ultra 12.0 software.

Compound	Name	Structure	FAAH IC ₅₀ (μM)	CEES % Inh.	TPA % Inh.	cLogP
4497	2-methoxy-4- (((phenoxycarbonyl)carbonyl]oxy} methyl)phenyl acetate		*0.640 ±0.3	63	97	4.12
4500	4-(((benzoylcarbonyl)oxy)methyl)-2- methoxyphenyl acetate		> 1 mM	NA	56	2.18
4369	phenyl (4-hydroxy-3- methoxybenzyl)carbamate		*2.2 ±0.4	76	87	2.16
4502	phenyl [(4-hydroxy-3- methoxybenzyl)carbonyl]carbamate		> 1 mM	82	83	2.09

Figure 26. Comparison of NDH Compound Structures with and without O-phenoxy group. Structures of two vanilloid compounds are shown. The O-phenoxy group in 4497 is labeled in red, the phenyl without oxygen is labeled in blue. Structures were drawn using ChemDraw Professional, Version 15.0.

4497



4500

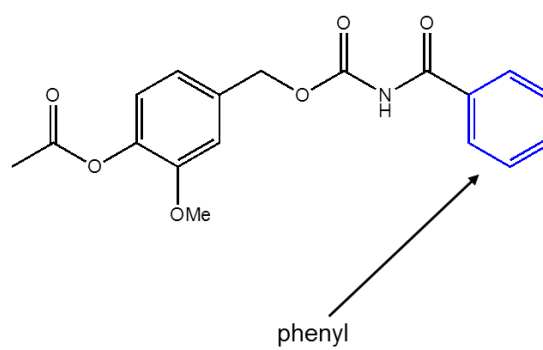
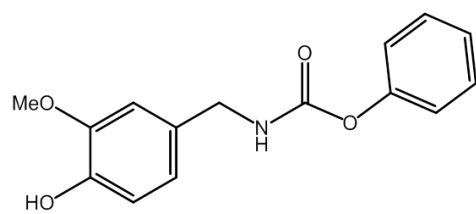


Figure 27. Comparison of NDH Compound Structures with and without additional amide group. Structures of two vanilloid compounds are shown. The extra amide group in 4502 is labeled in red. Structures were drawn using ChemDraw Professional, Version 15.0.

4369



4502

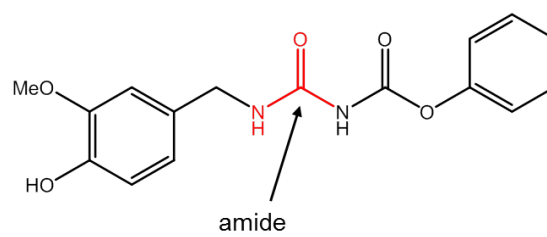
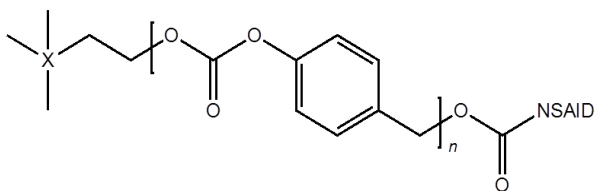


Figure 28. General structure of Ester-Carbonate and Ester series NSAIDs.

Compounds are divided into two classes: V(a) ester-carbonate linkage; V(b) ester linkage. Structures were drawn using ChemDraw Professional, Version 15.0.

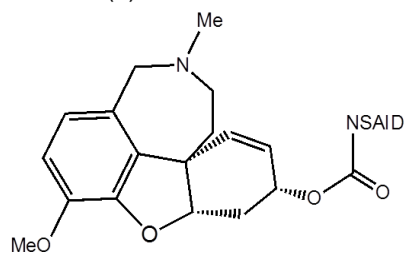
Class V(a).



X = C, Si, Ni⁺

NSAID = indomethacin

Class V(b).

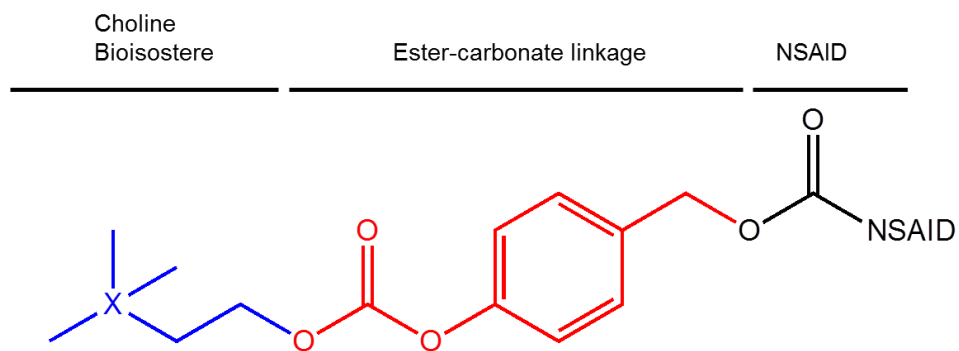


NSAID = indomethacin

naproxen

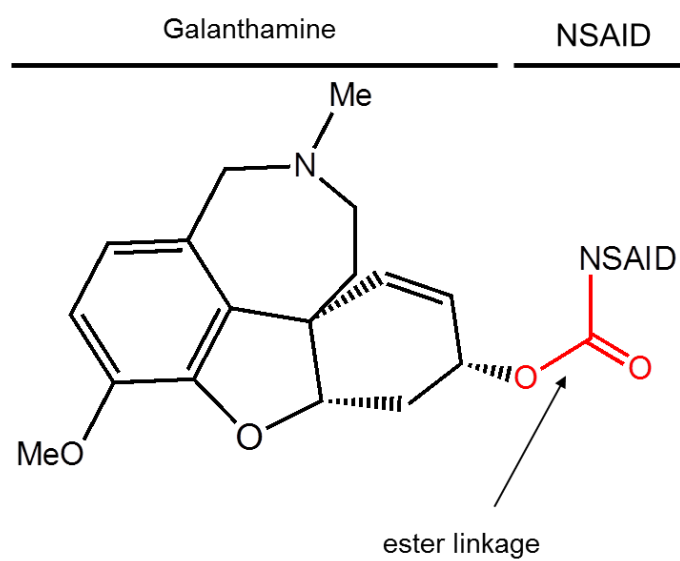
ibuprofen

Figure 29. General structure of Class V(a) Ester-Carbonate NSAID (4338). 4338 is divided into three components: a choline bioisostere (blue) linked to an NSAID (black) by an ester-carbonate (red). Structures were drawn using ChemDraw Professional, Version 15.0.



X = C
NSAID = indomethacin

Figure 30. General structure of Class V(b) Galantamine-NSAID. Galantamine and an NSAID are linked by an ester. Structures were drawn using ChemDraw Professional, Version 15.0.



NSAID = naproxen or indomethacin

Table 9. Activities of the Class V compounds as FAAH, COX-1, COX-2 and AChE inhibitors, and suppressors of inflammation in the mouse ear vesicant model (MEVM). *In vitro* compound activities are expressed as IC₅₀s, the inhibitor concentration necessary to reduce enzyme activity by half. FAAH hydrolyzes AEA and other *N*-acylethanolamines; AEA to AA and ethanolamine. Compounds are listed in order of increasing FAAH IC₅₀. COX-1 (constitutive) and COX-2 (inducible) convert AA to PGH₂, which can be further metabolized to pro-inflammatory prostaglandins. NSAIDs linked to AChE inhibitors have been reported to greatly reduce SM-induced damage and inflammation in the MEVM (Amitai et al., 2006). IC₅₀ data were calculated using GraphPad Prism 6.0; FAAH: n=2, †n=1; COX: n=3 ± S.E.M; AChE: n=3 ± S.E.M. CEES and TPA data are percent inhibition of inflammatory response by each compound compared to positive controls, n=3. The cLogP is the calculated logarithm of the partition coefficient between n-octanol and water and is used as a measure of compound hydrophilicity. A high cLogP indicates low hydrophilicity. The cLogP for each compound was determined using ChemBioDraw Ultra 12.0 software. *Class V(a) compound.

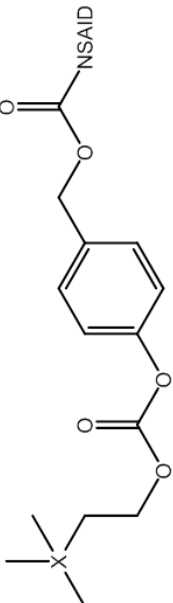
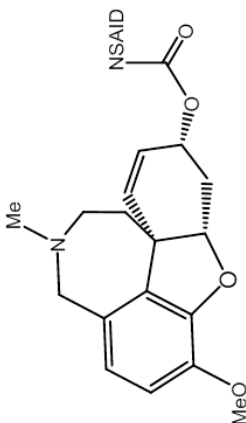
Class V(a)*		Class V(b)							
									
Compound	Name	NSAID	FAAH IC ₅₀ (μM)	COX-1 IC ₅₀ (μM)	COX-2 IC ₅₀ (μM)	AChE IC ₅₀ (μM)	CEES % Inhib.	TPA % Inhib.	cLogP
4338*	IndoSuc	Indomethacin; X=C	†0.82	49± 0.028	3.77 ±0.3	2.29 ±0.94	91	58	7.87
4461	Napro-Gal	Naproxen	66.2	3.35 ±0.16	0.18	37	88	97	5.01
4462	Indo-Gal	Indomethacin	113	0.032± 0.21	478 ±3.6	0.49 ±0.02	75	89	6.38

Figure 31. Activity of the Ester-carbonate 4338 as an inhibitor of the FAAH enzyme. Effects of increasing concentrations of 4338 on FAAH activity. IC₅₀ curve was drawn using GraphPad Prism 6.0. Data are n=2.

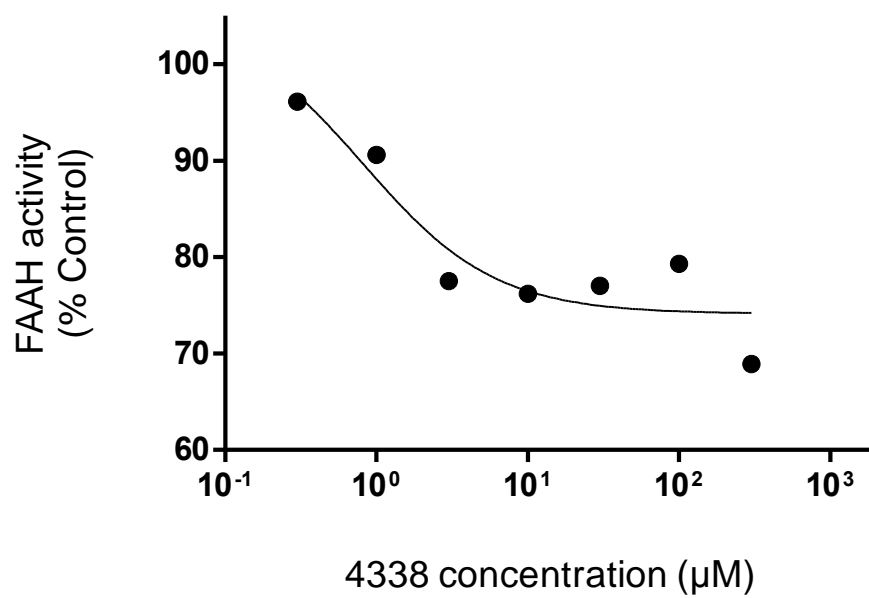
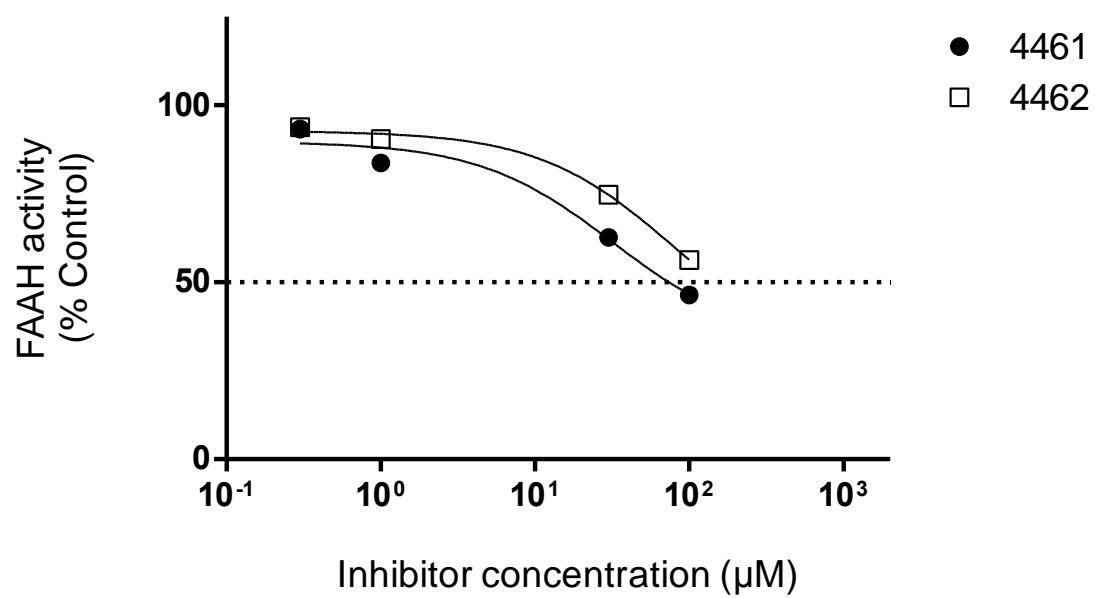


Figure 32. Activities of the Galantamine-NSAID compounds as inhibitors of FAAH enzyme activity. Effects of varying NSAID substituents on FAAH activity. IC_{50} curves were drawn using GraphPad Prism 6.0. Data are n=2.



CONCLUDING REMARKS

The first aim of this dissertation was to determine whether the endocannabinoid system was present in mouse skin and dermal appendages. Previously published reports were conflicting and used *in vitro* models with human skin-derived cells, for example HaCaT keratinocytes and SZ95 sebocytes. Since both CD-1 and SHK1-Hr mice are used by our group and others to study vesicant-induced skin injury, it was important to characterize the ECS before and after vesicant treatment in these models. Immunohistochemistry was used to provide a visual map of the location and expression level of CB1, CB2 and PPAR α in untreated animals. We also use immunohistochemistry to characterize FAAH expression, which to our knowledge had not yet been this well-visualized in skin. Our findings indicate that FAAH, a key catabolic enzyme important in regulating levels of various fatty acid amides including AEA and many N-acylethanolamines, as well as receptors for these mediators including CB1, CB2 and PPAR α , were present in mouse skin, particularly in the interfollicular epidermis and dermal appendages.

Secondly, we attempted to characterize the endocannabinoid system response to vesicant exposure in mouse skin. Using immunohistochemistry, we found that these proteins were markedly upregulated following treatment with NM and SM, suggesting that the endocannabinoid system plays a role in mustard-induced skin injury and/or repair. In addition, we observed changes in endocannabinoid system protein expression over a 21-day time course, indicating these proteins may also play a role in the healing process.

The third aim was to study structure activity relationships for different classes of FAAH inhibitors *in vitro*, then apply the most effective candidates to mouse skin to determine if inhibition of FAAH would have an effect on TPA- and/or vesicant-induced inflammation and injury. Our results showed that topical application of compounds found

to inhibit FAAH *in vitro* decreased inflammation in both the MEVM and in dorsal-skin application models for NM and SM. Of the five classes of compounds assayed, the olvanil-NSAIDs were the most potent against FAAH, CEES- and TPA-induced edema. Compound 4496, an indomethacin derivative also significantly inhibited COX-2, a known pro-inflammatory enzyme, suggesting activity as a dual FAAH-COX-2 inhibitor. Dual inhibition would not only play a role in preventing generation of arachidonic acid by FAAH, but also its cyclooxygenation by COX-2 and subsequent metabolism to pro-inflammatory prostaglandins, prostacyclins and leukotrienes. 4496 also was active against AChE, possibly an additional mechanism anti-inflammatory activity.

In all compound classes, there were agents with different levels of effectiveness against either CEES or TPA. Some potently suppressed edema induced by both irritants, others were more effective against one or the other. Although both irritants induce an inflammatory response, there are differences in structure and mechanism of toxicity. CEES is a vesicant, similar to the mustards structurally, mechanistically and in its effects on skin. CEES effects are similar to those observed post NM- or SM-exposure, lesions are slow to develop, and toxicity results from alkylation of DNA, RNA and proteins, activation of proteases, and an inflammatory response that can be delayed as long as 24 hours. In contrast, TPA is a tetracyclic diterpenoid known for its tumor-promoting activity and skin irritant effects (Goel *et al.*, 2007). An amphiphilic molecule, it binds phospholipid membrane receptors inducing arachidonic acid release, prostaglandin synthesis, altered lipid synthesis and cell adhesion, and release of histamine and IL-2 (Weinstein *et al.*, 1979). TPA is structurally analogous to diacylglycerol, which activates PKC by binding to its C1-domain. TPA potently activates PKC, triggering cell proliferation and differentiation through activation of MAPK pathways (Maccarrone *et al.*, 2003; Goel *et al.*, 2007). Interestingly, in HaCaT and NHEK cells, TPA treatment increased FAAH expression and activity, reducing AEA, while exogenous

AEA reduced PKC activity through CB1 signaling (Maccarrone *et al.*, 2003). This suggests a role for reduction of TPA-induced inflammation through FAAH inhibition, and supports our findings that our most effective FAAH inhibitors were more potent against TPA. Possible future studies could address whether vesicant exposure also modulates PKC activity through CB1, and if there are any reductions in vesicant-induced genotoxicity by modulation of this pathway.

Taken together, the data support the hypothesis that the endocannabinoids function in regulating skin homeostasis as well as responses to chemical inflammation and injury. Further studies are needed to better understand the role of the endocannabinoid system in mediating vesicant-induced injury as this will be important in identifying therapeutic targets that may reduce or prevent vesicant-induced skin damage.

REFERENCES

- Ahn, K., Johnson, D.S., Cravatt, B.F., 2009. Fatty acid amide hydrolase as a potential therapeutic target for the treatment of pain and CNS disorders. *Expert Opin Drug Discov* **4**, 763-784.
- Aldinger, K.A., Sokoloff, G., Rosenberg, D.M., Palmer, A.A., Millen, K.J., 2009. Genetic variation and population substructure in outbred CD-1 mice: implications for genome-wide association studies. *PloS one* **4**, e4729.
- Alexander, J.P., Cravatt, B.F., 2005. Mechanism of carbamate inactivation of FAAH: implications for the design of covalent inhibitors and in vivo functional probes for enzymes. *Chemistry & biology* **12**, 1179-1187.
- Alonso, L., Fuchs, E., 2006. The hair cycle. *Journal of cell science* **119**, 391-393.
- Amitai, G., Adani, R., Fishbein, E., Meshulam, H., Laish, I., Dachir, S., 2006. Bifunctional compounds eliciting anti-inflammatory and anti-cholinesterase activity as potential treatment of nerve and blister chemical agents poisoning. *Journal of applied toxicology* : JAT **26**, 81-87.
- Andradas, C., Caffarel, M.M., Perez-Gomez, E., Salazar, M., Lorente, M., Velasco, G., Guzman, M., Sanchez, C., 2011. The orphan G protein-coupled receptor GPR55 promotes cancer cell proliferation via ERK. *Oncogene* **30**, 245-252.
- Ansari, K.M., Rundhaug, J.E., Fischer, S.M., 2008. Multiple signaling pathways are responsible for prostaglandin E2-induced murine keratinocyte proliferation. *Molecular cancer research* : MCR **6**, 1003-1016.
- Ansell, D.M., Kloepper, J.E., Thomason, H.A., Paus, R., Hardman, M.J., 2011. Exploring the "hair growth-wound healing connection": anagen phase promotes wound re-epithelialization. *The Journal of investigative dermatology* **131**, 518-528.
- Arabzadeh, A., Troy, T.C., Turksen, K., 2009. Insights into the role of the calcium sensing receptor in epidermal differentiation in vivo. *Mol Biotechnol* **43**, 264-272.
- Arroyo, C.M., Burman, D.L., Kahler, D.W., Nelson, M.R., Corun, C.M., Guzman, J.J., Smith, M.A., Purcell, E.D., Hackley, B.E., Jr., Soni, S.D., Broomfield, C.A., 2004. TNF-alpha expression patterns as potential molecular biomarker for human skin cells exposed to vesicant chemical warfare agents: sulfur mustard (HD) and Lewisite (L). *Cell biology and toxicology* **20**, 345-359.
- Avci, P., Sadasivam, M., Gupta, A., De Melo, W.C., Huang, Y.Y., Yin, R., Chandran, R., Kumar, R., Otufowora, A., Nyame, T., Hamblin, M.R., 2013. Animal models of skin disease for drug discovery. *Expert Opin Drug Discov* **8**, 331-355.
- Babaev, V.R., Ishiguro, H., Ding, L., Yancey, P.G., Dove, D.E., Kovacs, W.J., Semenkovich, C.F., Fazio, S., Linton, M.F., 2007. Macrophage expression of peroxisome proliferator-activated receptor-alpha reduces atherosclerosis in low-density lipoprotein receptor-deficient mice. *Circulation* **116**, 1404-1412.
- Babin, M.C., Ricketts, K., Skvorak, J.P., Gazaway, M., Mitcheltree, L.W., Casillas, R.P., 2000. Systemic administration of candidate antivesicants to protect against topically applied sulfur mustard in the mouse ear vesicant model (MEVM). *Journal of applied toxicology* : JAT **20 Suppl 1**, S141-144.
- Balali-Mood, M., Hefazi, M., 2005. The pharmacology, toxicology, and medical treatment of sulphur mustard poisoning. *Fundamental & clinical pharmacology* **19**, 297-315.
- Balali-Mood, M., Hefazi, M., Mahmoudi, M., Jalali, E., Attaran, D., Maleki, M., Razavi, M.E., Zare, G., Tabatabaee, A., Jaafari, M.R., 2005. Long-term complications of sulphur mustard poisoning in severely intoxicated Iranian veterans. *Fundamental & clinical pharmacology* **19**, 713-721.

- Balszuweit, F., Menacher, G., Bloemeke, B., Schmidt, A., Worek, F., Thiermann, H., Steinritz, D., 2014. Development of a co-culture of keratinocytes and immune cells for in vitro investigation of cutaneous sulfur mustard toxicity. *Chemico-biological interactions* **223C**, 117-124.
- Benavides, F., Oberyshyn, T.M., VanBuskirk, A.M., Reeve, V.E., Kusewitt, D.F., 2009. The hairless mouse in skin research. *Journal of dermatological science* **53**, 10-18.
- Benson, J.M., Seagrave, J., Weber, W.M., Santistevan, C.D., Grotendorst, G.R., Schultz, G.S., March, T.H., 2011. Time course of lesion development in the hairless guinea-pig model of sulfur mustard-induced dermal injury. *Wound repair and regeneration : official publication of the Wound Healing Society [and] the European Tissue Repair Society* **19**, 348-357.
- Berglund, B.A., Boring, D.L., Howlett, A.C., 1999. Investigation of structural analogs of prostaglandin amides for binding to and activation of CB1 and CB2 cannabinoid receptors in rat brain and human tonsils. *Advances in experimental medicine and biology* **469**, 527-533.
- Bertolacci, L., Romeo, E., Veronesi, M., Magotti, P., Albani, C., Dionisi, M., Lambruschini, C., Scarpelli, R., Cavalli, A., De Vivo, M., Piomelli, D., Garau, G., 2013. A binding site for nonsteroidal anti-inflammatory drugs in fatty acid amide hydrolase. *Journal of the American Chemical Society* **135**, 22-25.
- Bikle, D.D., Ratnam, A., Mauro, T., Harris, J., Pillai, S., 1996. Changes in calcium responsiveness and handling during keratinocyte differentiation. Potential role of the calcium receptor. *The Journal of clinical investigation* **97**, 1085-1093.
- Bikle, D.D., Xie, Z., Tu, C.L., 2012. Calcium regulation of keratinocyte differentiation. *Expert Rev Endocrinol Metab* **7**, 461-472.
- Billiau, A., Matthys, P., 2001. Modes of action of Freund's adjuvants in experimental models of autoimmune diseases. *Journal of leukocyte biology* **70**, 849-860.
- Biro, T., Toth, B.I., Hasko, G., Paus, R., Pacher, P., 2009. The endocannabinoid system of the skin in health and disease: novel perspectives and therapeutic opportunities. *Trends in pharmacological sciences* **30**, 411-420.
- Black, A.T., Hayden, P.J., Casillas, R.P., Heck, D.E., Gerecke, D.R., Sinko, P.J., Laskin, D.L., Laskin, J.D., 2010a. Expression of proliferative and inflammatory markers in a full-thickness human skin equivalent following exposure to the model sulfur mustard vesicant, 2-chloroethyl ethyl sulfide. *Toxicology and applied pharmacology* **249**, 178-187.
- Black, A.T., Joseph, L.B., Casillas, R.P., Heck, D.E., Gerecke, D.R., Sinko, P.J., Laskin, D.L., Laskin, J.D., 2010b. Role of MAP kinases in regulating expression of antioxidants and inflammatory mediators in mouse keratinocytes following exposure to the half mustard, 2-chloroethyl ethyl sulfide. *Toxicology and applied pharmacology* **245**, 352-360.
- Blanco, F.J., Guitian, R., Moreno, J., de Toro, F.J., Galdo, F., 1999. Effect of antiinflammatory drugs on COX-1 and COX-2 activity in human articular chondrocytes. *The Journal of rheumatology* **26**, 1366-1373.
- Blanpain, C., Fuchs, E., 2009. Epidermal homeostasis: a balancing act of stem cells in the skin. *Nat Rev Mol Cell Biol* **10**, 207-217.
- Boger, D.L., Sato, H., Lerner, A.E., Hedrick, M.P., Fecik, R.A., Miyauchi, H., Wilkie, G.D., Austin, B.J., Patricelli, M.P., Cravatt, B.F., 2000. Exceptionally potent inhibitors of fatty acid amide hydrolase: the enzyme responsible for degradation of endogenous oleamide and anandamide. *Proceedings of the National Academy of Sciences of the United States of America* **97**, 5044-5049.

- Brown, I., Cascio, M.G., Rotondo, D., Pertwee, R.G., Heys, S.D., Wahle, K.W., 2013. Cannabinoids and omega-3/6 endocannabinoids as cell death and anticancer modulators. *Progress in lipid research* **52**, 80-109.
- Brown, R.F., Rice, P., 1997. Histopathological changes in Yucatan minipig skin following challenge with sulphur mustard. A sequential study of the first 24 hours following challenge. *Int J Exp Pathol* **78**, 9-20.
- Calandra, B., Portier, M., Kerneis, A., Delpech, M., Carillon, C., Le Fur, G., Ferrara, P., Shire, D., 1999. Dual intracellular signaling pathways mediated by the human cannabinoid CB1 receptor. *European journal of pharmacology* **374**, 445-455.
- Campora, L., Miragliotta, V., Ricci, E., Cristino, L., Di Marzo, V., Albanese, F., Federica Della Valle, M., Abramo, F., 2012. Cannabinoid receptor type 1 and 2 expression in the skin of healthy dogs and dogs with atopic dermatitis. *Am J Vet Res* **73**, 988-995.
- Casillas, R.P., Kiser, R.C., Truxall, J.A., Singer, A.W., Shumaker, S.M., Niemuth, N.A., Ricketts, K.M., Mitcheltree, L.W., Castrejon, L.R., Blank, J.A., 2000. Therapeutic approaches to dermatotoxicity by sulfur mustard. I. Modulation of sulfur mustard-induced cutaneous injury in the mouse ear vesicant model. *Journal of applied toxicology : JAT* **20 Suppl 1**, S145-151.
- Chang, J., Carlson, R.P., O'Neill-Davis, L., Lamb, B., Sharma, R.N., Lewis, A.J., 1986. Correlation between mouse skin inflammation induced by arachidonic acid and eicosanoid synthesis. *Inflammation* **10**, 205-214.
- Chang, Y.C., Wang, J.D., Hahn, R.A., Gordon, M.K., Joseph, L.B., Heck, D.E., Heindel, N.D., Young, S.C., Sinko, P.J., Casillas, R.P., Laskin, J.D., Laskin, D.L., Gerecke, D.R., 2014. Therapeutic potential of a non-steroidal bifunctional anti-inflammatory and anti-cholinergic agent against skin injury induced by sulfur mustard. *Toxicology and applied pharmacology* **280**, 236-244.
- Chia, R., Achilli, F., Festing, M.F., Fisher, E.M., 2005. The origins and uses of mouse outbred stocks. *Nature genetics* **37**, 1181-1186.
- Chiba, T., Takeuchi, S., Esaki, H., Yamamura, K., Kurihara, Y., Moroi, Y., Furue, M., 2012. Topical application of PPARalpha (but not beta/delta or gamma) suppresses atopic dermatitis in NC/Nga mice. *Allergy* **67**, 936-942.
- Chiurchiu, V., Lanuti, M., Catanzaro, G., Fezza, F., Rapino, C., Maccarrone, M., 2014. Detailed characterization of the endocannabinoid system in human macrophages and foam cells, and anti-inflammatory role of type-2 cannabinoid receptor. *Atherosclerosis* **233**, 55-63.
- Chivers, C.J., 2014. The Secret Casualties of Iraq's Abandoned Chemical Weapons., *The New York Times*, <http://www.nytimes.com>.
- Cipriano, M., Bjorklund, E., Wilson, A.A., Congiu, C., Onnis, V., Fowler, C.J., 2013. Inhibition of fatty acid amide hydrolase and cyclooxygenase by the N-(3-methylpyridin-2-yl)amide derivatives of flurbiprofen and naproxen. *European journal of pharmacology* **720**, 383-390.
- Clery-Barraud, C., Nguon, N., Vallet, V., Sentenac, C., Four, E., Arlaud, C., Coulon, D., Boudry, I., 2013. Sulfur mustard cutaneous injury characterization based on SKH-1 mouse model: relevance of non-invasive methods in terms of wound healing process analyses. *Skin Res Technol* **19**, e146-156.
- Colovic, M.B., Krstic, D.Z., Lazarevic-Pasti, T.D., Bondzic, A.M., Vasic, V.M., 2013. Acetylcholinesterase inhibitors: pharmacology and toxicology. *Curr Neuropharmacol* **11**, 315-335.
- Costa, B., Bettoni, I., Petrosino, S., Comelli, F., Giagnoni, G., Di Marzo, V., 2010. The dual fatty acid amide hydrolase/TRPV1 blocker, N-arachidonoyl-serotonin, relieves carrageenan-

- induced inflammation and hyperalgesia in mice. *Pharmacological research : the official journal of the Italian Pharmacological Society* **61**, 537-546.
- Cravatt, B.F., Demarest, K., Patricelli, M.P., Bracey, M.H., Giang, D.K., Martin, B.R., Lichtman, A.H., 2001. Supersensitivity to anandamide and enhanced endogenous cannabinoid signaling in mice lacking fatty acid amide hydrolase. *Proceedings of the National Academy of Sciences of the United States of America* **98**, 9371-9376.
- Cravatt, B.F., Saghatelian, A., Hawkins, E.G., Clement, A.B., Bracey, M.H., Lichtman, A.H., 2004. Functional disassociation of the central and peripheral fatty acid amide signaling systems. *Proceedings of the National Academy of Sciences of the United States of America* **101**, 10821-10826.
- Cui, S., Chesson, C., Hope, R., 1993. Genetic variation within and between strains of outbred Swiss mice. *Lab Anim* **27**, 116-123.
- Cummings, J.L., Nadel, A., Masterman, D., Cyrus, P.A., 2001. Efficacy of metrifonate in improving the psychiatric and behavioral disturbances of patients with Alzheimer's disease. *J Geriatr Psychiatry Neurol* **14**, 101-108.
- Cunard, R., DiCampli, D., Archer, D.C., Stevenson, J.L., Ricote, M., Glass, C.K., Kelly, C.J., 2002. WY14,643, a PPAR alpha ligand, has profound effects on immune responses in vivo. *J Immunol* **169**, 6806-6812.
- D'Agostino, G., La Rana, G., Russo, R., Sasso, O., Iacono, A., Esposito, E., Mattace Raso, G., Cuzzocrea, S., Loverme, J., Piomelli, D., Meli, R., Calignano, A., 2009. Central administration of palmitoylethanolamide reduces hyperalgesia in mice via inhibition of NF-kappaB nuclear signalling in dorsal root ganglia. *European journal of pharmacology* **613**, 54-59.
- D'Agostino, G., La Rana, G., Russo, R., Sasso, O., Iacono, A., Esposito, E., Raso, G.M., Cuzzocrea, S., Lo Verme, J., Piomelli, D., Meli, R., Calignano, A., 2007. Acute intracerebroventricular administration of palmitoylethanolamide, an endogenous peroxisome proliferator-activated receptor-alpha agonist, modulates carrageenan-induced paw edema in mice. *The Journal of pharmacology and experimental therapeutics* **322**, 1137-1143.
- Dachir, S., Cohen, M., Kamus-Elimeleh, D., Fishbine, E., Sahar, R., Gez, R., Brandeis, R., Horwitz, V., Kadar, T., 2012. Characterization of acute and long-term pathologies of superficial and deep dermal sulfur mustard skin lesions in the hairless guinea pig model. *Wound repair and regeneration : official publication of the Wound Healing Society [and] the European Tissue Repair Society* **20**, 852-861.
- Dachir, S., Fishbeine, E., Meshulam, Y., Sahar, R., Amir, A., Kadar, T., 2002. Potential anti-inflammatory treatments against cutaneous sulfur mustard injury using the mouse ear vesicant model. *Hum Exp Toxicol* **21**, 197-203.
- Daley, J.M., Brancato, S.K., Thomay, A.A., Reichner, J.S., Albina, J.E., 2010. The phenotype of murine wound macrophages. *Journal of leukocyte biology* **87**, 59-67.
- Darlenski, R., Kazandijeva, J., Tsankov, N., 2011. Skin Barrier Function: Morphological Basis and Regulatory Mechanisms. *J Clin Med* **4**, 36-45.
- Darvesh, S., Darvesh, K.V., McDonald, R.S., Mataija, D., Walsh, R., Mothana, S., Lockridge, O., Martin, E., 2008. Carbamates with differential mechanism of inhibition toward acetylcholinesterase and butyrylcholinesterase. *Journal of medicinal chemistry* **51**, 4200-4212.
- De Petrocellis, L., Ligresti, A., Moriello, A.S., Allara, M., Bisogno, T., Petrosino, S., Stott, C.G., Di Marzo, V., 2011. Effects of cannabinoids and cannabinoid-enriched Cannabis extracts on TRP channels and endocannabinoid metabolic enzymes. *British journal of pharmacology* **163**, 1479-1494.

- Deng, L., Cornett, B.L., Mackie, K., Hohmann, A.G., 2015. CB1 Knockout Mice Unveil Sustained CB2-Mediated Antiallodynic Effects of the Mixed CB1/CB2 Agonist CP55,940 in a Mouse Model of Paclitaxel-Induced Neuropathic Pain. *Molecular pharmacology* **88**, 64-74.
- DeVita, V.T., Jr., Chu, E., 2008. A history of cancer chemotherapy. *Cancer research* **68**, 8643-8653.
- Di-Poi, N., Michalik, L., Desvergne, B., Wahli, W., 2004. Functions of peroxisome proliferator-activated receptors (PPAR) in skin homeostasis. *Lipids* **39**, 1093-1099.
- Di Marzo, V., Melck, D., Orlando, P., Bisogno, T., Zagoory, O., Bifulco, M., Vogel, Z., De Petrocellis, L., 2001. Palmitoylethanolamide inhibits the expression of fatty acid amide hydrolase and enhances the anti-proliferative effect of anandamide in human breast cancer cells. *The Biochemical journal* **358**, 249-255.
- Di Marzo, V., Petrosino, S., 2007. Endocannabinoids and the regulation of their levels in health and disease. *Curr Opin Lipidol* **18**, 129-140.
- Di Pasquale, E., Chahinian, H., Sanchez, P., Fantini, J., 2009. The insertion and transport of anandamide in synthetic lipid membranes are both cholesterol-dependent. *PloS one* **4**, e4989.
- Dobrosi, N., Toth, B.I., Nagy, G., Dozsa, A., Geczy, T., Nagy, L., Zouboulis, C.C., Paus, R., Kovacs, L., Biro, T., 2008. Endocannabinoids enhance lipid synthesis and apoptosis of human sebocytes via cannabinoid receptor-2-mediated signaling. *FASEB journal : official publication of the Federation of American Societies for Experimental Biology* **22**, 3685-3695.
- Downie, M.M., Sanders, D.A., Maier, L.M., Stock, D.M., Kealey, T., 2004. Peroxisome proliferator-activated receptor and farnesoid X receptor ligands differentially regulate sebaceous differentiation in human sebaceous gland organ cultures in vitro. *The British journal of dermatology* **151**, 766-775.
- Dubrac, S., Schmuth, M., 2011. PPAR-alpha in cutaneous inflammation. *Dermato-endocrinology* **3**, 23-26.
- Dvorak, M., Watkinson, A., McGlone, F., Rukwied, R., 2003. Histamine induced responses are attenuated by a cannabinoid receptor agonist in human skin. *Inflammation research : official journal of the European Histamine Research Society ... [et al.]* **52**, 238-245.
- Elias, P.M., Feingold, K.R., 2001. Coordinate regulation of epidermal differentiation and barrier homeostasis. *Skin Pharmacol Appl Skin Physiol* **14 Suppl 1**, 28-34.
- Ellman, G.L., Courtney, K.D., Andres, V., Jr., Feather-Stone, R.M., 1961. A new and rapid colorimetric determination of acetylcholinesterase activity. *Biochemical pharmacology* **7**, 88-95.
- Favia, A.D., Habrant, D., Scarpelli, R., Migliore, M., Albani, C., Bertozzi, S.M., Dionisi, M., Tarozzo, G., Piomelli, D., Cavalli, A., De Vivo, M., 2012. Identification and characterization of carprofen as a multitarget fatty acid amide hydrolase/cyclooxygenase inhibitor. *Journal of medicinal chemistry* **55**, 8807-8826.
- Fegley, D., Gaetani, S., Duranti, A., Tontini, A., Mor, M., Tarzia, G., Piomelli, D., 2005. Characterization of the fatty acid amide hydrolase inhibitor cyclohexyl carbamic acid 3'-carbamoyl-biphenyl-3-yl ester (URB597): effects on anandamide and oleoylethanolamide deactivation. *The Journal of pharmacology and experimental therapeutics* **313**, 352-358.
- Fehrenbacher, J.C., Vasko, M.R., Duarte, D.B., 2012. Models of inflammation: Carrageenan- or complete Freund's Adjuvant (CFA)-induced edema and hypersensitivity in the rat. *Curr Protoc Pharmacol* **Chapter 5**, Unit5 4.

- Fezza, F., Bari, M., Florio, R., Talamonti, E., Feole, M., Maccarrone, M., 2014. Endocannabinoids, related compounds and their metabolic routes. *Molecules* **19**, 17078-17106.
- Firooz, A., Sadr, B., Davoudi, S.M., Nassiri-Kashani, M., Panahi, Y., Dowlati, Y., 2011. Long-term skin damage due to chemical weapon exposure. *Cutaneous and ocular toxicology* **30**, 64-68.
- Fogh, K., Herlin, T., Kragballe, K., 1989. Eicosanoids in skin of patients with atopic dermatitis: prostaglandin E2 and leukotriene B4 are present in biologically active concentrations. *The Journal of allergy and clinical immunology* **83**, 450-455.
- Fonseca, B.M., Costa, M.A., Almada, M., Correia-da-Silva, G., Teixeira, N.A., 2013. Endogenous cannabinoids revisited: a biochemistry perspective. *Prostaglandins Other Lipid Mediat* **102-103**, 13-30.
- Fowler, C.J., Holt, S., Tiger, G., 2003. Acidic nonsteroidal anti-inflammatory drugs inhibit rat brain fatty acid amide hydrolase in a pH-dependent manner. *Journal of enzyme inhibition and medicinal chemistry* **18**, 55-58.
- Fu, J., Gaetani, S., Oveisi, F., Lo Verme, J., Serrano, A., Rodriguez De Fonseca, F., Rosengarth, A., Luecke, H., Di Giacomo, B., Tarzia, G., Piomelli, D., 2003. Oleyethanolamide regulates feeding and body weight through activation of the nuclear receptor PPAR-alpha. *Nature* **425**, 90-93.
- Futagami, A., Ishizaki, M., Fukuda, Y., Kawana, S., Yamanaka, N., 2002. Wound healing involves induction of cyclooxygenase-2 expression in rat skin. *Laboratory investigation; a journal of technical methods and pathology* **82**, 1503-1513.
- Gaffal, E., Cron, M., Glodde, N., Bald, T., Kuner, R., Zimmer, A., Lutz, B., Tuting, T., 2013. Cannabinoid 1 receptors in keratinocytes modulate proinflammatory chemokine secretion and attenuate contact allergic inflammation. *J Immunol* **190**, 4929-4936.
- Gaffal, E., Glodde, N., Jakobs, M., Bald, T., Tuting, T., 2014. Cannabinoid 1 receptors in keratinocytes attenuate fluorescein isothiocyanate-induced mouse atopic-like dermatitis. *Experimental dermatology* **23**, 401-406.
- Galiegue, S., Mary, S., Marchand, J., Dussossoy, D., Carriere, D., Carayon, P., Bouaboula, M., Shire, D., Le Fur, G., Casellas, P., 1995. Expression of central and peripheral cannabinoid receptors in human immune tissues and leukocyte subpopulations. *European journal of biochemistry / FEBS* **232**, 54-61.
- Garcia, M., Llames, S., Garcia, E., Meana, A., Cuadrado, N., Recasens, M., Puig, S., Nagore, E., Illera, N., Jorcano, J.L., Del Rio, M., Larcher, F., 2010. In vivo assessment of acute UVB responses in normal and Xeroderma Pigmentosum (XP-C) skin-humanized mouse models. *The American journal of pathology* **177**, 865-872.
- Ghabili, K., Agutter, P.S., Ghanei, M., Ansarin, K., Shoja, M.M., 2010. Mustard gas toxicity: the acute and chronic pathological effects. *Journal of applied toxicology : JAT* **30**, 627-643.
- Giang, D.K., Cravatt, B.F., 1997. Molecular characterization of human and mouse fatty acid amide hydrolases. *Proceedings of the National Academy of Sciences of the United States of America* **94**, 2238-2242.
- Goel, G., Makkar, H.P., Francis, G., Becker, K., 2007. Phorbol esters: structure, biological activity, and toxicity in animals. *Int J Toxicol* **26**, 279-288.
- Gordon, M.K., DeSantis Rodrigues, A.S., Hahn, R.A., Gerecke, D.R., Svoboda, K.H 2013. Hydroxamates inhibit EMMPRIN as well as ADAM17/TACE and MMPs. *FASEB J.* **27**, 754.752.
- Goren, I., Lee, S.Y., Maucher, D., Nusing, R., Schlich, T., Pfeilschifter, J., Frank, S., 2015. Inhibition of cyclooxygenase-1 and -2 activity in keratinocytes inhibits PGE formation and impairs

- vascular endothelial growth factor release and neovascularisation in skin wounds. *Int Wound J.*
- Graham, J.S., Chilcott, R.P., Rice, P., Milner, S.M., Hurst, C.G., Maliner, B.I., 2005. Wound healing of cutaneous sulfur mustard injuries: strategies for the development of improved therapies. *Journal of burns and wounds* **4**, e1.
- Graham, J.S., Stevenson, R.S., Mitcheltree, L.W., Hamilton, T.A., Deckert, R.R., Lee, R.B., Schiavetta, A.M., 2009. Medical management of cutaneous sulfur mustard injuries. *Toxicology* **263**, 47-58.
- Grando, S.A., 1997. Biological functions of keratinocyte cholinergic receptors. *The journal of investigative dermatology. Symposium proceedings / the Society for Investigative Dermatology, Inc. [and] European Society for Dermatological Research* **2**, 41-48.
- Greenhalgh, D.G., 2005. Models of wound healing. *The Journal of burn care & rehabilitation* **26**, 293-305.
- Grim, T.W., Ghosh, S., Hsu, K.L., Cravatt, B.F., Kinsey, S.G., Lichtman, A.H., 2014. Combined inhibition of FAAH and COX produces enhanced anti-allodynic effects in mouse neuropathic and inflammatory pain models. *Pharmacology, biochemistry, and behavior* **124**, 405-411.
- Grygiel-Gorniak, B., 2014. Peroxisome proliferator-activated receptors and their ligands: nutritional and clinical implications - a review. *Nutrition Journal* **13**.
- Gui, H., Tong, Q., Qu, W., Mao, C.M., Dai, S.M., 2015. The endocannabinoid system and its therapeutic implications in rheumatoid arthritis. *International immunopharmacology* **26**, 86-91.
- Han, S., Espinoza, L.A., Liao, H., Boulares, A.H., Smulson, M.E., 2004. Protection by antioxidants against toxicity and apoptosis induced by the sulphur mustard analog 2-chloroethylethyl sulphide (CEES) in Jurkat T cells and normal human lymphocytes. *British journal of pharmacology* **141**, 795-802.
- Hanley, K., Jiang, Y., He, S.S., Friedman, M., Elias, P.M., Bikle, D.D., Williams, M.L., Feingold, K.R., 1998. Keratinocyte differentiation is stimulated by activators of the nuclear hormone receptor PPARalpha. *The Journal of investigative dermatology* **110**, 368-375.
- Hansch, C., Bonavida, B., Jazirehi, A.R., Cohen, J.J., Milliron, C., Kurup, A., 2003. Quantitative structure-activity relationships of phenolic compounds causing apoptosis. *Bioorganic & medicinal chemistry* **11**, 617-620.
- Haslam, I.S., Pitre, A., Schuetz, J.D., Paus, R., 2013. Protection against chemotherapy-induced alopecia: targeting ATP-binding cassette transporters in the hair follicle? *Trends in pharmacological sciences* **34**, 599-604.
- Hawk, J.L., Black, A.K., Jaenicke, K.F., Barr, R.M., Soter, N.A., Mallett, A.I., Gilchrest, B.A., Hensby, C.N., Parrish, J.A., Greaves, M.W., 1983. Increased concentrations of arachidonic acid, prostaglandins E2, D2, and 6-oxo-F1 alpha, and histamine in human skin following UVA irradiation. *The Journal of investigative dermatology* **80**, 496-499.
- Hefazi, M., Maleki, M., Mahmoudi, M., Tabatabaee, A., Balali-Mood, M., 2006. Delayed complications of sulfur mustard poisoning in the skin and the immune system of Iranian veterans 16-20 years after exposure. *International journal of dermatology* **45**, 1025-1031.
- Ho, W.S., Barrett, D.A., Randall, M.D., 2008. 'Entourage' effects of N-palmitoylethanolamide and N-oleoylethanolamide on vasorelaxation to anandamide occur through TRPV1 receptors. *British journal of pharmacology* **155**, 837-846.
- Hogg, N., Kalyanaraman, B., 1999. Nitric oxide and lipid peroxidation. *Biochimica et biophysica acta* **1411**, 378-384.

- Holt, S., Comelli, F., Costa, B., Fowler, C.J., 2005. Inhibitors of fatty acid amide hydrolase reduce carrageenan-induced hind paw inflammation in pentobarbital-treated mice: comparison with indomethacin and possible involvement of cannabinoid receptors. *British journal of pharmacology* **146**, 467-476.
- Holt, S., Nilsson, J., Omeir, R., Tiger, G., Fowler, C.J., 2001. Effects of pH on the inhibition of fatty acid amidohydrolase by ibuprofen. *British journal of pharmacology* **133**, 513-520.
- Holt, S., Paylor, B., Boldrup, L., Alajakku, K., Vandevoorde, S., Sundstrom, A., Cocco, M.T., Onnis, V., Fowler, C.J., 2007. Inhibition of fatty acid amide hydrolase, a key endocannabinoid metabolizing enzyme, by analogues of ibuprofen and indomethacin. *European journal of pharmacology* **565**, 26-36.
- Howlett, A.C., 2002. The cannabinoid receptors. *Prostaglandins Other Lipid Mediat* **68-69**, 619-631.
- Howlett, A.C., 2005. Cannabinoid receptor signaling. *Handb Exp Pharmacol*, 53-79.
- Howlett, A.C., Blume, L.C., Dalton, G.D., 2010. CB(1) cannabinoid receptors and their associated proteins. *Current medicinal chemistry* **17**, 1382-1393.
- Ito, M., Liu, Y., Yang, Z., Nguyen, J., Liang, F., Morris, R.J., Cotsarelis, G., 2005. Stem cells in the hair follicle bulge contribute to wound repair but not to homeostasis of the epidermis. *Nature medicine* **11**, 1351-1354.
- Jain, A.K., Tewari-Singh, N., Inturi, S., Orlicky, D.J., White, C.W., Agarwal, R., 2014. Histopathological and immunohistochemical evaluation of nitrogen mustard-induced cutaneous effects in SKH-1 hairless and C57BL/6 mice. *Experimental and toxicologic pathology : official journal of the Gesellschaft fur Toxikologische Pathologie* **66**, 129-138.
- Jan, Y.H., Heck, D.E., Gray, J.P., Zheng, H., Casillas, R.P., Laskin, D.L., Laskin, J.D., 2010. Selective targeting of selenocysteine in thioredoxin reductase by the half mustard 2-chloroethyl ethyl sulfide in lung epithelial cells. *Chemical research in toxicology* **23**, 1045-1053.
- Janusz, J.M., Buckwalter, B.L., Young, P.A., LaHann, T.R., Farmer, R.W., Kasting, G.B., Loomans, M.E., Kerckaert, G.A., Maddin, C.S., Berman, E.F., et al., 1993. Vanilloids. 1. Analogs of capsaicin with antinociceptive and antiinflammatory activity. *Journal of medicinal chemistry* **36**, 2595-2604.
- Jayamanne, A., Greenwood, R., Mitchell, V.A., Aslan, S., Piomelli, D., Vaughan, C.W., 2006. Actions of the FAAH inhibitor URB597 in neuropathic and inflammatory chronic pain models. *British journal of pharmacology* **147**, 281-288.
- Jhaveri, M.D., Richardson, D., Robinson, I., Garle, M.J., Patel, A., Sun, Y., Sagar, D.R., Bennett, A.J., Alexander, S.P., Kendall, D.A., Barrett, D.A., Chapman, V., 2008. Inhibition of fatty acid amide hydrolase and cyclooxygenase-2 increases levels of endocannabinoid related molecules and produces analgesia via peroxisome proliferator-activated receptor-alpha in a model of inflammatory pain. *Neuropharmacology* **55**, 85-93.
- Jia, W., Hegde, V.L., Singh, N.P., Sisco, D., Grant, S., Nagarkatti, M., Nagarkatti, P.S., 2006. Delta9-tetrahydrocannabinol-induced apoptosis in Jurkat leukemia T cells is regulated by translocation of Bad to mitochondria. *Molecular cancer research : MCR* **4**, 549-562.
- Joseph, L.B., Gerecke, D.R., Heck, D.E., Black, A.T., Sinko, P.J., Cervelli, J.A., Casillas, R.P., Babin, M.C., Laskin, D.L., Laskin, J.D., 2011. Structural changes in the skin of hairless mice following exposure to sulfur mustard correlate with inflammation and DNA damage. *Experimental and molecular pathology* **91**, 515-527.
- Joseph, L.B., Heck, D.E., Cervelli, J.A., Composto, G.M., Babin, M.C., Casillas, R.P., Sinko, P.J., Gerecke, D.R., Laskin, D.L., Laskin, J.D., 2014. Structural changes in hair follicles and sebaceous glands of hairless mice following exposure to sulfur mustard. *Experimental and molecular pathology* **96**, 316-327.

- Jung, H.J., Song, Y.S., Lim, C.J., Park, E.H., 2008. Anti-angiogenic, anti-inflammatory and anti-nociceptive activities of vanillyl alcohol. *Archives of pharmacal research* **31**, 1275-1279.
- Kampfer, H., Brautigam, L., Geisslinger, G., Pfeilschifter, J., Frank, S., 2003. Cyclooxygenase-1-coupled prostaglandin biosynthesis constitutes an essential prerequisite for skin repair. *The Journal of investigative dermatology* **120**, 880-890.
- Kampfer, H., Schmidt, R., Geisslinger, G., Pfeilschifter, J., Frank, S., 2005. Wound inflammation in diabetic ob/ob mice: functional coupling of prostaglandin biosynthesis to cyclooxygenase-1 activity in diabetes-impaired wound healing. *Diabetes* **54**, 1543-1551.
- Karaliota, S., Siafaka-Kapadai, A., Gontinou, C., Psarra, K., Mavri-Vavayanni, M., 2009. Anandamide increases the differentiation of rat adipocytes and causes PPARgamma and CB1 receptor upregulation. *Obesity (Silver Spring)* **17**, 1830-1838.
- Karsak, M., Gaffal, E., Date, R., Wang-Eckhardt, L., Rehnelt, J., Petrosino, S., Starowicz, K., Steuder, R., Schlicker, E., Cravatt, B., Mechoulam, R., Buettner, R., Werner, S., Di Marzo, V., Tuting, T., Zimmer, A., 2007. Attenuation of allergic contact dermatitis through the endocannabinoid system. *Science* **316**, 1494-1497.
- Kathuria, S., Gaetani, S., Fegley, D., Valino, F., Duranti, A., Tontini, A., Mor, M., Tarzia, G., La Rana, G., Calignano, A., Giustino, A., Tattoli, M., Palmery, M., Cuomo, V., Piomelli, D., 2003. Modulation of anxiety through blockade of anandamide hydrolysis. *Nature medicine* **9**, 76-81.
- Kehe, K., Balszuweit, F., Steinritz, D., Thiermann, H., 2009a. Molecular toxicology of sulfur mustard-induced cutaneous inflammation and blistering. *Toxicology* **263**, 12-19.
- Kehe, K., Thiermann, H., Balszuweit, F., Eyer, F., Steinritz, D., Zilker, T., 2009j. Acute effects of sulfur mustard injury--Munich experiences. *Toxicology* **263**, 3-8.
- Keith, J.M., Apodaca, R., Tichenor, M., Xiao, W., Jones, W., Pierce, J., Seierstad, M., Palmer, J., Webb, M., Karbarz, M., Scott, B., Wilson, S., Luo, L., Wennerholm, M., Chang, L., Brown, S., Rizzolio, M., Rynberg, R., Chaplan, S., Breitenbucher, J.G., 2012. Aryl Piperaziny Ureas as Inhibitors of Fatty Acid Amide Hydrolase (FAAH) in Rat, Dog, and Primate. *ACS medicinal chemistry letters* **3**, 823-827.
- Keith, J.M., Jones, W.M., Pierce, J.M., Seierstad, M., Palmer, J.A., Webb, M., Karbarz, M.J., Scott, B.P., Wilson, S.J., Luo, L., Wennerholm, M.L., Chang, L., Brown, S.M., Rizzolio, M., Rynberg, R., Chaplan, S.R., Breitenbucher, J.G., 2014. Heteroarylureas with spirocyclic diamine cores as inhibitors of fatty acid amide hydrolase. *Bioorganic & medicinal chemistry letters* **24**, 737-741.
- Kendall, A.C., Nicolaou, A., 2013. Bioactive lipid mediators in skin inflammation and immunity. *Progress in lipid research* **52**, 141-164.
- Kendall, A.C., Pilkington, S.M., Massey, K.A., Sassano, G., Rhodes, L.E., Nicolaou, A., 2015. Distribution of Bioactive Lipid Mediators in Human Skin. *The Journal of investigative dermatology*.
- Khallouki, F., Haubner, R., Ulrich, C.M., Owen, R.W., 2011. Ethnobotanical survey, chemical composition, and antioxidant capacity of methanolic extract of the root bark of *Annona cuneata* Oliv. *J Med Food* **14**, 1397-1402.
- Khansari, N., Shakiba, Y., Mahmoudi, M., 2009. Chronic inflammation and oxidative stress as a major cause of age-related diseases and cancer. *Recent patents on inflammation & allergy drug discovery* **3**, 73-80.
- Khateri, S., Ghanei, M., Keshavarz, S., Soroush, M., Haines, D., 2003. Incidence of lung, eye, and skin lesions as late complications in 34,000 Iranians with wartime exposure to mustard agent. *Journal of occupational and environmental medicine / American College of Occupational and Environmental Medicine* **45**, 1136-1143.

- Kishimoto, S., Muramatsu, M., Gokoh, M., Oka, S., Waku, K., Sugiura, T., 2005. Endogenous cannabinoid receptor ligand induces the migration of human natural killer cells. *Journal of biochemistry* **137**, 217-223.
- Klein, T.W., Newton, C., Larsen, K., Lu, L., Perkins, I., Nong, L., Friedman, H., 2003. The cannabinoid system and immune modulation. *Journal of leukocyte biology* **74**, 486-496.
- Korkmaz, A., Tan, D.X., Reiter, R.J., 2008. Acute and delayed sulfur mustard toxicity; novel mechanisms and future studies. *Interdiscip Toxicol* **1**, 22-26.
- Koster, M.I., 2009. Making an epidermis. *Annals of the New York Academy of Sciences* **1170**, 7-10.
- Kozak, K.R., Crews, B.C., Morrow, J.D., Wang, L.H., Ma, Y.H., Weinander, R., Jakobsson, P.J., Marnett, L.J., 2002. Metabolism of the endocannabinoids, 2-arachidonylglycerol and anandamide, into prostaglandin, thromboxane, and prostacyclin glycerol esters and ethanolamides. *The Journal of biological chemistry* **277**, 44877-44885.
- Kozono, S., Matsuyama, T., Biwasa, K.K., Kawahara, K., Nakajima, Y., Yoshimoto, T., Yonamine, Y., Kadomatsu, H., Tanchaoen, S., Hashiguchi, T., Noguchi, K., Maruyama, I., 2010. Involvement of the endocannabinoid system in periodontal healing. *Biochemical and biophysical research communications* **394**, 928-933.
- Krampert, M., Bloch, W., Sasaki, T., Bugnon, P., Rulicke, T., Wolf, E., Aumailley, M., Parks, W.C., Werner, S., 2004. Activities of the matrix metalloproteinase stromelysin-2 (MMP-10) in matrix degradation and keratinocyte organization in wounded skin. *Molecular biology of the cell* **15**, 5242-5254.
- Kumar, D., Tewari-Singh, N., Agarwal, C., Jain, A.K., Inturi, S., Kant, R., White, C.W., Agarwal, R., 2015. Nitrogen mustard exposure of murine skin induces DNA damage, oxidative stress and activation of MAPK/Akt-AP1 pathway leading to induction of inflammatory and proteolytic mediators. *Toxicology letters* **235**, 161-171.
- Kupczyk, P., Reich, A., Szepietowski, J.C., 2009. Cannabinoid system in the skin - a possible target for future therapies in dermatology. *Experimental dermatology* **18**, 669-679.
- Lambert, D.M., 2007. Allergic contact dermatitis and the endocannabinoid system: from mechanisms to skin care. *ChemMedChem* **2**, 1701-1702.
- Laskin, J.D., Black, A.T., Jan, Y.H., Sinko, P.J., Heindel, N.D., Sunil, V., Heck, D.E., Laskin, D.L., 2010. Oxidants and antioxidants in sulfur mustard-induced injury. *Annals of the New York Academy of Sciences* **1203**, 92-100.
- Laskin, J.D., Heck, D.E., Huang, M-T., Fabio, K., Lacey, C.J., Young, S., Mohanta, P., Guillon, C., & Heindel, N.D. , 2012. Unique Dual-Action Therapeutics. In Office, U.S.P., (Ed.), United States, pp.
- Laskin, J.D., Heck, D.E., Lacey, C.J., Aponte, E., Huang, M-T., & Heindel, N.D. , 2013. Pharmacologically-Active Vanilloid Carbamates. In Office, U.S.P., (Ed.), United States, pp.
- Laulederkind, S.J., Thompson-Jaeger, S., Goorha, S., Chen, Q., Fu, A., Rho, J.Y., Ballou, L.R., Raghov, R., 2002. Both constitutive and inducible prostaglandin H synthase affect dermal wound healing in mice. *Laboratory investigation; a journal of technical methods and pathology* **82**, 919-927.
- Lee, B., Vouthounis, C., Stojadinovic, O., Brem, H., Im, M., Tomic-Canic, M., 2005. From an enhanceosome to a repressosome: molecular antagonism between glucocorticoids and EGF leads to inhibition of wound healing. *Journal of molecular biology* **345**, 1083-1097.
- Lehmann, J.M., Lenhard, J.M., Oliver, B.B., Ringold, G.M., Kliewer, S.A., 1997. Peroxisome proliferator-activated receptors alpha and gamma are activated by indomethacin and other non-steroidal anti-inflammatory drugs. *The Journal of biological chemistry* **272**, 3406-3410.

- Lenglet, S., Thomas, A., Soehnlein, O., Montecucco, F., Burger, F., Pelli, G., Galan, K., Cravatt, B., Staub, C., Steffens, S., 2013. Fatty acid amide hydrolase deficiency enhances intraplaque neutrophil recruitment in atherosclerotic mice. *Arteriosclerosis, thrombosis, and vascular biology* **33**, 215-223.
- Li, L., Tucker, R.W., Hennings, H., Yuspa, S.H., 1995. Chelation of intracellular Ca^{2+} inhibits murine keratinocyte differentiation in vitro. *Journal of cellular physiology* **163**, 105-114.
- Lichtman, A.H., Leung, D., Shelton, C.C., Saghatelian, A., Hardouin, C., Boger, D.L., Cravatt, B.F., 2004. Reversible inhibitors of fatty acid amide hydrolase that promote analgesia: evidence for an unprecedented combination of potency and selectivity. *The Journal of pharmacology and experimental therapeutics* **311**, 441-448.
- Lindahl, L.M., Fenger-Gron, M., Iversen, L., 2013. Topical nitrogen mustard therapy in patients with mycosis fungoides or parapsoriasis. *Journal of the European Academy of Dermatology and Venereology : JEADV* **27**, 163-168.
- Lo Verme, J., Fu, J., Astarita, G., La Rana, G., Russo, R., Calignano, A., Piomelli, D., 2005. The nuclear receptor peroxisome proliferator-activated receptor- α mediates the anti-inflammatory actions of palmitoylethanolamide. *Molecular pharmacology* **67**, 15-19.
- Lodola, A., Capoferri, L., Rivara, S., Chudyk, E., Sirirak, J., Dyguda-Kazimierowicz, E., Andrzej Sokalski, W., Mileni, M., Tarzia, G., Piomelli, D., Mor, M., Mulholland, A.J., 2011. Understanding the role of carbamate reactivity in fatty acid amide hydrolase inhibition by QM/MM mechanistic modelling. *Chem Commun (Camb)* **47**, 2517-2519.
- LoVerme, J., Russo, R., La Rana, G., Fu, J., Farthing, J., Mattace-Raso, G., Meli, R., Hohmann, A., Calignano, A., Piomelli, D., 2006. Rapid broad-spectrum analgesia through activation of peroxisome proliferator-activated receptor- α . *The Journal of pharmacology and experimental therapeutics* **319**, 1051-1061.
- Maccarrone, M., Bab, I., Biro, T., Cabral, G.A., Dey, S.K., Di Marzo, V., Konje, J.C., Kunos, G., Mechoulam, R., Pacher, P., Sharkey, K.A., Zimmer, A., 2015. Endocannabinoid signaling at the periphery: 50 years after THC. *Trends in pharmacological sciences*.
- Maccarrone, M., Dainese, E., Oddi, S., 2010. Intracellular trafficking of anandamide: new concepts for signaling. *Trends in biochemical sciences* **35**, 601-608.
- Maccarrone, M., Di Rienzo, M., Battista, N., Gasperi, V., Guerrieri, P., Rossi, A., Finazzi-Agro, A., 2003. The endocannabinoid system in human keratinocytes. Evidence that anandamide inhibits epidermal differentiation through CB1 receptor-dependent inhibition of protein kinase C, activation protein-1, and transglutaminase. *The Journal of biological chemistry* **278**, 33896-33903.
- Malek, N., Mrugala, M., Makuch, W., Kolosowska, N., Przewlocka, B., Binkowski, M., Czaja, M., Morera, E., Di Marzo, V., Starowicz, K., 2015. A multi-target approach for pain treatment: dual inhibition of fatty acid amide hydrolase and TRPV1 in a rat model of osteoarthritis. *Pain* **156**, 890-903.
- Mansour Razavi, S., Salamati, P., Saghafein, M., Abdollahi, M., 2012. A review on delayed toxic effects of sulfur mustard in Iranian veterans. *Daru* **20**, 51.
- Massa, F., Marsicano, G., Hermann, H., Cannich, A., Monory, K., Cravatt, B.F., Ferri, G.L., Sibaev, A., Storr, M., Lutz, B., 2004. The endogenous cannabinoid system protects against colonic inflammation. *The Journal of clinical investigation* **113**, 1202-1209.
- Matsuda, L.A., Lolait, S.J., Brownstein, M.J., Young, A.C., Bonner, T.I., 1990. Structure of a cannabinoid receptor and functional expression of the cloned cDNA. *Nature* **346**, 561-564.
- Matsui, T., Amagai, M., 2015. Dissecting the formation, structure and barrier function of the stratum corneum. *Int Immunol* **27**, 269-280.

- McKinney, M.K., Cravatt, B.F., 2003. Evidence for distinct roles in catalysis for residues of the serine-serine-lysine catalytic triad of fatty acid amide hydrolase. *The Journal of biological chemistry* **278**, 37393-37399.
- McMahon, S.B., Wood, M.A., Cole, M.D., 2000. The essential cofactor TRRAP recruits the histone acetyltransferase hGCN5 to c-Myc. *Molecular and cellular biology* **20**, 556-562.
- Medicherla, S., Wadsworth, S., Cullen, B., Silcock, D., Ma, J.Y., Mangadu, R., Kerr, I., Chakravarty, S., Luedtke, G.L., Dugar, S., Protter, A.A., Higgins, L.S., 2009. p38 MAPK inhibition reduces diabetes-induced impairment of wound healing. *Diabetes Metab Syndr Obes* **2**, 91-100.
- Menon, G.K., Elias, P.M., Lee, S.H., Feingold, K.R., 1992. Localization of calcium in murine epidermis following disruption and repair of the permeability barrier. *Cell and tissue research* **270**, 503-512.
- Michalik, L., Desvergne, B., Tan, N.S., Basu-Modak, S., Escher, P., Rieusset, J., Peters, J.M., Kaya, G., Gonzalez, F.J., Zakany, J., Metzger, D., Chambon, P., Duboule, D., Wahli, W., 2001. Impaired skin wound healing in peroxisome proliferator-activated receptor (PPAR)alpha and PPARbeta mutant mice. *The Journal of cell biology* **154**, 799-814.
- Mileni, M., Garfinkle, J., Ezzili, C., Kimball, F.S., Cravatt, B.F., Stevens, R.C., Boger, D.L., 2010. X-ray crystallographic analysis of alpha-ketoheterocycle inhibitors bound to a humanized variant of fatty acid amide hydrolase. *Journal of medicinal chemistry* **53**, 230-240.
- Min, X., Thibault, S.T., Porter, A.C., Gustin, D.J., Carlson, T.J., Xu, H., Lindstrom, M., Xu, G., Uyeda, C., Ma, Z., Li, Y., Kayser, F., Walker, N.P., Wang, Z., 2011. Discovery and molecular basis of potent noncovalent inhibitors of fatty acid amide hydrolase (FAAH). *Proceedings of the National Academy of Sciences of the United States of America* **108**, 7379-7384.
- Mitchell, J.A., Akaraseenont, P., Thiemermann, C., Flower, R.J., Vane, J.R., 1993. Selectivity of nonsteroidal antiinflammatory drugs as inhibitors of constitutive and inducible cyclooxygenase. *Proceedings of the National Academy of Sciences of the United States of America* **90**, 11693-11697.
- Mor, M., Rivara, S., Lodola, A., Plazzi, P.V., Tarzia, G., Duranti, A., Tontini, A., Piersanti, G., Kathuria, S., Piomelli, D., 2004. Cyclohexylcarbamic acid 3'- or 4'-substituted biphenyl-3-yl esters as fatty acid amide hydrolase inhibitors: synthesis, quantitative structure-activity relationships, and molecular modeling studies. *Journal of medicinal chemistry* **47**, 4998-5008.
- Munro, S., Thomas, K.L., Abu-Shaar, M., 1993. Molecular characterization of a peripheral receptor for cannabinoids. *Nature* **365**, 61-65.
- Murakami, M., Nakatani, Y., Tanioka, T., Kudo, I., 2002. Prostaglandin E synthase. *Prostaglandins Other Lipid Mediat* **68-69**, 383-399.
- Naghii, M.R., 2002. Sulfur mustard intoxication, oxidative stress, and antioxidants. *Military medicine* **167**, 573-575.
- Neff, G.W., O'Brien, C.B., Reddy, K.R., Bergasa, N.V., Regev, A., Molina, E., Amaro, R., Rodriguez, M.J., Chase, V., Jeffers, L., Schiff, E., 2002. Preliminary observation with dronabinol in patients with intractable pruritus secondary to cholestatic liver disease. *The American journal of gastroenterology* **97**, 2117-2119.
- Nguyen, V.T., Ndoeye, A., Grando, S.A., 2000. Novel human alpha9 acetylcholine receptor regulating keratinocyte adhesion is targeted by Pemphigus vulgaris autoimmunity. *The American journal of pathology* **157**, 1377-1391.
- Nicolussi, S., Gertsch, J., 2015. Endocannabinoid transport revisited. *Vitamins and hormones* **98**, 441-485.

- Nyska, A., Lomnitski, L., Maronpot, R., Moomaw, C., Brodsky, B., Sintov, A., Wormser, U., 2001. Effects of iodine on inducible nitric oxide synthase and cyclooxygenase-2 expression in sulfur mustard-induced skin. *Arch Toxicol* **74**, 768-774.
- O'Sullivan, S.E., Kendall, D.A., 2010. Cannabinoid activation of peroxisome proliferator-activated receptors: potential for modulation of inflammatory disease. *Immunobiology* **215**, 611-616.
- Oddi, S., Bari, M., Battista, N., Barsacchi, D., Cozzani, I., Maccarrone, M., 2005. Confocal microscopy and biochemical analysis reveal spatial and functional separation between anandamide uptake and hydrolysis in human keratinocytes. *Cellular and molecular life sciences : CMLS* **62**, 386-395.
- Oka, S., Wakui, J., Ikeda, S., Yanagimoto, S., Kishimoto, S., Gokoh, M., Nasui, M., Sugiura, T., 2006. Involvement of the cannabinoid CB2 receptor and its endogenous ligand 2-arachidonoylglycerol in oxazolone-induced contact dermatitis in mice. *J Immunol* **177**, 8796-8805.
- Oka, S., Yanagimoto, S., Ikeda, S., Gokoh, M., Kishimoto, S., Waku, K., Ishima, Y., Sugiura, T., 2005. Evidence for the involvement of the cannabinoid CB2 receptor and its endogenous ligand 2-arachidonoylglycerol in 12-O-tetradecanoylphorbol-13-acetate-induced acute inflammation in mouse ear. *The Journal of biological chemistry* **280**, 18488-18497.
- Olah, A., Ambrus, L., Nicolussi, S., Gertsch, J., Tubak, V., Kemeny, L., Soeberdt, M., Abels, C., Biro, T., 2016. Inhibition of fatty acid amide hydrolase exerts cutaneous anti-inflammatory effects both in vitro and in vivo. *Experimental dermatology*.
- Opas, E.E., Bonney, R.J., Humes, J.L., 1985. Prostaglandin and leukotriene synthesis in mouse ears inflamed by arachidonic acid. *The Journal of investigative dermatology* **84**, 253-256.
- Orrenius, S., McConkey, D.J., Bellomo, G., Nicotera, P., 1989. Role of Ca²⁺ in toxic cell killing. *Trends in pharmacological sciences* **10**, 281-285.
- Otrubova, K., Cravatt, B.F., Boger, D.L., 2014. Design, synthesis, and characterization of alpha-ketoheterocycles that additionally target the cytosolic port Cys269 of fatty acid amide hydrolase. *Journal of medicinal chemistry* **57**, 1079-1089.
- Otrubova, K., Ezzili, C., Boger, D.L., 2011. The discovery and development of inhibitors of fatty acid amide hydrolase (FAAH). *Bioorganic & medicinal chemistry letters* **21**, 4674-4685.
- Ottaviani, M., Alestas, T., Flori, E., Mastrofrancesco, A., Zouboulis, C.C., Picardo, M., 2006. Peroxidated squalene induces the production of inflammatory mediators in HaCaT keratinocytes: a possible role in acne vulgaris. *The Journal of investigative dermatology* **126**, 2430-2437.
- Ottaviani, M., Camera, E., Picardo, M., 2010. Lipid mediators in acne. *Mediators of inflammation* **2010**.
- Ozaita, A., Puighermanal, E., Maldonado, R., 2007. Regulation of PI3K/Akt/GSK-3 pathway by cannabinoids in the brain. *Journal of neurochemistry* **102**, 1105-1114.
- Pacher, P., Mechoulam, R., 2011. Is lipid signaling through cannabinoid 2 receptors part of a protective system? *Progress in lipid research* **50**, 193-211.
- Pal, A., Tewari-Singh, N., Gu, M., Agarwal, C., Huang, J., Day, B.J., White, C.W., Agarwal, R., 2009a. Sulfur mustard analog induces oxidative stress and activates signaling cascades in the skin of SKH-1 hairless mice. *Free radical biology & medicine* **47**, 1640-1651.
- Pal, M., Angaru, S., Kodimuthali, A., Dhingra, N., 2009c. Vanilloid receptor antagonists: emerging class of novel anti-inflammatory agents for pain management. *Current pharmaceutical design* **15**, 1008-1026.

- Paladini, R.D., Takahashi, K., Bravo, N.S., Coulombe, P.A., 1996. Onset of re-epithelialization after skin injury correlates with a reorganization of keratin filaments in wound edge keratinocytes: defining a potential role for keratin 16. *The Journal of cell biology* **132**, 381-397.
- Palumbo-Zerr, K., Horn, A., Distler, A., Zerr, P., Dees, C., Beyer, C., Selvi, E., Cravatt, B.F., Distler, O., Schett, G., Distler, J.H., 2012. Inactivation of fatty acid amide hydrolase exacerbates experimental fibrosis by enhanced endocannabinoid-mediated activation of CB1. *Annals of the rheumatic diseases* **71**, 2051-2054.
- Panteleyev, A.A., Paus, R., Christiano, A.M., 2000. Patterns of hairless (hr) gene expression in mouse hair follicle morphogenesis and cycling. *The American journal of pathology* **157**, 1071-1079.
- Panteleyev, A.A., van der Veen, C., Rosenbach, T., Muller-Rover, S., Sokolov, V.E., Paus, R., 1998. Towards defining the pathogenesis of the hairless phenotype. *The Journal of investigative dermatology* **110**, 902-907.
- Papirmeister, B., Gross, C.L., Meier, H.L., Petrali, J.P., Johnson, J.B., 1985. Molecular basis for mustard-induced vesication. *Fundamental and applied toxicology : official journal of the Society of Toxicology* **5**, S134-149.
- Paradisi, A., Pasquariello, N., Barcaroli, D., Maccarrone, M., 2008. Anandamide regulates keratinocyte differentiation by inducing DNA methylation in a CB1 receptor-dependent manner. *The Journal of biological chemistry* **283**, 6005-6012.
- Paromov, V., Suntres, Z., Smith, M., Stone, W.L., 2007. Sulfur mustard toxicity following dermal exposure: role of oxidative stress, and antioxidant therapy. *Journal of burns and wounds* **7**, e7.
- Pastar, I., Stojadinovic, O., Yin, N.C., Ramirez, H., Nusbaum, A.G., Sawaya, A., Patel, S.B., Khalid, L., Isseroff, R.R., Tomic-Canic, M., 2014. Epithelialization in Wound Healing: A Comprehensive Review. *Advances in wound care* **3**, 445-464.
- Paus, R., Schmelz, M., Biro, T., Steinhoff, M., 2006. Frontiers in pruritus research: scratching the brain for more effective itch therapy. *The Journal of clinical investigation* **116**, 1174-1186.
- Perez-Gomez, E., Andradas, C., Flores, J.M., Quintanilla, M., Paramio, J.M., Guzman, M., Sanchez, C., 2013. The orphan receptor GPR55 drives skin carcinogenesis and is upregulated in human squamous cell carcinomas. *Oncogene* **32**, 2534-2542.
- Pertwee, R.G., 2005. Pharmacological actions of cannabinoids. *Handb Exp Pharmacol*, 1-51.
- Pertwee, R.G., 2010. Receptors and channels targeted by synthetic cannabinoid receptor agonists and antagonists. *Current medicinal chemistry* **17**, 1360-1381.
- Pertwee, R.G., 2014. Elevating endocannabinoid levels: pharmacological strategies and potential therapeutic applications. *Proc Nutr Soc* **73**, 96-105.
- Pertwee, R.G., Howlett, A.C., Abood, M.E., Alexander, S.P., Di Marzo, V., Elphick, M.R., Greasley, P.J., Hansen, H.S., Kunos, G., Mackie, K., Mechoulam, R., Ross, R.A., 2010. International Union of Basic and Clinical Pharmacology. LXXIX. Cannabinoid receptors and their ligands: beyond CB(1) and CB(2). *Pharmacological reviews* **62**, 588-631.
- Petit, F., Donlan, M., Michel, A., 2006. GPR55 as a new cannabinoid receptor: still a long way to prove it. *Chem Biol Drug Des* **67**, 252-253.
- Petrosino, S., Cristino, L., Karsak, M., Gaffal, E., Ueda, N., Tuting, T., Bisogno, T., De Filippis, D., D'Amico, A., Saturnino, C., Orlando, P., Zimmer, A., Iuvone, T., Di Marzo, V., 2010. Protective role of palmitoylethanolamide in contact allergic dermatitis. *Allergy* **65**, 698-711.

- Pilcher, B.K., Wang, M., Qin, X.J., Parks, W.C., Senior, R.M., Welgus, H.G., 1999. Role of matrix metalloproteinases and their inhibition in cutaneous wound healing and allergic contact hypersensitivity. *Ann Ny Acad Sci* **878**, 12-24.
- Piomelli, D., Tarzia, G., Duranti, A., Tontini, A., Mor, M., Compton, T.R., Dasse, O., Monaghan, E.P., Parrott, J.A., Putman, D., 2006. Pharmacological profile of the selective FAAH inhibitor KDS-4103 (URB597). *CNS drug reviews* **12**, 21-38.
- Pita, R., Vidal-Asensi, S., 2010. [Cutaneous and systemic toxicology of vesicants used in warfare]. *Actas Dermosifiliogr* **101**, 7-18.
- Popp, T., Egea, V., Kehe, K., Steinritz, D., Schmidt, A., Jochum, M., Ries, C., 2011. Sulfur mustard induces differentiation in human primary keratinocytes: opposite roles of p38 and ERK1/2 MAPK. *Toxicology letters* **204**, 43-51.
- Potenzieri, C., Brink, T.S., Pacharinsak, C., Simone, D.A., 2008. Cannabinoid modulation of cutaneous Adelta nociceptors during inflammation. *J Neurophysiol* **100**, 2794-2806.
- Potten, C.S., Saffhill, R., Maibach, H.I., 1987. Measurement of the transit time for cells through the epidermis and stratum corneum of the mouse and guinea-pig. *Cell Tissue Kinet* **20**, 461-472.
- Potter, G.B., Beaudoin, G.M., 3rd, DeRenzo, C.L., Zarach, J.M., Chen, S.H., Thompson, C.C., 2001. The hairless gene mutated in congenital hair loss disorders encodes a novel nuclear receptor corepressor. *Genes & development* **15**, 2687-2701.
- Poursaleh, Z., Harandi, A.A., Vahedi, E., Ghanei, M., 2012. Treatment for sulfur mustard lung injuries; new therapeutic approaches from acute to chronic phase. *Daru* **20**, 27.
- Quistad, G.B., Sparks, S.E., Casida, J.E., 2001. Fatty acid amide hydrolase inhibition by neurotoxic organophosphorus pesticides. *Toxicology and applied pharmacology* **173**, 48-55.
- Raffai, G., Khang, G., Vanhoutte, P.M., 2015. Vanillin and vanillin analogs relax porcine coronary and basilar arteries by inhibiting L-type Ca²⁺ channels. *The Journal of pharmacology and experimental therapeutics* **352**, 14-22.
- Ramarao, M.K., Murphy, E.A., Shen, M.W., Wang, Y., Bushell, K.N., Huang, N., Pan, N., Williams, C., Clark, J.D., 2005. A fluorescence-based assay for fatty acid amide hydrolase compatible with high-throughput screening. *Analytical biochemistry* **343**, 143-151.
- Ramot, Y., Sugawara, K., Zakany, N., Toth, B.I., Biro, T., Paus, R., 2013. A novel control of human keratin expression: cannabinoid receptor 1-mediated signaling down-regulates the expression of keratins K6 and K16 in human keratinocytes in vitro and in situ. *PeerJ* **1**, e40.
- Ray, R., Legere, R.H., Majerus, B.J., Petrali, J.P., 1995. Sulfur mustard-induced increase in intracellular free calcium level and arachidonic acid release from cell membrane. *Toxicology and applied pharmacology* **131**, 44-52.
- Rebholz, B., Kehe, K., Ruzicka, T., Rupec, R.A., 2008. Role of NF-kappaB/RelA and MAPK pathways in keratinocytes in response to sulfur mustard. *The Journal of investigative dermatology* **128**, 1626-1632.
- Rettori, E., De Laurentiis, A., Zorrilla Zubilete, M., Rettori, V., Elverdin, J.C., 2012. Anti-inflammatory effect of the endocannabinoid anandamide in experimental periodontitis and stress in the rat. *Neuroimmunomodulation* **19**, 293-303.
- Rhee, D.J., Katz, L.J., Spaeth, G.L., Myers, J.S., 2001. Complementary and alternative medicine for glaucoma. *Surv Ophthalmol* **46**, 43-55.
- Rice, P., 2003. Sulphur mustard injuries of the skin. *Pathophysiology and management. Toxicol Rev* **22**, 111-118.
- Richardson, D., Pearson, R.G., Kurian, N., Latif, M.L., Garle, M.J., Barrett, D.A., Kendall, D.A., Scammell, B.E., Reeve, A.J., Chapman, V., 2008. Characterisation of the cannabinoid

- receptor system in synovial tissue and fluid in patients with osteoarthritis and rheumatoid arthritis. *Arthritis Res Ther* **10**, R43.
- Ricketts, K.M., Santai, C.T., France, J.A., Graziosi, A.M., Doyel, T.D., Gazaway, M.Y., Casillas, R.P., 2000. Inflammatory cytokine response in sulfur mustard-exposed mouse skin. *Journal of applied toxicology : JAT* **20 Suppl 1**, S73-76.
- Rikimaru, T., Nakamura, M., Yano, T., Beck, G., Habicht, G.S., Rennie, L.L., Widra, M., Hirshman, C.A., Boulay, M.G., Spannhake, E.W., et al., 1991. Mediators, initiating the inflammatory response, released in organ culture by full-thickness human skin explants exposed to the irritant, sulfur mustard. *The Journal of investigative dermatology* **96**, 888-897.
- Rishikaysh, P., Dev, K., Diaz, D., Qureshi, W.M., Filip, S., Mokry, J., 2014. Signaling involved in hair follicle morphogenesis and development. *International journal of molecular sciences* **15**, 1647-1670.
- Roelandt, T., Heughebaert, C., Bredif, S., Giddelo, C., Baudouin, C., Msika, P., Roseeuw, D., Uchida, Y., Elias, P.M., Hachem, J.P., 2012. Cannabinoid receptors 1 and 2 oppositely regulate epidermal permeability barrier status and differentiation. *Experimental dermatology* **21**, 688-693.
- Romani, R., Galeazzi, R., Rosi, G., Fiorini, R., Pirisinu, I., Ambrosini, A., Zolese, G., 2011. Anandamide and its congeners inhibit human plasma butyrylcholinesterase. Possible new roles for these endocannabinoids? *Biochimie* **93**, 1584-1591.
- Rosenthal, D.S., Simbulan-Rosenthal, C.M., Iyer, S., Spoonde, A., Smith, W., Ray, R., Smulson, M.E., 1998. Sulfur mustard induces markers of terminal differentiation and apoptosis in keratinocytes via a Ca²⁺-calmodulin and caspase-dependent pathway. *The Journal of investigative dermatology* **111**, 64-71.
- Rosenthal, D.S., Velena, A., Chou, F.P., Schlegel, R., Ray, R., Benton, B., Anderson, D., Smith, W.J., Simbulan-Rosenthal, C.M., 2003. Expression of dominant-negative Fas-associated death domain blocks human keratinocyte apoptosis and vesication induced by sulfur mustard. *The Journal of biological chemistry* **278**, 8531-8540.
- Ruzicka, T., Simmet, T., Peskar, B.A., Ring, J., 1986. Skin levels of arachidonic acid-derived inflammatory mediators and histamine in atopic dermatitis and psoriasis. *The Journal of investigative dermatology* **86**, 105-108.
- Ryberg, E., Larsson, N., Sjogren, S., Hjorth, S., Hermansson, N.O., Leonova, J., Elebring, T., Nilsson, K., Drmota, T., Greasley, P.J., 2007. The orphan receptor GPR55 is a novel cannabinoid receptor. *British journal of pharmacology* **152**, 1092-1101.
- Rys-Sikora, K.E., Konger, R.L., Schoggins, J.W., Malaviya, R., Pentland, A.P., 2000. Coordinate expression of secretory phospholipase A(2) and cyclooxygenase-2 in activated human keratinocytes. *American journal of physiology. Cell physiology* **278**, C822-833.
- Sabourin, C.L., Petrali, J.P., Casillas, R.P., 2000. Alterations in inflammatory cytokine gene expression in sulfur mustard-exposed mouse skin. *Journal of biochemical and molecular toxicology* **14**, 291-302.
- Schlosburg, J.E., Kinsey, S.G., Lichtman, A.H., 2009. Targeting fatty acid amide hydrolase (FAAH) to treat pain and inflammation. *The AAPS journal* **11**, 39-44.
- Schmid, M.A., Harris, E., 2014. Monocyte recruitment to the dermis and differentiation to dendritic cells increases the targets for dengue virus replication. *PLoS pathogens* **10**, e1004541.
- Schmuth, M., Haqq, C.M., Cairns, W.J., Holder, J.C., Dorsam, S., Chang, S., Lau, P., Fowler, A.J., Chuang, G., Moser, A.H., Brown, B.E., Mao-Qiang, M., Uchida, Y., Schoonjans, K., Auwerx, J., Chambon, P., Willson, T.M., Elias, P.M., Feingold, K.R., 2004. Peroxisome

- proliferator-activated receptor (PPAR)-beta/delta stimulates differentiation and lipid accumulation in keratinocytes. *The Journal of investigative dermatology* **122**, 971-983.
- Schneider, M.R., Paus, R., 2010. Sebocytes, multifaceted epithelial cells: lipid production and holocrine secretion. *The international journal of biochemistry & cell biology* **42**, 181-185.
- Seierstad, M., Breitenbucher, J.G., 2008. Discovery and development of fatty acid amide hydrolase (FAAH) inhibitors. *Journal of medicinal chemistry* **51**, 7327-7343.
- Sertznig, P., Seifert, M., Tilgen, W., Reichrath, J., 2008. Peroxisome proliferator-activated receptors (PPARs) and the human skin: importance of PPARs in skin physiology and dermatologic diseases. *American journal of clinical dermatology* **9**, 15-31.
- Shakarjian, M.P., Heck, D.E., Gray, J.P., Sinko, P.J., Gordon, M.K., Casillas, R.P., Heindel, N.D., Gerecke, D.R., Laskin, D.L., Laskin, J.D., 2010. Mechanisms mediating the vesicant actions of sulfur mustard after cutaneous exposure. *Toxicological sciences : an official journal of the Society of Toxicology* **114**, 5-19.
- Shen, W., Chen, H., Jia, K., Ni, J., Yan, X., Li, S., 2012. Cloning and characterization of a novel amidase from *Paracoccus* sp. M-1, showing aryl acylamidase and acyl transferase activities. *Appl Microbiol Biotechnol* **94**, 1007-1018.
- Sheu, M.Y., Fowler, A.J., Kao, J., Schmuth, M., Schoonjans, K., Auwerx, J., Fluhr, J.W., Man, M.Q., Elias, P.M., Feingold, K.R., 2002. Topical peroxisome proliferator activated receptor-alpha activators reduce inflammation in irritant and allergic contact dermatitis models. *The Journal of investigative dermatology* **118**, 94-101.
- Simbulan-Rosenthal, C.M., Ray, R., Benton, B., Soeda, E., Daher, A., Anderson, D., Smith, W.J., Rosenthal, D.S., 2006. Calmodulin mediates sulfur mustard toxicity in human keratinocytes. *Toxicology* **227**, 21-35.
- Slipetz, D.M., O'Neill, G.P., Favreau, L., Dufresne, C., Gallant, M., Gareau, Y., Guay, D., Labelle, M., Metters, K.M., 1995. Activation of the human peripheral cannabinoid receptor results in inhibition of adenylyl cyclase. *Molecular pharmacology* **48**, 352-361.
- Smith, K.R., Thiboutot, D.M., 2008. Thematic review series: skin lipids. Sebaceous gland lipids: friend or foe? *Journal of lipid research* **49**, 271-281.
- Smith, L.T., Holbrook, K.A., 1982. Development of dermal connective tissue in human embryonic and fetal skin. *Scan Electron Microsc*, 1745-1751.
- Smith, L.T., Holbrook, K.A., Byers, P.H., 1982. Structure of the dermal matrix during development and in the adult. *The Journal of investigative dermatology* **79 Suppl 1**, 93s-104s.
- Snider, N.T., Nast, J.A., Tesmer, L.A., Hollenberg, P.F., 2009. A cytochrome P450-derived epoxygenated metabolite of anandamide is a potent cannabinoid receptor 2-selective agonist. *Molecular pharmacology* **75**, 965-972.
- Soldani, C., Scovassi, A.I., 2002. Poly(ADP-ribose) polymerase-1 cleavage during apoptosis: an update. *Apoptosis* **7**, 321-328.
- Song, Z.H., Bonner, T.I., 1996. A lysine residue of the cannabinoid receptor is critical for receptor recognition by several agonists but not WIN55212-2. *Molecular pharmacology* **49**, 891-896.
- Sotiropoulou, P.A., Blanpain, C., 2012. Development and homeostasis of the skin epidermis. *Cold Spring Harb Perspect Biol* **4**, a008383.
- Sourdeval, M., Lemaire, C., Deniaud, A., Taysse, L., Daulon, S., Breton, P., Brenner, C., Boisvieux-Ulrich, E., Marano, F., 2006. Inhibition of caspase-dependent mitochondrial permeability transition protects airway epithelial cells against mustard-induced apoptosis. *Apoptosis* **11**, 1545-1559.

- Sridar, C., Snider, N.T., Hollenberg, P.F., 2011. Anandamide oxidation by wild-type and polymorphically expressed CYP2B6 and CYP2D6. *Drug metabolism and disposition: the biological fate of chemicals* **39**, 782-788.
- Stander, S., Schmelz, M., Metze, D., Luger, T., Rukwied, R., 2005. Distribution of cannabinoid receptor 1 (CB1) and 2 (CB2) on sensory nerve fibers and adnexal structures in human skin. *Journal of dermatological science* **38**, 177-188.
- Starr, B., Sciutto, J. Labott, E., 2015. U.S. Investigating credible reports ISIS used chemical weapons., CNN Politics, <http://www.cnn.com>.
- Stojadinovic, O., Pastar, I., Vukelic, S., Mahoney, M.G., Brennan, D., Krzyzanowska, A., Golinko, M., Brem, H., Tomic-Canic, M., 2008. Deregulation of keratinocyte differentiation and activation: a hallmark of venous ulcers. *Journal of cellular and molecular medicine* **12**, 2675-2690.
- Storr, M.A., Keenan, C.M., Emmerdinger, D., Zhang, H., Yuce, B., Sibaev, A., Massa, F., Buckley, N.E., Lutz, B., Goke, B., Brand, S., Patel, K.D., Sharkey, K.A., 2008. Targeting endocannabinoid degradation protects against experimental colitis in mice: involvement of CB1 and CB2 receptors. *J Mol Med (Berl)* **86**, 925-936.
- Straus, D.S., Glass, C.K., 2007. Anti-inflammatory actions of PPAR ligands: new insights on cellular and molecular mechanisms. *Trends Immunol* **28**, 551-558.
- Sturm, A., Sudermann, T., Schulte, K.M., Goebell, H., Dignass, A.U., 1999. Modulation of intestinal epithelial wound healing in vitro and in vivo by lysophosphatidic acid. *Gastroenterology* **117**, 368-377.
- Sugawara, K., Biro, T., Tsuruta, D., Toth, B.I., Kromminga, A., Zakany, N., Zimmer, A., Funk, W., Gibbs, B.F., Zimmer, A., Paus, R., 2012. Endocannabinoids limit excessive mast cell maturation and activation in human skin. *The Journal of allergy and clinical immunology* **129**, 726-738 e728.
- Sun, Y., Alexander, S.P., Kendall, D.A., Bennett, A.J., 2006. Cannabinoids and PPARalpha signalling. *Biochemical Society transactions* **34**, 1095-1097.
- Szallasi, A., Cortright, D.N., Blum, C.A., Eid, S.R., 2007. The vanilloid receptor TRPV1: 10 years from channel cloning to antagonist proof-of-concept. *Nat Rev Drug Discov* **6**, 357-372.
- Tai, A., Sawano, T., Yazama, F., 2011. Antioxidant properties of ethyl vanillin in vitro and in vivo. *Bioscience, biotechnology, and biochemistry* **75**, 2346-2350.
- Tai, T., Tsuboi, K., Uyama, T., Masuda, K., Cravatt, B.F., Houchi, H., Ueda, N., 2012. Endogenous molecules stimulating N-acyl ethanolamine-hydrolyzing acid amidase (NAAA). *ACS chemical neuroscience* **3**, 379-385.
- Takata, M., Homma, Y., Kurosaki, T., 1995. Requirement of phospholipase C-gamma 2 activation in surface immunoglobulin M-induced B cell apoptosis. *The Journal of experimental medicine* **182**, 907-914.
- Telek, A., Biro, T., Bodo, E., Toth, B.I., Borbiri, I., Kunos, G., Paus, R., 2007. Inhibition of human hair follicle growth by endo- and exocannabinoids. *FASEB journal : official publication of the Federation of American Societies for Experimental Biology* **21**, 3534-3541.
- Tewari-Singh, N., Jain, A.K., Inturi, S., White, C.W., Agarwal, R., 2013. Clinically-relevant cutaneous lesions by nitrogen mustard: useful biomarkers of vesicants skin injury in SKH-1 hairless and C57BL/6 mice. *PloS one* **8**, e67557.
- Tewari-Singh, N., Jain, A.K., Orlicky, D.J., White, C.W., Agarwal, R., 2014. Cutaneous injury-related structural changes and their progression following topical nitrogen mustard exposure in hairless and haired mice. *PloS one* **9**, e85402.
- Thorburn, A., 2004. Death receptor-induced cell killing. *Cellular signalling* **16**, 139-144.

- Tian, X., Guo, J., Yao, F., Yang, D.P., Makriyannis, A., 2005. The conformation, location, and dynamic properties of the endocannabinoid ligand anandamide in a membrane bilayer. *The Journal of biological chemistry* **280**, 29788-29795.
- Tochio, T., Tanaka, H., Nakata, S., Ikeno, H., 2009. Accumulation of lipid peroxide in the content of comedones may be involved in the progression of comedogenesis and inflammatory changes in comedones. *J Cosmet Dermatol* **8**, 152-158.
- Tomar, S., E, E.Z., Nagarkatti, M., Nagarkatti, P.S., 2015. Protective Role of Cannabinoid Receptor 2 Activation in Galactosamine/Lipopolysaccharide-Induced Acute Liver Failure through Regulation of Macrophage Polarization and MicroRNAs. *The Journal of pharmacology and experimental therapeutics* **353**, 369-379.
- Tomohiro, D., Mizuta, K., Fujita, T., Nishikubo, Y., Kumamoto, E., 2013. Inhibition by capsaicin and its related vanilloids of compound action potentials in frog sciatic nerves. *Life sciences* **92**, 368-378.
- Toth, B.I., Dobrosi, N., Dajnoki, A., Czifra, G., Olah, A., Szollosi, A.G., Juhasz, I., Sugawara, K., Paus, R., Biro, T., 2011a. Endocannabinoids modulate human epidermal keratinocyte proliferation and survival via the sequential engagement of cannabinoid receptor-1 and transient receptor potential vanilloid-1. *The Journal of investigative dermatology* **131**, 1095-1104.
- Toth, B.I., Olah, A., Szollosi, A.G., Czifra, G., Biro, T., 2011e. "Sebocytes' makeup": novel mechanisms and concepts in the physiology of the human sebaceous glands. *Pflugers Archiv : European journal of physiology* **461**, 593-606.
- Tu, C.L., Crumrine, D.A., Man, M.Q., Chang, W., Elalieh, H., You, M., Elias, P.M., Bikle, D.D., 2012. Ablation of the calcium-sensing receptor in keratinocytes impairs epidermal differentiation and barrier function. *The Journal of investigative dermatology* **132**, 2350-2359.
- Turcotte, C., Chouinard, F., Lefebvre, J.S., Flamand, N., 2015. Regulation of inflammation by cannabinoids, the endocannabinoids 2-arachidonoyl-glycerol and arachidonoyl-ethanolamide, and their metabolites. *Journal of leukocyte biology* **97**, 1049-1070.
- Ueda, Y., Miyagawa, N., Matsui, T., Kaya, T., Iwamura, H., 2005. Involvement of cannabinoid CB(2) receptor-mediated response and efficacy of cannabinoid CB(2) receptor inverse agonist, JTE-907, in cutaneous inflammation in mice. *European journal of pharmacology* **520**, 164-171.
- Vacondio, F., Silva, C., Lodola, A., Carmi, C., Rivara, S., Duranti, A., Tontini, A., Sanchini, S., Clapper, J.R., Piomelli, D., Tarzia, G., Mor, M., 2011. Biphenyl-3-yl alkylcarbamates as fatty acid amide hydrolase (FAAH) inhibitors: steric effects of N-alkyl chain on rat plasma and liver stability. *European journal of medicinal chemistry* **46**, 4466-4473.
- Vane, S.J., 1998. Differential inhibition of cyclooxygenase isoforms: an explanation of the action of NSAIDs. *J Clin Rheumatol* **4**, s3-10.
- Walpole, C.S., Wrigglesworth, R., Bevan, S., Campbell, E.A., Dray, A., James, I.F., Masdin, K.J., Perkins, M.N., Winter, J., 1993. Analogues of capsaicin with agonist activity as novel analgesic agents; structure-activity studies. 3. The hydrophobic side-chain "C-region". *Journal of medicinal chemistry* **36**, 2381-2389.
- Wang, Y., Ramirez, F., Krishnamurthy, G., Gilbert, A., Kadakia, N., Xu, J., Kalgaonkar, G., Ramarao, M.K., Edris, W., Rogers, K.E., Jones, P.G., 2006. High-throughput screening for the discovery of inhibitors of fatty acid amide hydrolase using a microsome-based fluorescent assay. *Journal of biomolecular screening* **11**, 519-527.
- Wattana, M., Bey, T., 2009. Mustard gas or sulfur mustard: an old chemical agent as a new terrorist threat. *Prehospital and disaster medicine* **24**, 19-29; discussion 30-11.

- Weber, A., Ni, J., Ling, K.H., Acheampong, A., Tang-Liu, D.D., Burk, R., Cravatt, B.F., Woodward, D., 2004. Formation of prostamides from anandamide in FAAH knockout mice analyzed by HPLC with tandem mass spectrometry. *Journal of lipid research* **45**, 757-763.
- Wei, B.Q., Mikkelsen, T.S., McKinney, M.K., Lander, E.S., Cravatt, B.F., 2006. A second fatty acid amide hydrolase with variable distribution among placental mammals. *The Journal of biological chemistry* **281**, 36569-36578.
- Weinstein, I.B., Lee, L.S., Fisher, P.B., Mufson, A., Yamasaki, H., 1979. Action of phorbol esters in cell culture: mimicry of transformation, altered differentiation, and effects on cell membranes. *J Supramol Struct* **12**, 195-208.
- Werner, S., Smola, H., Liao, X., Longaker, M.T., Krieg, T., Hofschneider, P.H., Williams, L.T., 1994. The function of KGF in morphogenesis of epithelium and reepithelialization of wounds. *Science* **266**, 819-822.
- Wickett R.R., a.V., M.O. , 2006. Structure and function of the epidermal barrier. *AmJ Inf Ctl* **34**, S98-110.
- Wikramanayake, T.C., Stojadinovic, O., Tomic-Canic, M., 2014. Epidermal Differentiation in Barrier Maintenance and Wound Healing. *Advances in wound care* **3**, 272-280.
- Williams, C.S., Mann, M., DuBois, R.N., 1999. The role of cyclooxygenases in inflammation, cancer, and development. *Oncogene* **18**, 7908-7916.
- Wise, L.E., Cannavacciuolo, R., Cravatt, B.F., Martin, B.F., Lichtman, A.H., 2008. Evaluation of fatty acid amides in the carrageenan-induced paw edema model. *Neuropharmacology* **54**, 181-188.
- Wong, V.W., Sorkin, M., Glotzbach, J.P., Longaker, M.T., Gurtner, G.C., 2011. Surgical approaches to create murine models of human wound healing. *Journal of biomedicine & biotechnology* **2011**, 969618.
- Woodward, D.F., Carling, R.W., Cornell, C.L., Fliri, H.G., Martos, J.L., Pettit, S.N., Liang, Y., Wang, J.W., 2008. The pharmacology and therapeutic relevance of endocannabinoid derived cyclo-oxygenase (COX)-2 products. *Pharmacology & therapeutics* **120**, 71-80.
- Woodward, D.F., Krauss, A.H., Chen, J., Liang, Y., Li, C., Protzman, C.E., Bogardus, A., Chen, R., Kedzie, K.M., Krauss, H.A., Gil, D.W., Kharlamb, A., Wheeler, L.A., Babusis, D., Welty, D., Tang-Liu, D.D., Cherukury, M., Andrews, S.W., Burk, R.M., Garst, M.E., 2003. Pharmacological characterization of a novel antiglaucoma agent, Bimatoprost (AGN 192024). *The Journal of pharmacology and experimental therapeutics* **305**, 772-785.
- Woodward, D.F., Wang, J.W., Poloso, N.J., 2013. Recent progress in prostaglandin F2alpha ethanolamide (prostamide F2alpha) research and therapeutics. *Pharmacological reviews* **65**, 1135-1147.
- Wormser, U., Brodsky, B., Proscura, E., Foley, J.F., Jones, T., Nyska, A., 2005. Involvement of tumor necrosis factor-alpha in sulfur mustard-induced skin lesion; effect of topical iodine. *Arch Toxicol* **79**, 660-670.
- Wormser, U., Langenbach, R., Peddada, S., Sintov, A., Brodsky, B., Nyska, A., 2004. Reduced sulfur mustard-induced skin toxicity in cyclooxygenase-2 knockout and celecoxib-treated mice. *Toxicology and applied pharmacology* **200**, 40-47.
- Wosicka, H., Cal, K., 2010. Targeting to the hair follicles: current status and potential. *Journal of dermatological science* **57**, 83-89.
- Wright, K., Rooney, N., Feeney, M., Tate, J., Robertson, D., Welham, M., Ward, S., 2005. Differential expression of cannabinoid receptors in the human colon: cannabinoids promote epithelial wound healing. *Gastroenterology* **129**, 437-453.

- Yamashita, A., Oka, S., Tanikawa, T., Hayashi, Y., Nemoto-Sasaki, Y., Sugiura, T., 2013. The actions and metabolism of lysophosphatidylinositol, an endogenous agonist for GPR55. *Prostaglandins Other Lipid Mediat* **107**, 103-116.
- Yates, M.L., Barker, E.L., 2009. Organized trafficking of anandamide and related lipids. *Vitamins and hormones* **81**, 25-53.
- Young, S., Fabio, K., Guillon, C., Mohanta, P., Halton, T.A., Heck, D.E., Flowers, R.A., 2nd, Laskin, J.D., Heindel, N.D., 2010. Peripheral site acetylcholinesterase inhibitors targeting both inflammation and cholinergic dysfunction. *Bioorganic & medicinal chemistry letters* **20**, 2987-2990.
- Young, S.C., Fabio, K.M., Huang, M.T., Saxena, J., Harman, M.P., Guillon, C.D., Vetrano, A.M., Heck, D.E., Flowers, R.A., 2nd, Heindel, N.D., Laskin, J.D., 2012. Investigation of anticholinergic and non-steroidal anti-inflammatory prodrugs which reduce chemically induced skin inflammation. *Journal of applied toxicology : JAT* **32**, 135-141.
- Yu, M., Ives, D., Ramesha, C.S., 1997. Synthesis of prostaglandin E2 ethanolamide from anandamide by cyclooxygenase-2. *The Journal of biological chemistry* **272**, 21181-21186.
- Zelasko, S., Arnold, W.R., Das, A., 2015. Endocannabinoid metabolism by cytochrome P450 monooxygenases. *Prostaglandins Other Lipid Mediat* **116-117**, 112-123.
- Zhang, J., Chen, L., Su, T., Cao, F., Meng, X., Pei, L., Shi, J., Pan, H.L., Li, M., 2010. Electroacupuncture increases CB2 receptor expression on keratinocytes and infiltrating inflammatory cells in inflamed skin tissues of rats. *The journal of pain : official journal of the American Pain Society* **11**, 1250-1258.
- Zheng, J.L., Yu, T.S., Li, X.N., Fan, Y.Y., Ma, W.X., Du, Y., Zhao, R., Guan, D.W., 2012. Cannabinoid receptor type 2 is time-dependently expressed during skin wound healing in mice. *International journal of legal medicine* **126**, 807-814.
- Zheng, R., Po, I., Mishin, V., Black, A.T., Heck, D.E., Laskin, D.L., Sinko, P.J., Gerecke, D.R., Gordon, M.K., Laskin, J.D., 2013. The generation of 4-hydroxynonenal, an electrophilic lipid peroxidation end product, in rabbit cornea organ cultures treated with UVB light and nitrogen mustard. *Toxicology and applied pharmacology* **272**, 345-355.
- Zhou, B.R., Zhang, J.A., Zhang, Q., Permatasari, F., Xu, Y., Wu, D., Yin, Z.Q., Luo, D., 2013. Palmitic acid induces production of proinflammatory cytokines interleukin-6, interleukin-1beta, and tumor necrosis factor-alpha via a NF-kappaB-dependent mechanism in HaCaT keratinocytes. *Mediators of inflammation* **2013**, 530429.
- Zouboulis, C.C., 2004. Acne and sebaceous gland function. *Clin Dermatol* **22**, 360-366.
- Zouboulis, C.C., Jourdan, E., Picardo, M., 2014. Acne is an inflammatory disease and alterations of sebum composition initiate acne lesions. *Journal of the European Academy of Dermatology and Venereology : JEADV* **28**, 527-532.
- Zouboulis, C.C., Schagen, S., Alestas, T., 2008. The sebocyte culture: a model to study the pathophysiology of the sebaceous gland in seborrhea and acne. *Arch Dermatol Res* **300**, 397-413.